



Porquerolles,
September 14th

Semi-conductor epitaxy

3D growth driven by elasticity

Leo Miglio

leo.miglio@unimib.it



with: F. Montalenti, A. Marzegalli,
R. Bergamaschini, F. Pezzoli, M. Salvalaglio,
M. Albani,

Past co-workers:

D. B. Migas, P. Raiteri, G. Vastola, D. Scopece, R. Gatti,
F. Boioli, S. Cereda, V.A. Zinoviev, F. Valentinotti

Main collaborations:

Guenther Bauer, Jerry Tersoff, Oliver Schmidt, Hans von Kaenel, Armando Rastelli, Giovanni Capellini...



Porquerolles,
September 14th

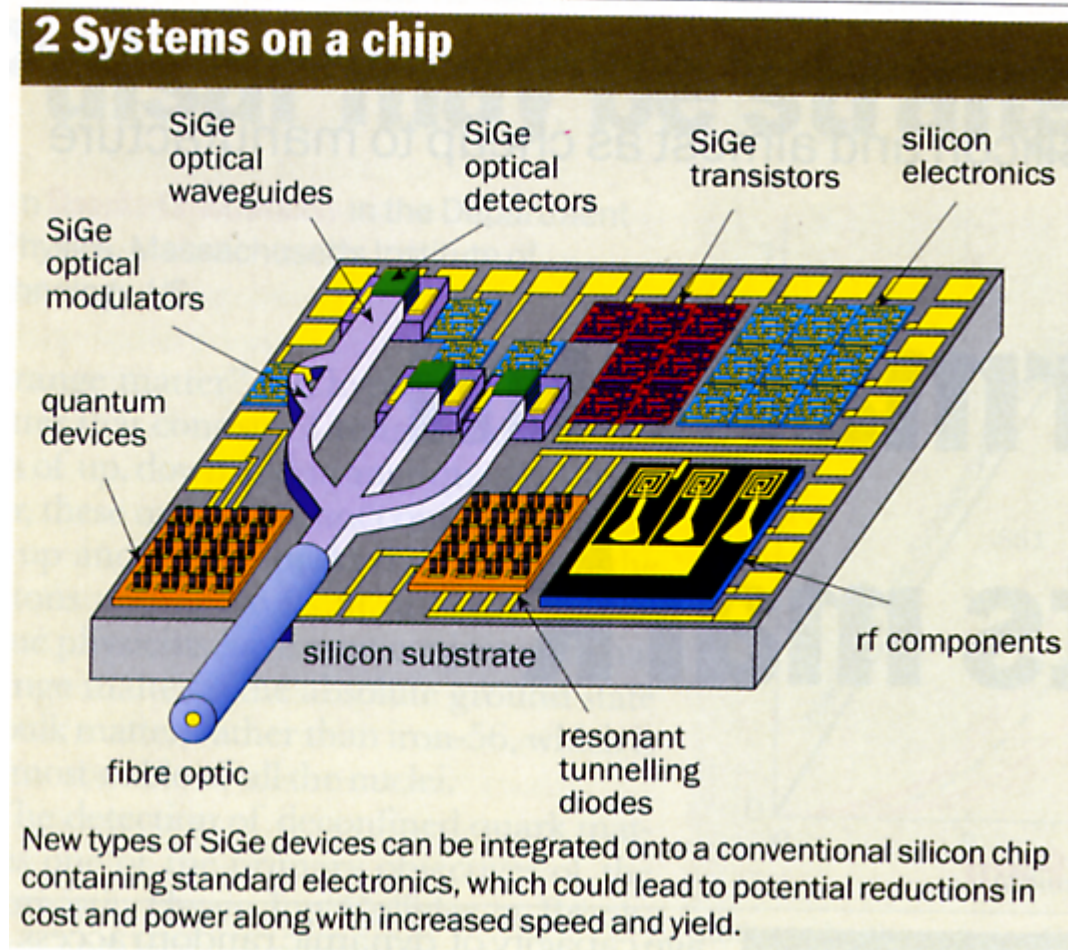
Semiconductor epitaxy

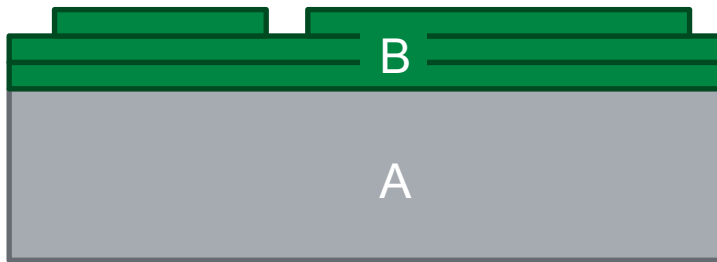


Introduction to heteroepitaxial islands and their formation mechanism



Ge(Si)/Si is a test example of full miscibility for epitaxy of nanostructures and a promising candidate for electronic and photonic integrated systems

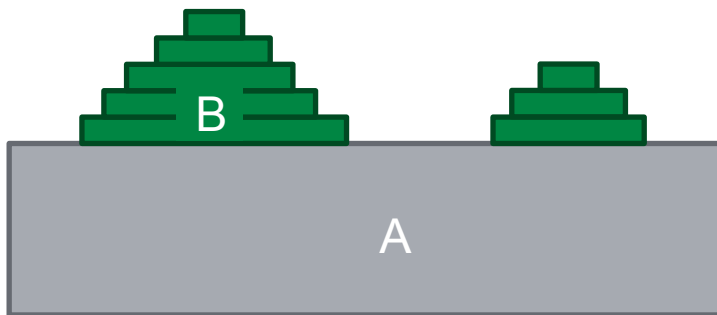




Frank – van der Merve

(lattice misfit < 1%)

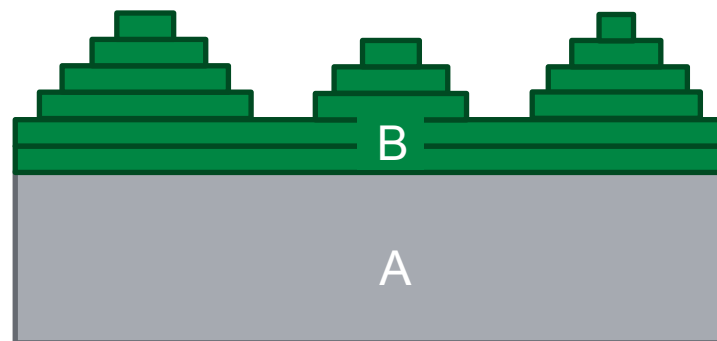
$$\gamma_{\downarrow A} > \gamma_{\downarrow B} + \gamma_{\downarrow AB}$$



Volmer – Weber

(lattice misfit > 6-8 %)

$$\gamma_{\downarrow A} < \gamma_{\downarrow B} + \gamma_{\downarrow AB}$$



Stranski – Krastanow

(lattice misfit 1-5%)

$$\gamma_{\downarrow A} > \gamma_{\downarrow B} + \gamma_{\downarrow AB} \rightarrow \text{Wetting layer}$$

+

$E(V) \rightarrow$ Island formation above a critical thickness to relieve strain

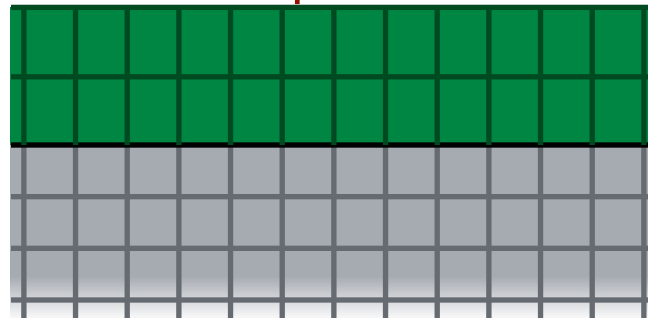
Stranski-Krastanow growth of SiGe/Si



Full miscibility, no polarity, just lattice mismatch up to 4.2 %

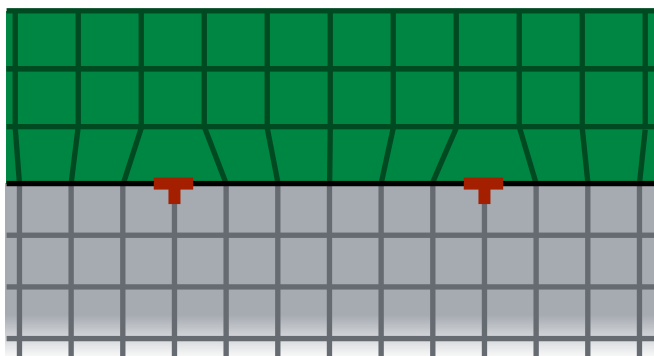


Pseudomorphic structure



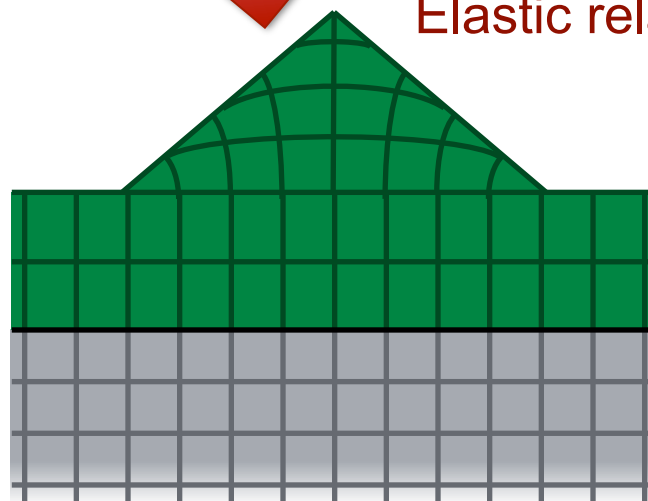
Small Ge Content

Plastic relaxation



Large Ge content

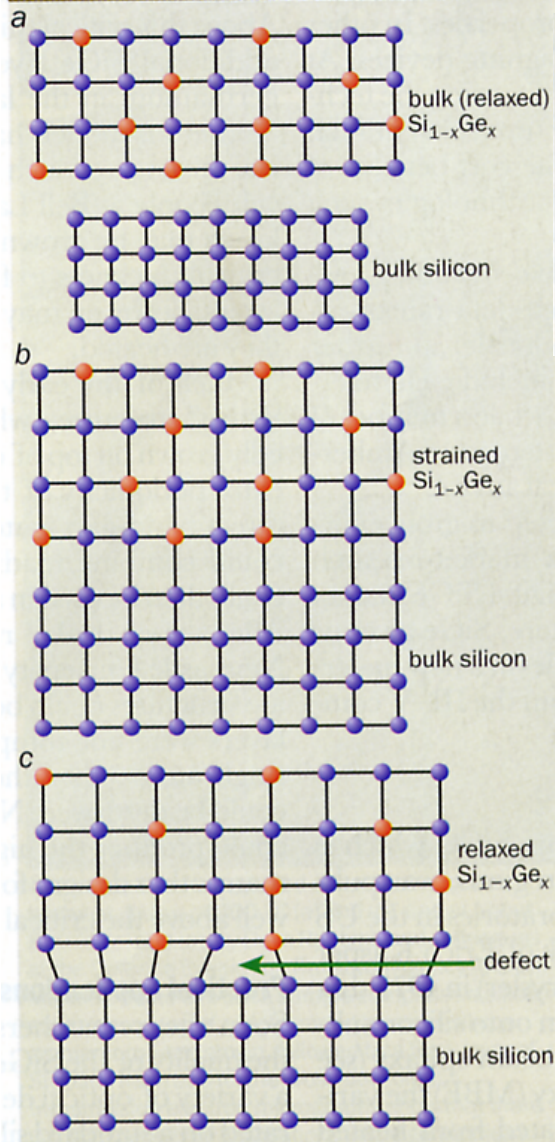
Elastic relaxation



Dislocations in a SiGe (graded) layer



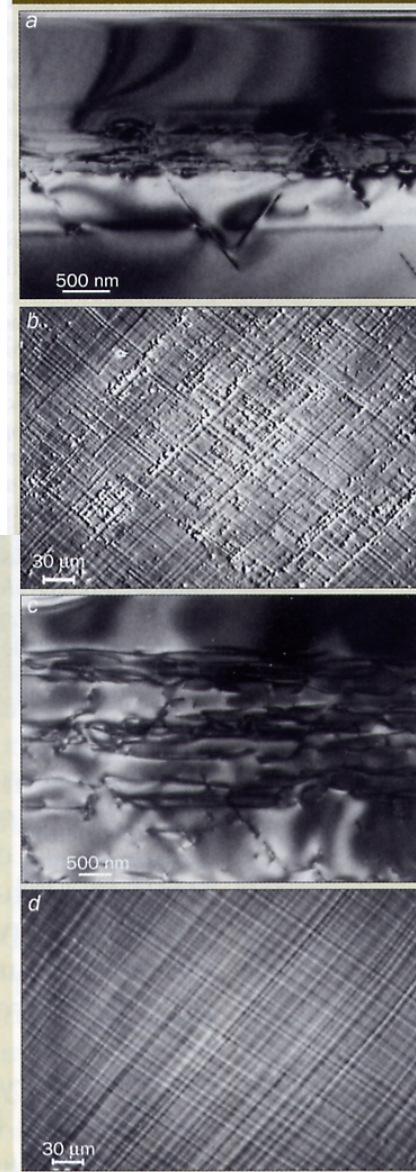
1 Crystal engineering



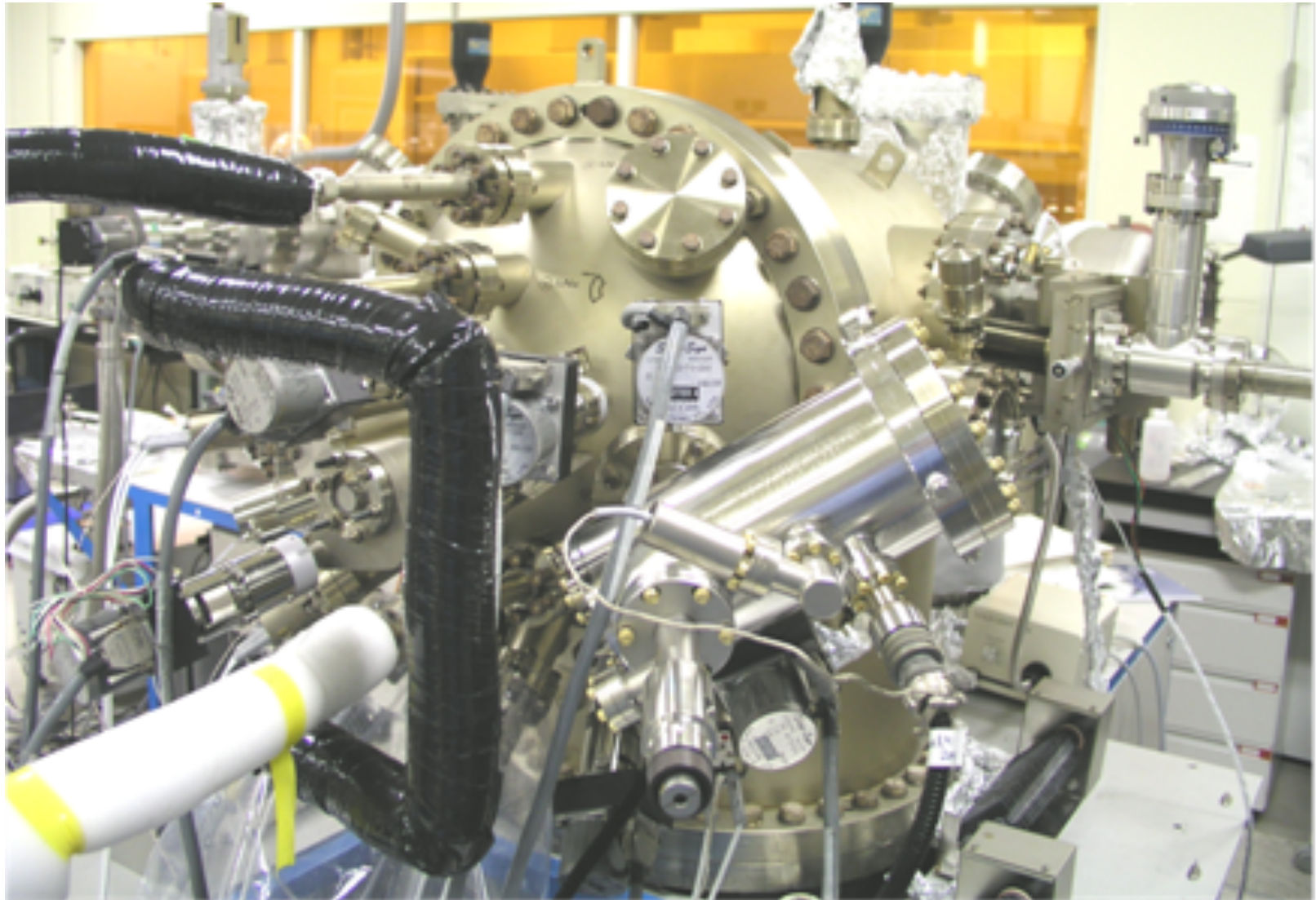
(a) The lattice constant of bulk silicon (blue) and $\text{Si}_{1-x}\text{Ge}_x$ crystals differ because the lattice constant in bulk germanium (red) is 4.2% larger than in silicon. (b) A thin layer of $\text{Si}_{1-x}\text{Ge}_x$ can be grown on top of a layer of silicon such that the lattice constant of the $\text{Si}_{1-x}\text{Ge}_x$ is matched to the silicon. The strain induced by the difference in the lattice constants can be used to engineer the band gap. (c) Beyond the so-called critical thickness, defects such as misfit dislocations form to relieve the system. This critical thickness depends on the fraction of germanium used.

A comparison of two graded silicon-germanium samples, grown at 600 °C (a) and (b), and at about 800 °C (c) and (d), by Dave Robbins and colleagues at the Defence Evaluation Research Agency (DERA), Malvern, in the UK. Each sample comprises a silicon substrate on top of which graded layers of silicon germanium were grown, followed by a thick layer of $\text{Si}_{1-x}\text{Ge}_x$. In (a) and (c) the cross-sectional transmission electron micrographs show that there is a high density of dislocations in the germanium-graded parts of the structures but the thick $\text{Si}_{1-x}\text{Ge}_x$ layer grown above the graded regions is free from defects. More surprising is that many of the dislocations thread down into the Si substrate rather than up to the surface. (b) and (d) show the difference in surface roughness from the different growth temperatures. There are fewer defects in the sample grown at higher temperatures. Indeed, the mobility of the charge carriers in the high-temperature substrate was 100 times better than in the one grown at the lower temperature.

3 Reducing the defect density



Deposition by MBE: close to equilibrium

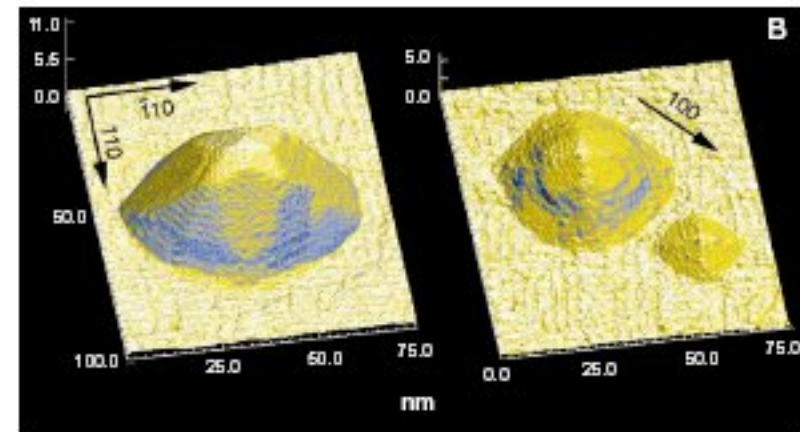
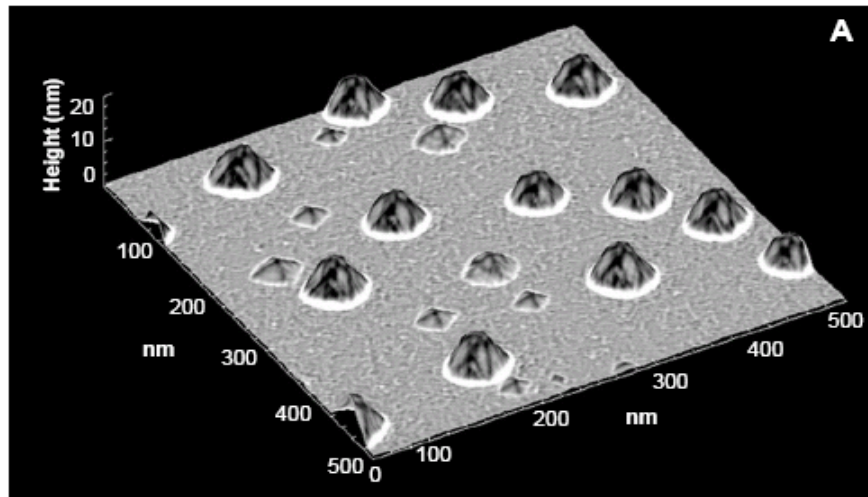




Shape Transition of Germanium Nanocrystals on a Silicon (001) Surface from Pyramids to Domes

Gilberto Medeiros-Ribeiro, Alexander M. Bratkovski,
Theodore I. Kamins, Douglas A. A. Ohlberg, R. Stanley Williams*

SCIENCE • VOL. 279 • 16 JANUARY 1998



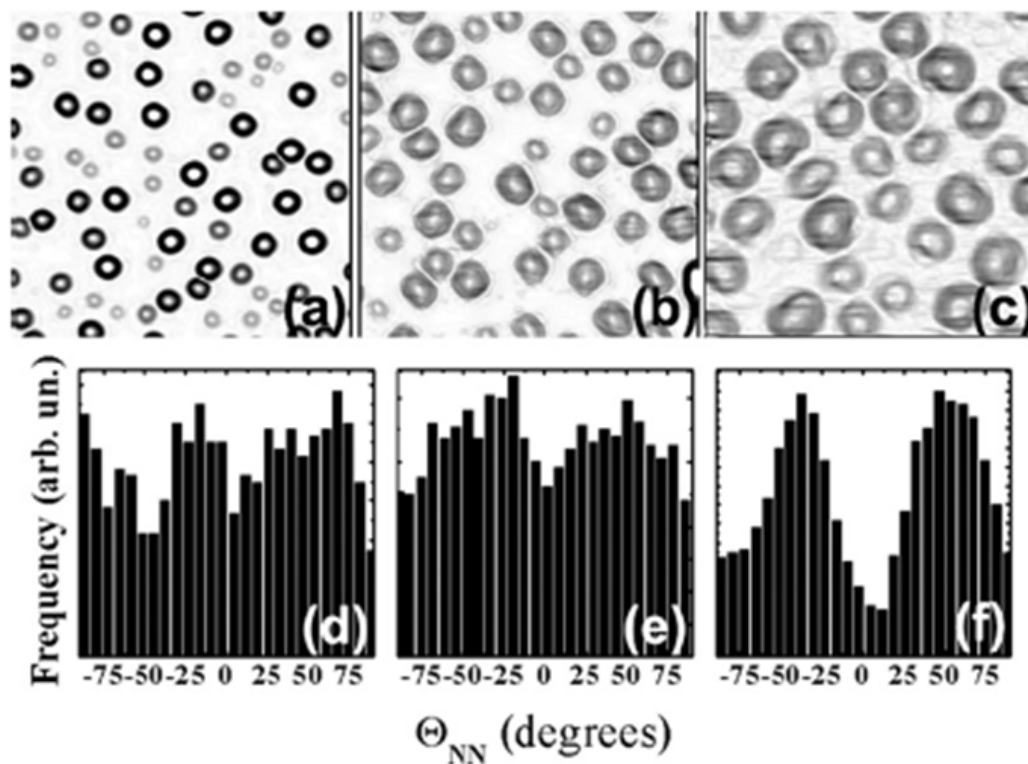
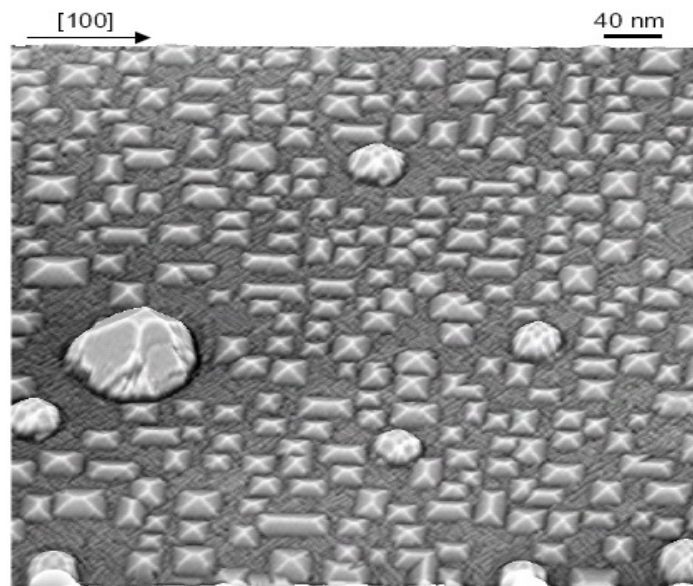
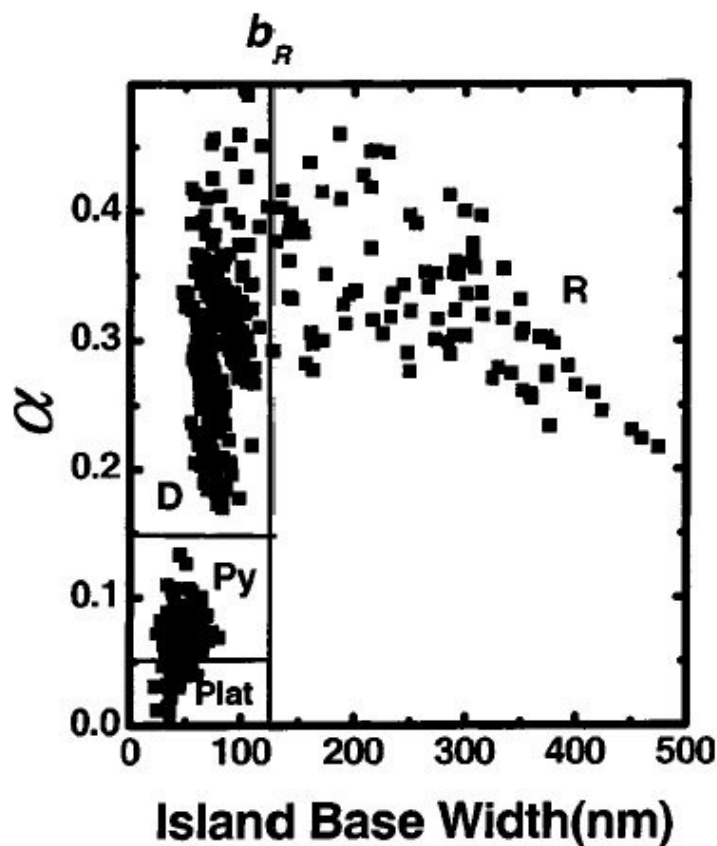


Figure 11. $2 \times 2 \mu\text{m}^2$ AFM images displayed in differential mode of a Ge island layer deposited at 750°C and having an equivalent thickness of 1.5 nm covered by a (a) 0 nm, (b) 1.8 nm, and (c) 6 nm thick silicon cap layer. Image sides are oriented along [110] directions. In panels (d)–(f) we display the corresponding angular distribution of the four nearest neighbours.



Different sizes \rightarrow different shapes
(AFM imaging)




A. Rastelli, private communication and Phd. thesis

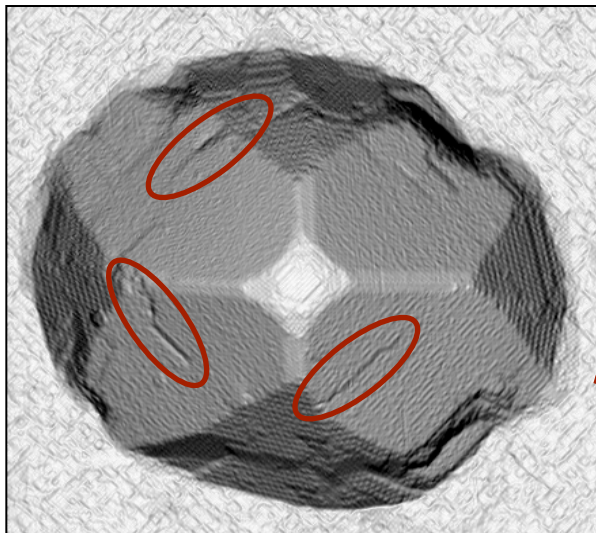
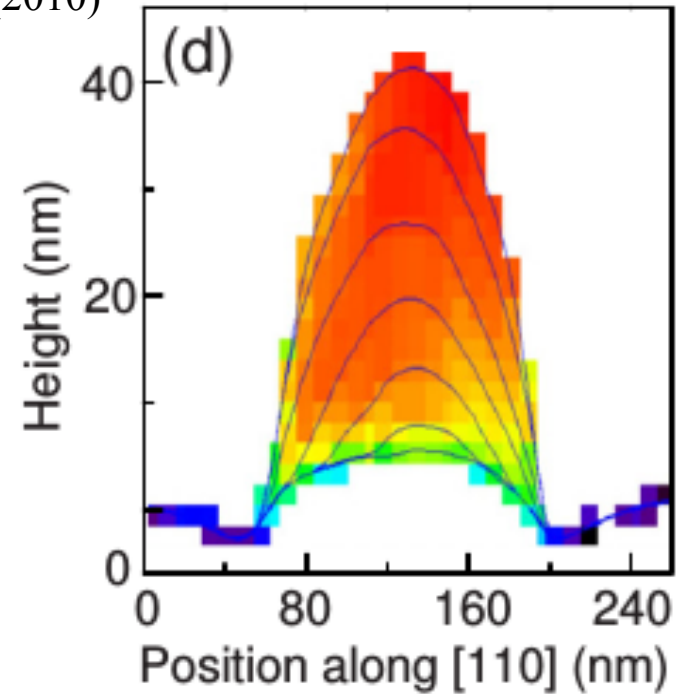
G. Cappellini, M. De Seta, F. Evangelisti, *J. Appl. Phys.* (2003)

Pbls for device appl: intermixing, dislocations



J. Zhang et al., *Appl. Phys. Lett.* **97**, 203103 (2010)

Ge fraction 0  0.43



Dislocations at large volumes (STM imaging)

0  48° STM 120×120×27 nm³

A. Rastelli, private communication and Phd. thesis



- Lower elastic energy in volume
- Different surface energies and area of facets
- THESE ARE THE WEAKER FORCES PRODUCING A HIERARCHY WITH STRONGER COVALENT FORCES, IN TURN ORIGINATING THE SELF-ASSEMBLY PROCESS

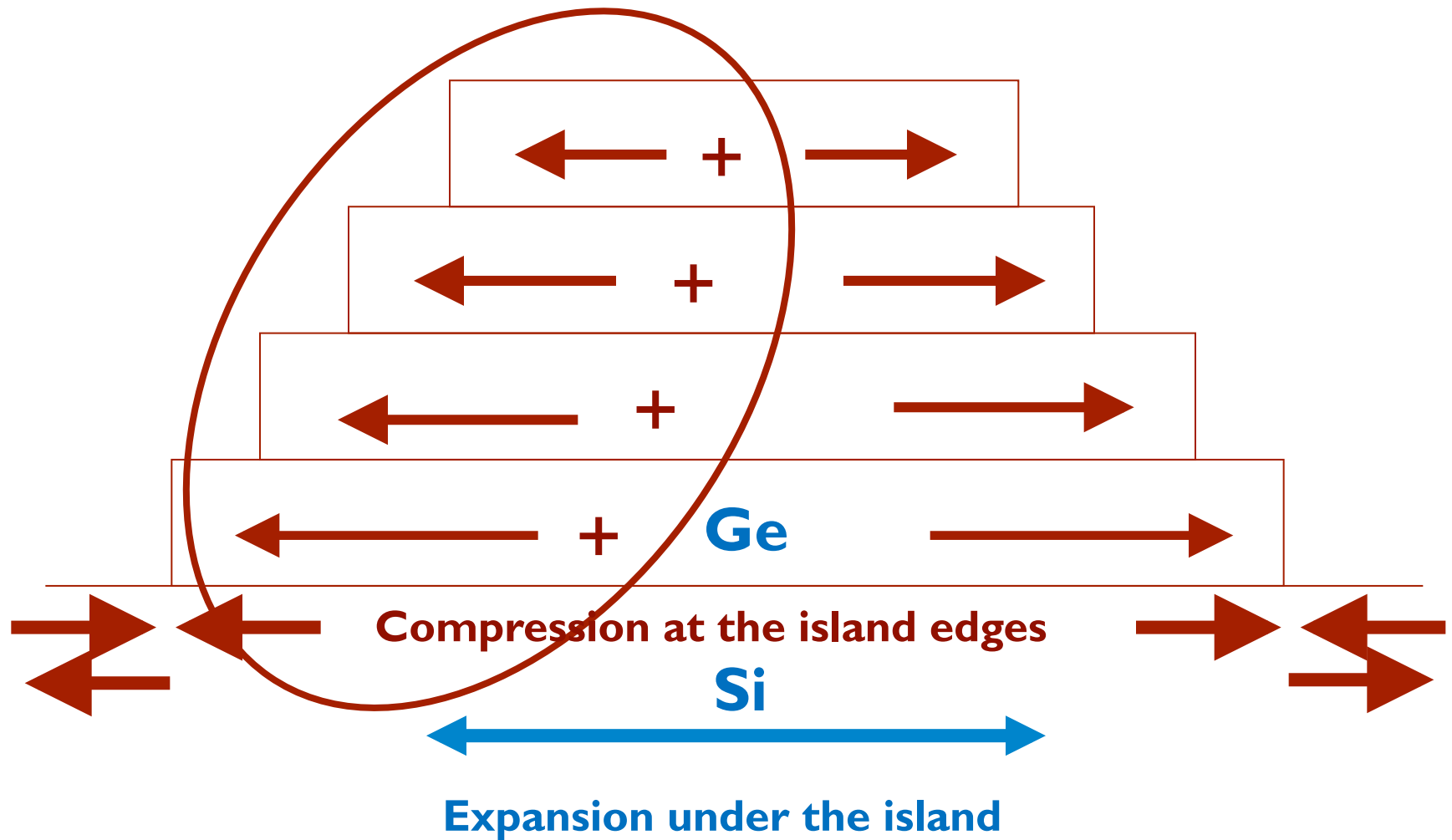


Elastic relaxation

- Transfer of the load to the Si substrate
- Expanding the Ge lattice at the free facets

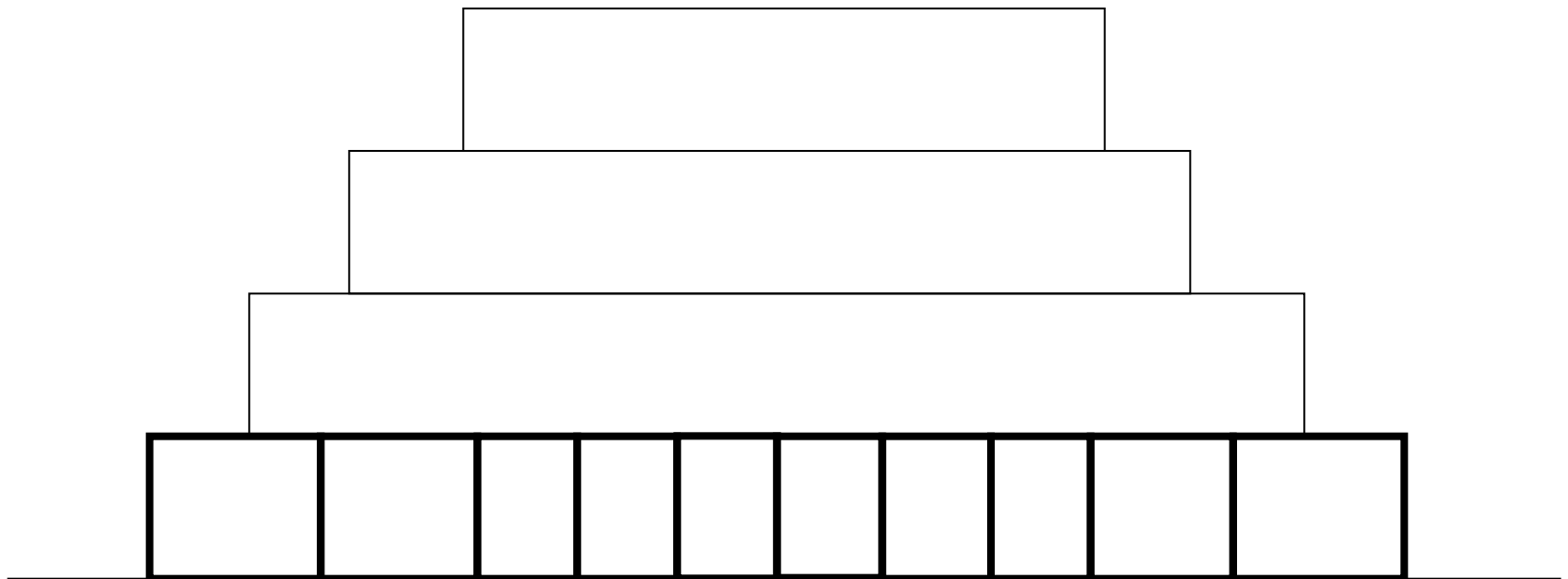
Other strategy: Intermixing Si-Ge

Other strategy: Plastic relaxation (dislocations)





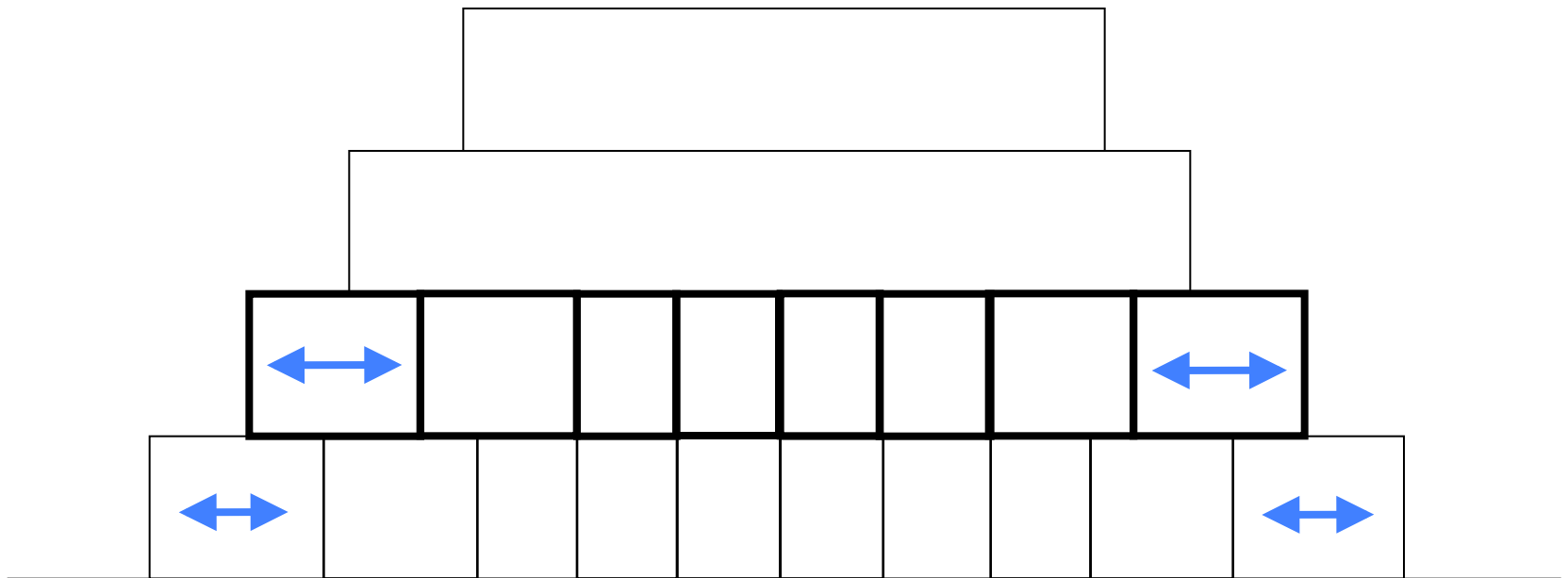
Ratch and Zangwill expansion on a fixed substrate



In continuum approach, this is just $\sigma \cdot n = 0$

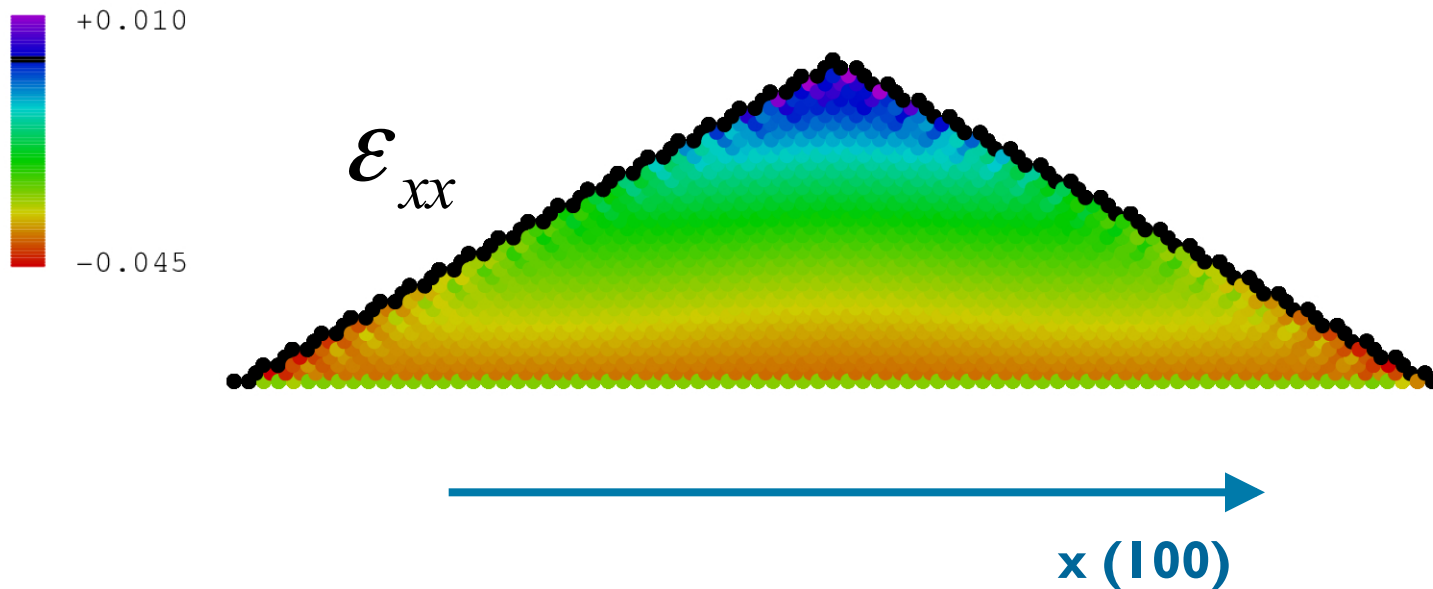


**The stress related to strain decreases
from the bottom to the top**





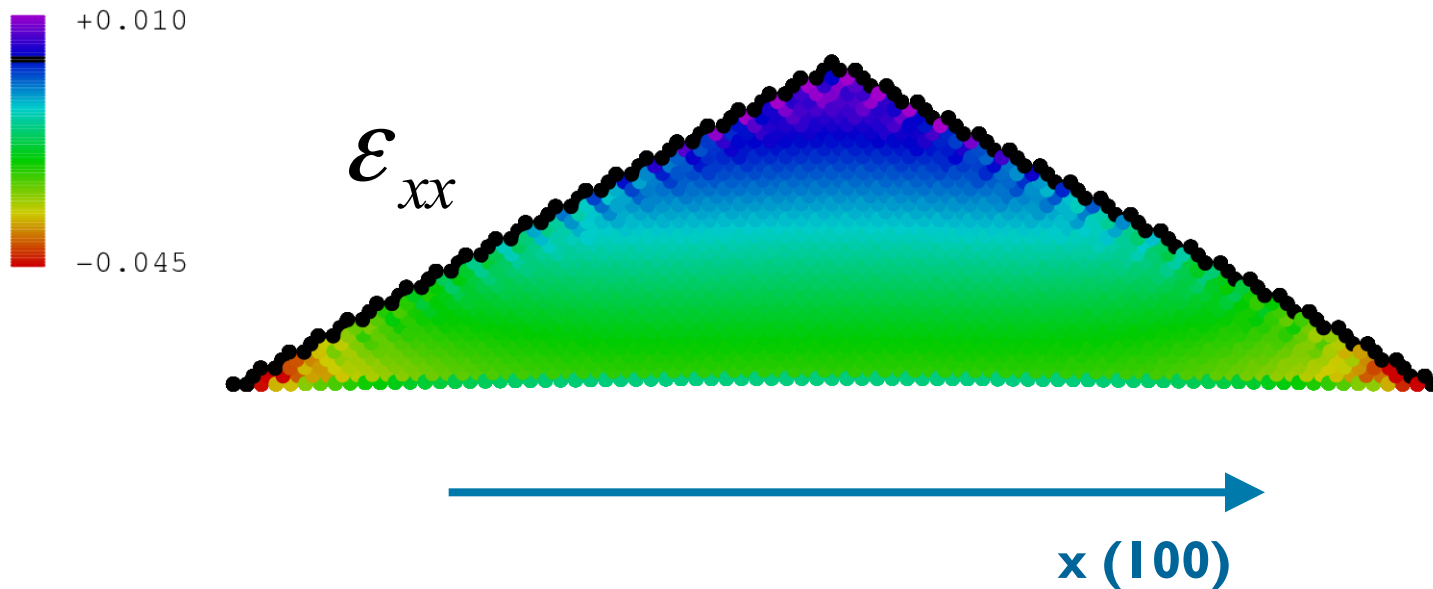
{102} Ge island on Si(001) by MD simulations



Second mechanism only: frozen Si substrate



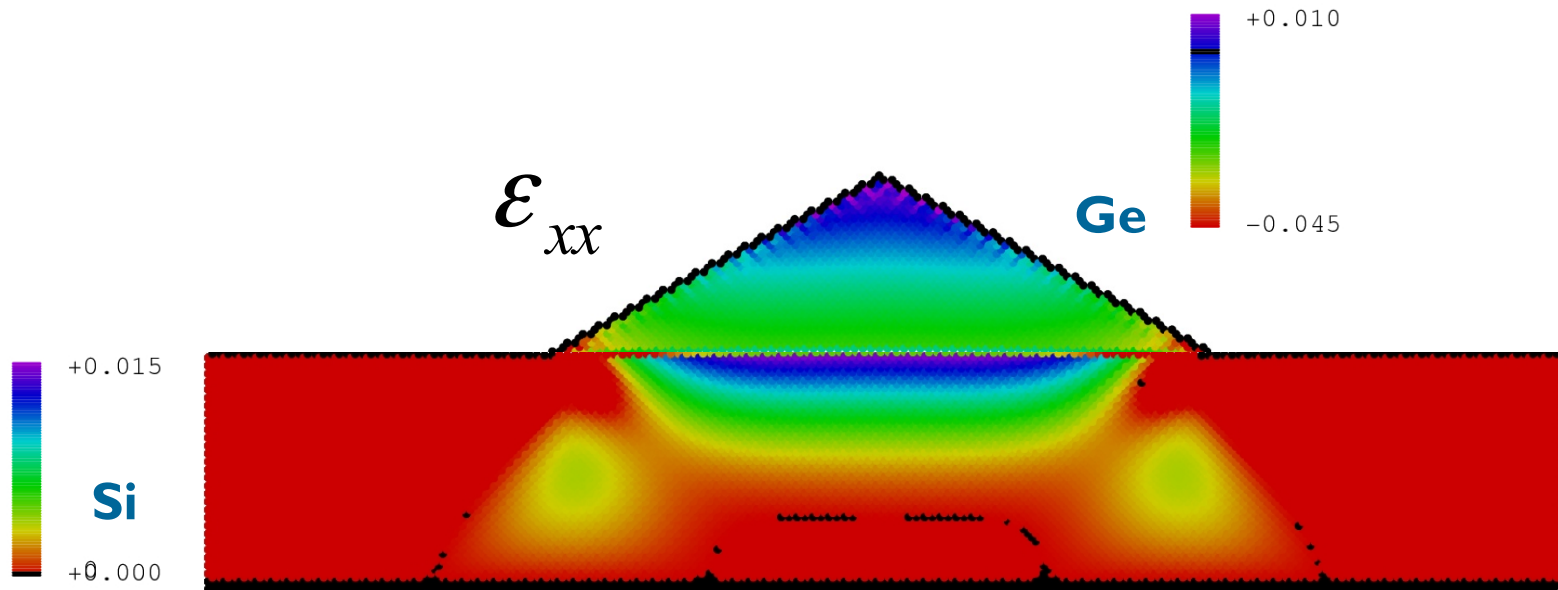
Two contributions to the total
relaxation mechanism



with Si-substrate distortion



..... the substrate is correspondingly loaded (but summing the two contribution we find that the elastic energy is lower)



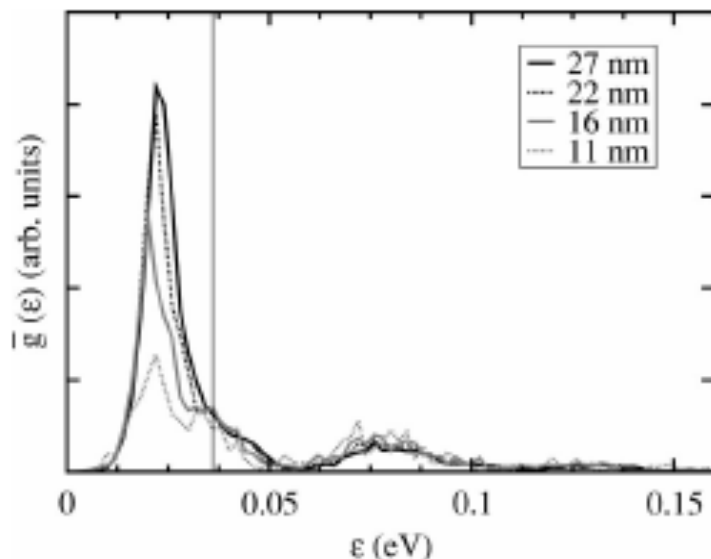


FIG. 6. Normalized distribution of the energy per atom in $\{1\ 0\ 5\}$ pyramids with different sizes for a spectral region corresponding to the energy contribution scaling as the number of atoms. The vertical line indicates the excess energy of a pseudomorphic Ge film without free surfaces (0.036 eV).

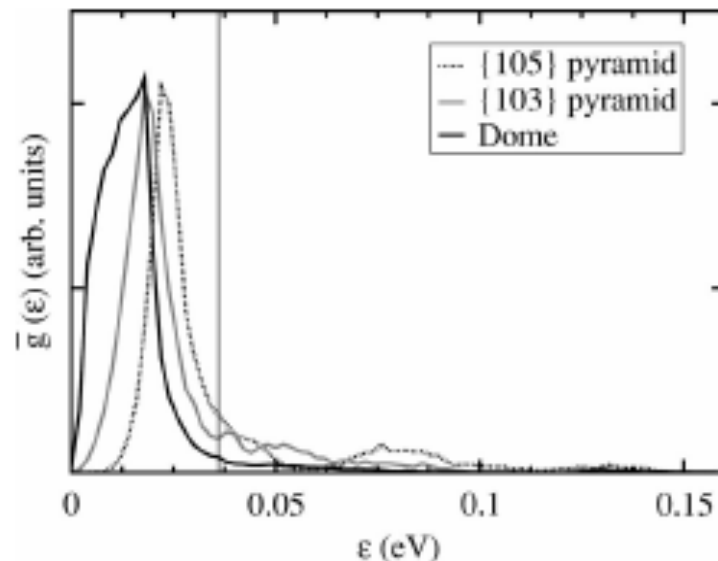
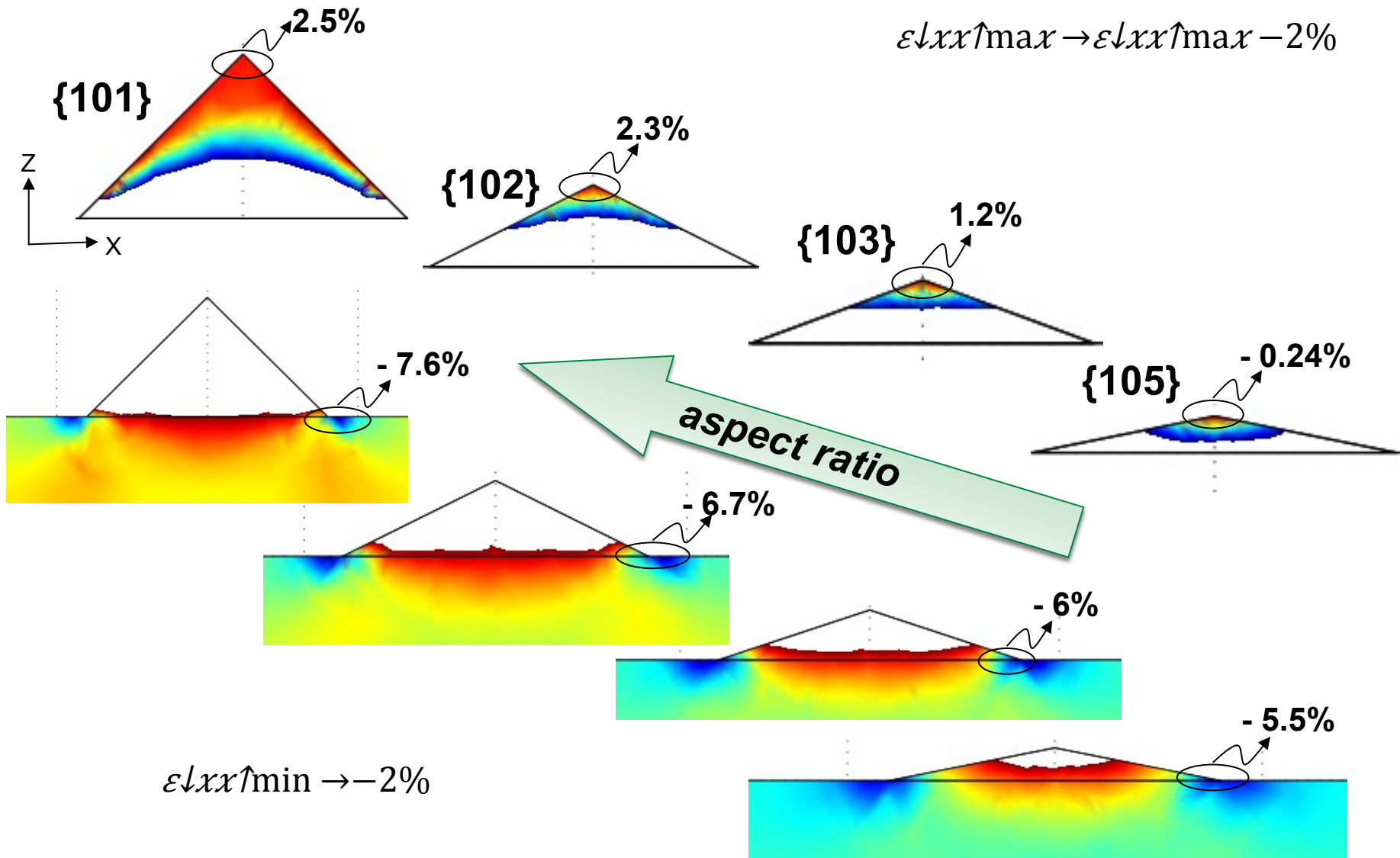


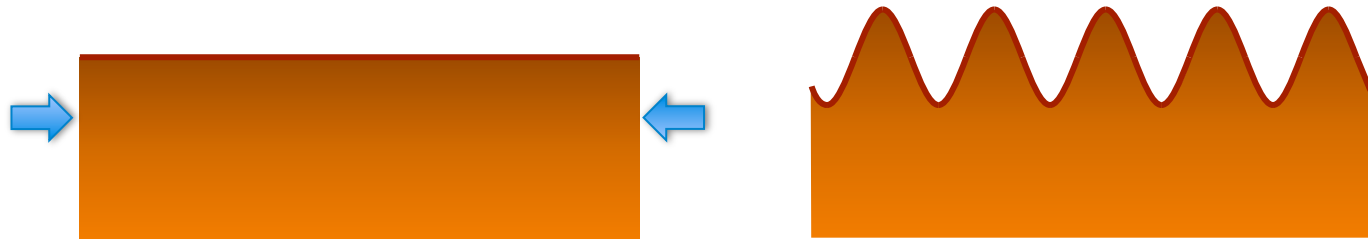
FIG. 7. The same as Fig. 6 for a dome (32 nm, solid black line), a $\{1\ 0\ 3\}$ pyramid (22 nm, solid gray line), and a $\{1\ 0\ 5\}$ pyramid (27 nm, dashed gray line).

P. Raiteri & L. Miglio, *Phys. Rev. B* **66**, 235408 (2002)

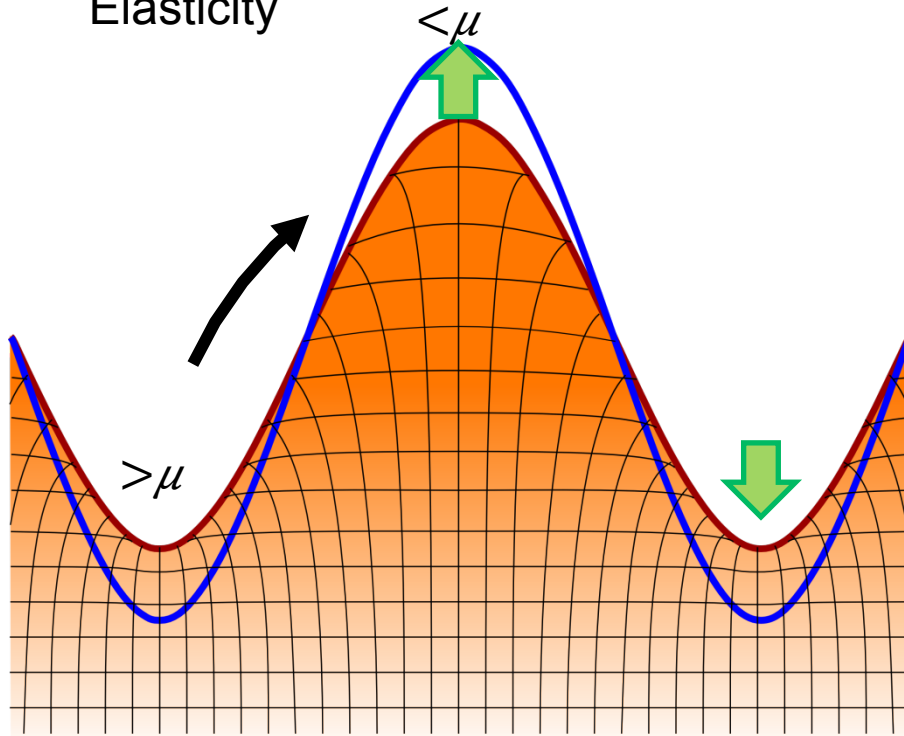
FEM analysis: strain relaxation with a.r.



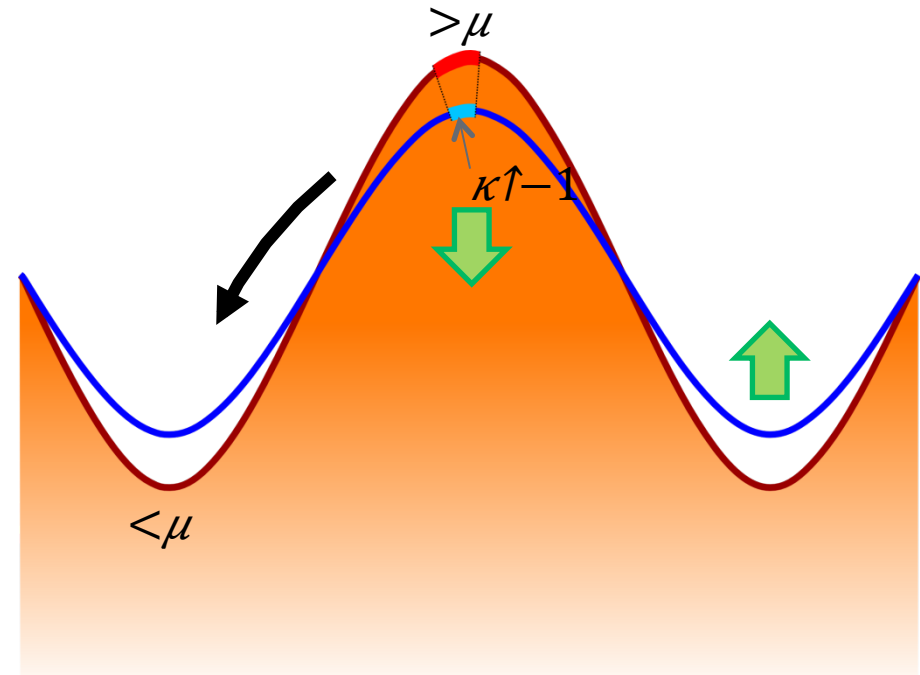
Explaining Island formation by rate equations



Elasticity



Surface energy



Modeling surface diffusion



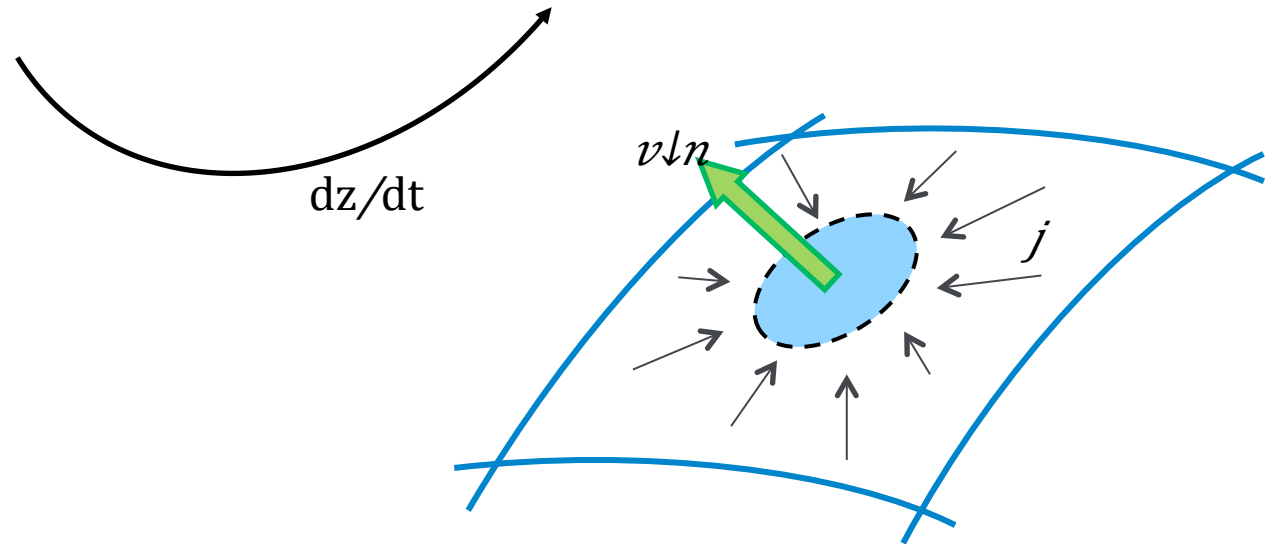
$$G \rightarrow \mu = \delta G$$

Elastic + surface energy

Onsager linear law: $j = -M \nabla \mu$

Continuity equation: $dN/dt = -\nabla \cdot j + \Phi$

$$\rightarrow v \downarrow n = \nabla \cdot [M \nabla \mu] + \Phi$$



No bulk diffusion

B.P. Uberuaga et al., *Phys. Rev. Lett.* **74**, 2441 (2000)

$M \neq 0$ only at the surface

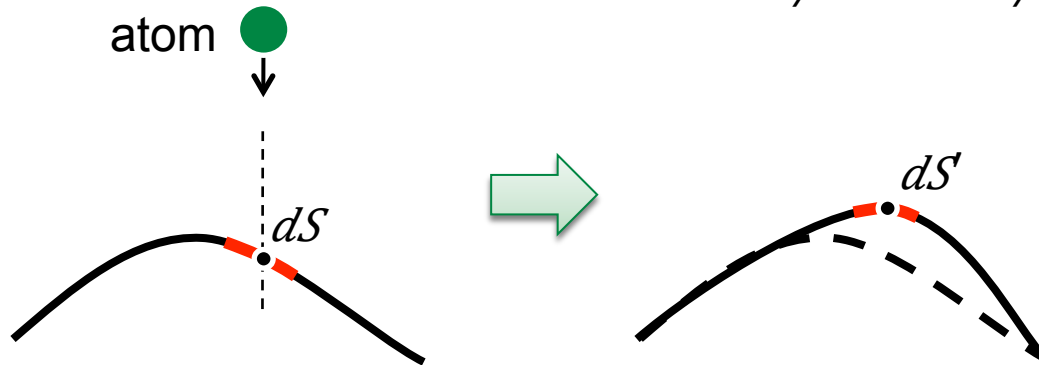
Gradients along the surface $\nabla \rightarrow \nabla \downarrow s$



$$G \downarrow \gamma = \int \Gamma \uparrow \gamma dS$$

γ = surface energy density (Hyp: isotropic)

$$2D: dS = dx / \cos\theta = dx / \sqrt{1 + z'^2}$$



$$\begin{aligned} \mu \downarrow \gamma &= \delta G \downarrow \gamma / \delta z = \gamma \delta / \delta z \left[\int \delta z / \sqrt{1 + z'^2} dx \right] = \\ &= \gamma \left[-z'' / (1 + z'^2)^{3/2} \right] = \gamma \kappa \end{aligned}$$

κ = local curvature (surface element extension)



$$G \downarrow \varepsilon = \int V \uparrow \rho(\varepsilon) dr$$

$\rho = 1/2 \boldsymbol{\sigma} : \boldsymbol{\varepsilon}$ = elastic energy density

$\boldsymbol{\sigma}$ = stress tensor

$\boldsymbol{\varepsilon}$ = strain tensor

$$\mu \downarrow \varepsilon = \rho(\varepsilon)$$

Hyp: isotropic
medium

$$\sigma_{ij} = \lambda \delta_{ij} \sum_k \varepsilon_{kk} + 2\mu (\varepsilon_{ij} - \varepsilon_{ij}^*)$$

$$\rho = \mu \sum_{k,l} \varepsilon_{kl}^2 + \lambda/2 \left[\sum_k \varepsilon_{kk} \right]^2$$

Mechanical equilibrium

$$\nabla \cdot \boldsymbol{\sigma} = 0 \quad (\sum F = 0)$$

$$\boldsymbol{\sigma} \cdot \mathbf{n} = 0 \quad \text{free surfaces}$$



$$G \downarrow \varepsilon = \int V \uparrow \rho(\varepsilon) dr$$

$\rho = 1/2 \boldsymbol{\sigma} : \boldsymbol{\varepsilon}$ = elastic energy density

$\boldsymbol{\sigma}$ = stress tensor

$\boldsymbol{\varepsilon}$ = strain tensor

$$\mu \downarrow \varepsilon = \rho(\varepsilon)$$

Hyp: isotropic medium

$$\sigma_{ij} = \lambda \delta_{ij} \sum_k \varepsilon_{kk} + 2\mu (\varepsilon_{ij} - \varepsilon_{ij}^*)$$

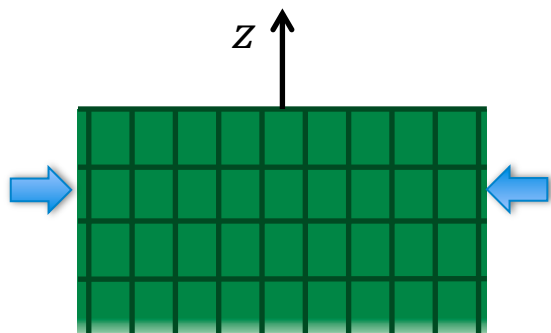
$$\rho = \mu \sum_{k,l} \varepsilon_{kl}^2 + \lambda/2 [\sum_k \varepsilon_{kk}]^2$$

Mechanical equilibrium

$$\nabla \cdot \boldsymbol{\sigma} = 0 \quad (\sum F = 0)$$

$$\boldsymbol{\sigma} \cdot \mathbf{n} = 0 \quad \text{free surfaces}$$

Flat film



$$\boldsymbol{\sigma} \cdot \mathbf{z} = 0 \rightarrow \sigma_{zz} = (\lambda + 2\mu) \varepsilon_{zz} + \lambda \varepsilon_{xx} = 0$$

$$\varepsilon_{zz} = \lambda / (\lambda + 2\mu) \varepsilon_{xx} = \nu / (1 - \nu) \varepsilon_{xx} \quad \boldsymbol{\varepsilon} = \begin{bmatrix} \varepsilon_{xx} & 0 & 0 \\ 0 & \varepsilon_{yy} & 0 \\ 0 & 0 & \varepsilon_{zz} \end{bmatrix}$$

$$\sigma_{xx} = (\lambda + 2\mu) \varepsilon_{xx} + \lambda \varepsilon_{zz} = -E / (1 - \nu^2) \varepsilon_{xx}$$

$$\rho_{f} = 1/2 \boldsymbol{\sigma} : \boldsymbol{\varepsilon} = 1/2 \sigma_{xx} \varepsilon_{xx} = E / (2(1 - \nu^2)) \varepsilon_{xx}^2$$

Elastic energy



$$G \downarrow \varepsilon = \int V \uparrow \rho(\varepsilon) dr$$

$\rho = 1/2 \sigma \cdot \varepsilon$ = elastic energy density

σ = stress tensor

ε = strain tensor

$$\mu \downarrow \varepsilon = \rho(\varepsilon)$$

Hyp: isotropic medium



$$\sigma_{\downarrow ij} = \lambda \delta_{\downarrow ij} \sum k \uparrow (\varepsilon_{\downarrow kk} - \varepsilon_{\downarrow kk}^*) + 2\mu (\varepsilon_{\downarrow ij} - \varepsilon_{\downarrow ij}^*)$$

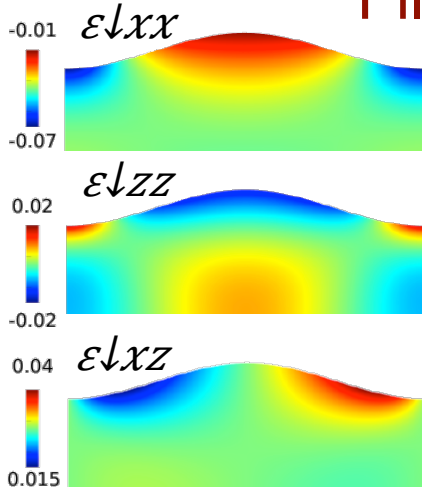
$$\rho = \mu \sum k \uparrow \varepsilon_{\downarrow kk}^2 + 2\mu \sum k, l \uparrow \varepsilon_{\downarrow kl}^2 + \lambda/2 [\sum k \uparrow \varepsilon_{\downarrow kk}]^2$$

Mechanical equilibrium

$$\nabla \cdot \sigma = 0 \quad (\sum F = 0)$$

$$\sigma \cdot n = 0 \quad \text{free surfaces}$$

Film perturbed by a cosine $z(x) = A \cos(qx)$



$$\sigma_{\downarrow xx} = \sigma_{\downarrow 0} [1 - A(q^2 z - 2q) e^{\downarrow -qz} \cos(qx)]$$

$$\sigma_{\downarrow zz} = -\sigma_{\downarrow 0} A q^2 z e^{\downarrow -qz} \cos(qx)$$

$$\sigma_{\downarrow xz} = -\sigma_{\downarrow 0} A q (1 - qz) e^{\downarrow -qz} \sin(qx)$$

R.J. Asaro & W.A. Tiller, *Metall. Trans.* **3**, 1789 (1972)

D.J. Srolovitz, *Acta Metal.* **37**, 621 (1989)

At the surface: $\varepsilon_{\downarrow xx}(x) = -\varepsilon_{\downarrow 0} [1 - 2qA$

$$\rho = 1/2 \sigma \cdot \varepsilon = 1/2 \sigma_{\downarrow xx} \varepsilon_{\downarrow xx} = \rho_{\downarrow f} [1 - 4qA \cos(qx) + 4q^2 A^2 \cos^2(qx)]$$

Asaro-Tiller-Grinfeld instability



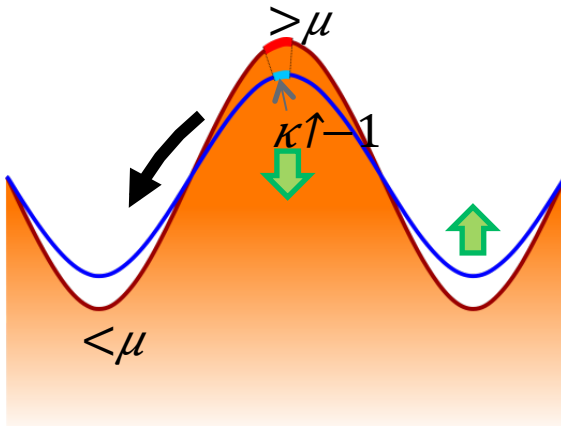
R.J. Asaro & W.A. Tiller, *Metall. Trans.* **3**, 1789 (1972)
 M.A. Grinfeld, *J. Nonlinear Sci.* **3**, 35 (1993)

Perturbation: $z(x) = A \cos(qx)$

Surface energy contribution

$$\mu \downarrow \gamma = \gamma \kappa = \gamma [-z'' / (1+z'^2)^{3/2}]$$

$$\rightarrow \gamma [-z''] = \gamma q^2 A \cos(qx) = \gamma q^2 z(x)$$

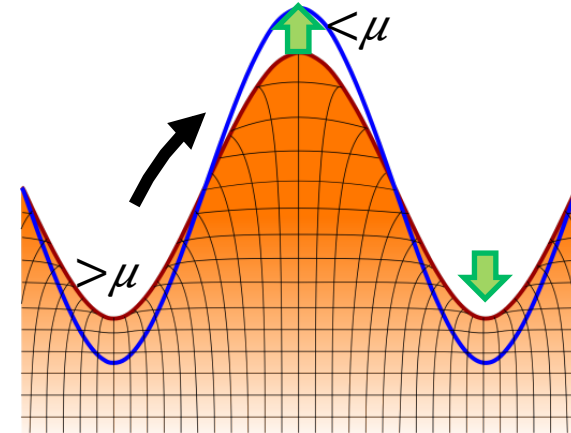


+

Elastic energy contribution

$$\epsilon_{xx}(x) = -\epsilon_0 [1 - 2qz(x)]$$

$$\mu \downarrow \epsilon = \rho \downarrow f [1 - 4qz(x) + 4q^2 z^2(x)] \rightarrow \rho \downarrow f [1 - 4qz(x)]$$



$$v \downarrow n = \nabla \cdot [M \nabla \mu]$$

$$\rightarrow dz/dt = M \partial^2 \mu / \partial x^2 = M [-4\rho \downarrow f q + \gamma q^2] \partial^2 / \partial x^2 [A \cos(qx)] = M [q \downarrow c q^3 - q^4] z(x)$$

$$z(t) = e^{\uparrow M [q \downarrow c q^3 - \gamma q^4] t} A \cos(qx)$$

$$q \downarrow c = 4\rho \downarrow f / \gamma$$

Asaro-Tiller-Grinfeld instability



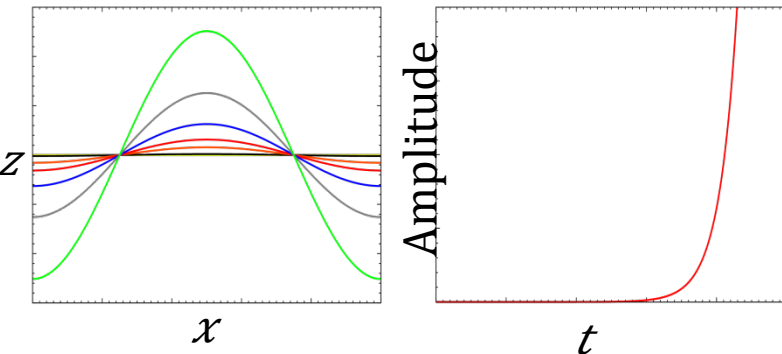
$$z(t) = e^{\uparrow} M [q \downarrow c \ q \uparrow 3 \ -q \uparrow 4 \] t A \cos(qx) = e^{\uparrow} t / \tau(q) A \cos(qx)$$

$$q \downarrow c = 4 \rho \downarrow f / \dots$$

$q > q \downarrow c \rightarrow$ flat film is stable

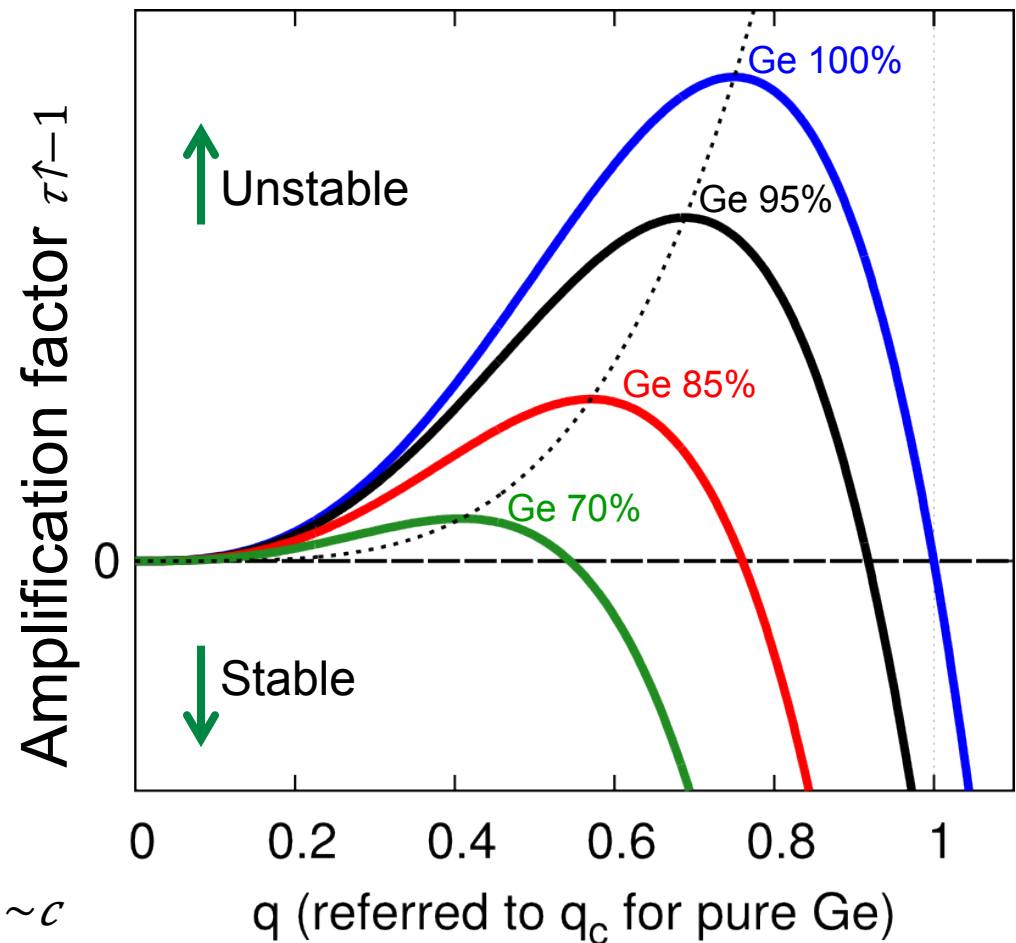
$q < q \downarrow c \rightarrow$ flat film is unstable (amplitude grows indefinitely)

$$q \downarrow max = 3/4 \ q \downarrow c$$



c (% Ge)	$\lambda \downarrow max = 2\pi / q \downarrow max$ (nm)
100	14
95	16
85	20
70	30
50	58
$\rightarrow 0$	$\rightarrow \infty$

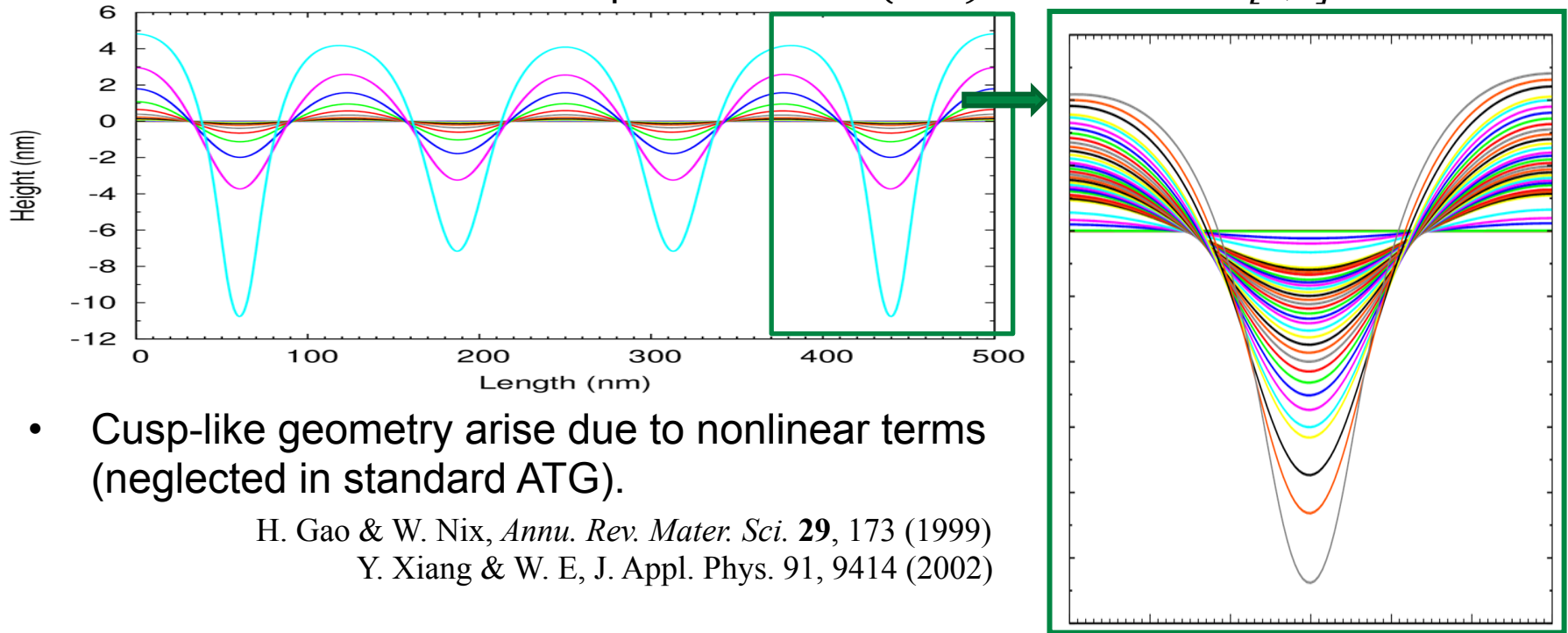
$$\epsilon \downarrow 0 \sim c$$





Arbitrary profiles can always be decomposed as Fourier series of cosine perturbations $\rightarrow \lambda \downarrow \text{max}$ dominates

Random initial perturbation: $z(t=0) = 10^{-5} \text{ rand}[0,1]$



- Cusp-like geometry arise due to nonlinear terms (neglected in standard ATG).

H. Gao & W. Nix, *Annu. Rev. Mater. Sci.* **29**, 173 (1999)

Y. Xiang & W. E, *J. Appl. Phys.* **91**, 9414 (2002)

- For high aspect ratio divergency at the trenches

Interaction with the substrate



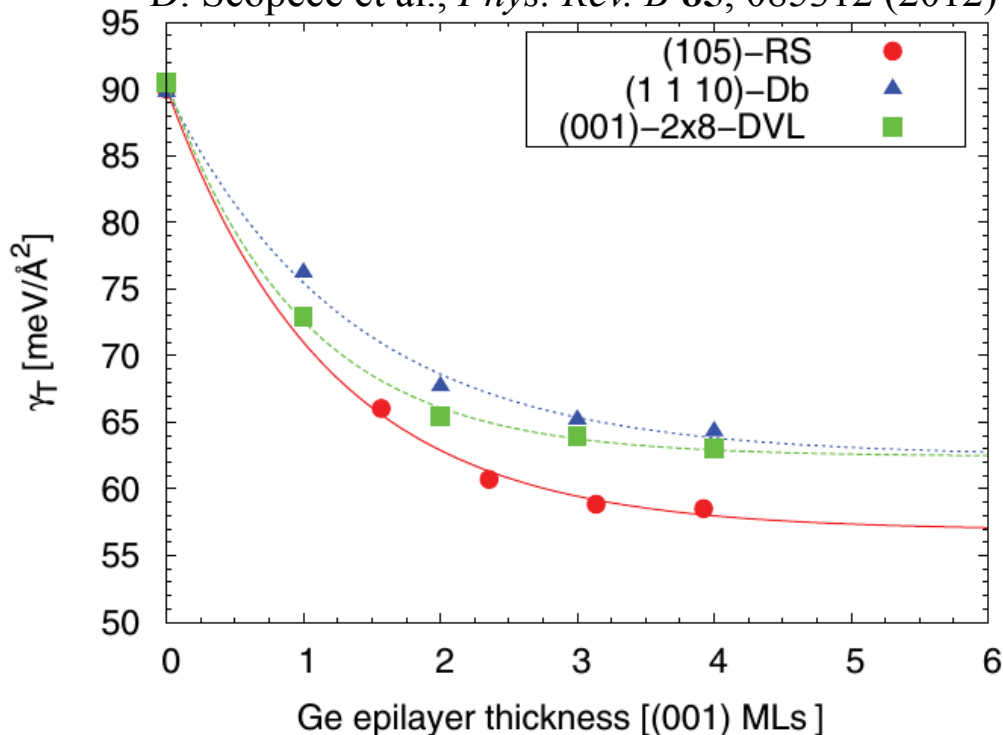
Wetting effects

Composition effects



G.-H. Lu & F. Liu, *Phys. Rev. Lett.* **94**, 176103 (2005)

D. Scopece et al., *Phys. Rev. B* **85**, 085312 (2012)



$$\gamma(h) = \gamma_0 [1 + c \exp(-h/\delta)]$$

$$\gamma_0 = 60 \text{ meV/Å}^2$$

$$c = 0.45$$

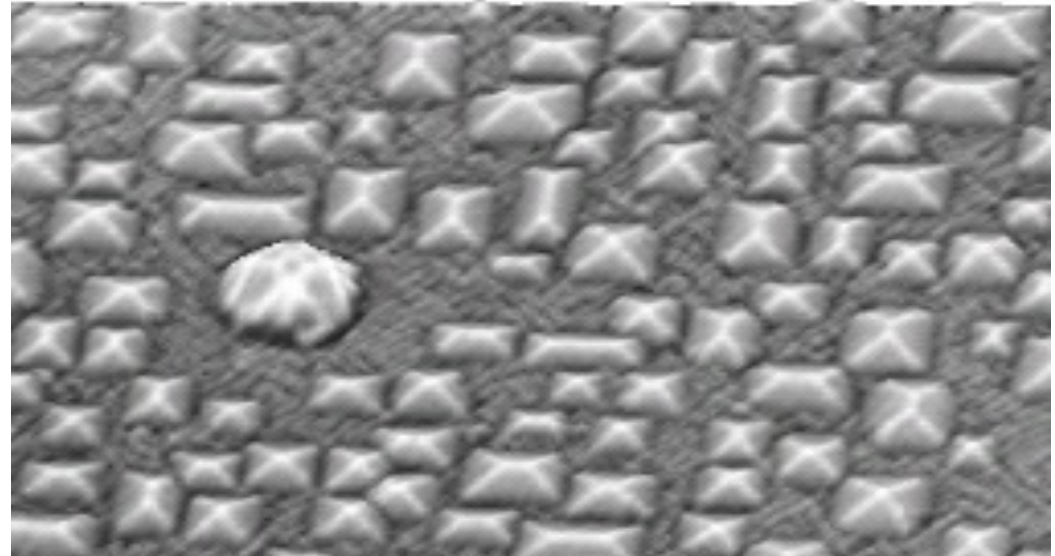
$$\delta = 1.21 ML = 0.177 \text{ nm}$$

FIG. 4. (Color online) DFT-LDA results for $\gamma_T(N_{\text{Ge}})$, i.e., the dependence of the surface energy on the Ge epilayer thickness. Points are the direct calculations; lines are the interpolation given by Eq. (4). See discussion at Sec. III A.

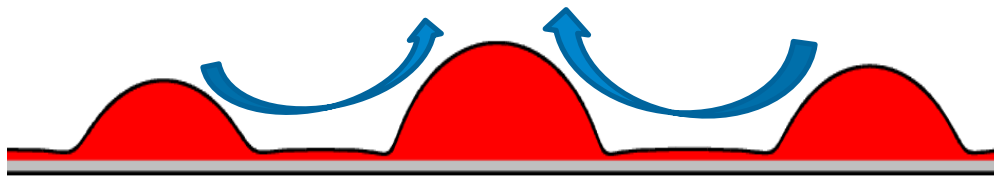
Ostwald ripening: the big fish eats the smaller



40 nm



A. Rastelli, private communication and Phd. thesis

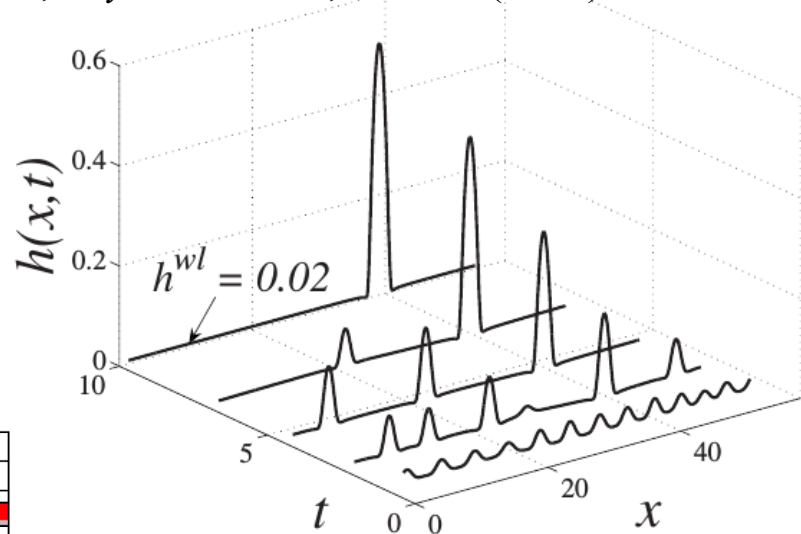
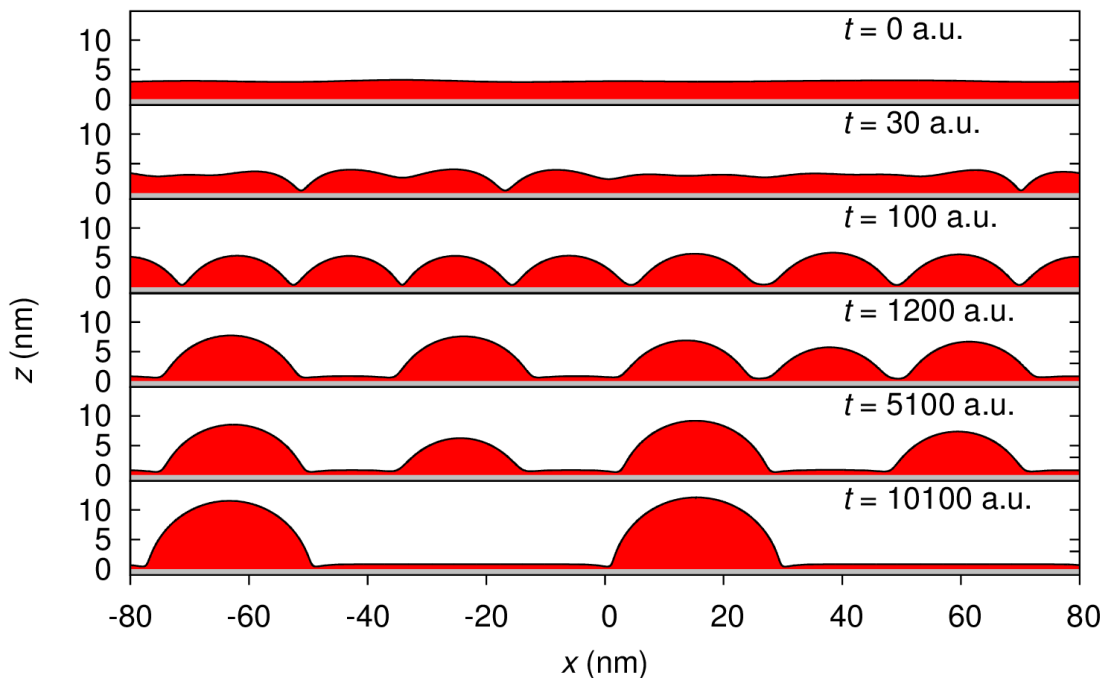


Pure Ge film: wetting effects & coarsening



J.-N. Aqua et al., *Phys. Rev. B* **76**, 165319 (2007)

- Trenches stop digging at the WL
- Progressive coarsening



M. Albani, *Master Thesis* (2015)



- Lower elastic energy in volume
- Different surface energies and areas of facets

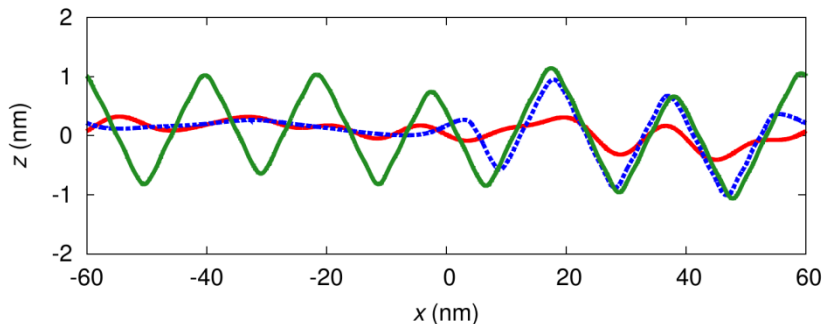
Evolution model including surface anisotropy:

$$\gamma = \gamma(\mathbf{n}) \quad \mathbf{n} = \text{surface orientation}$$

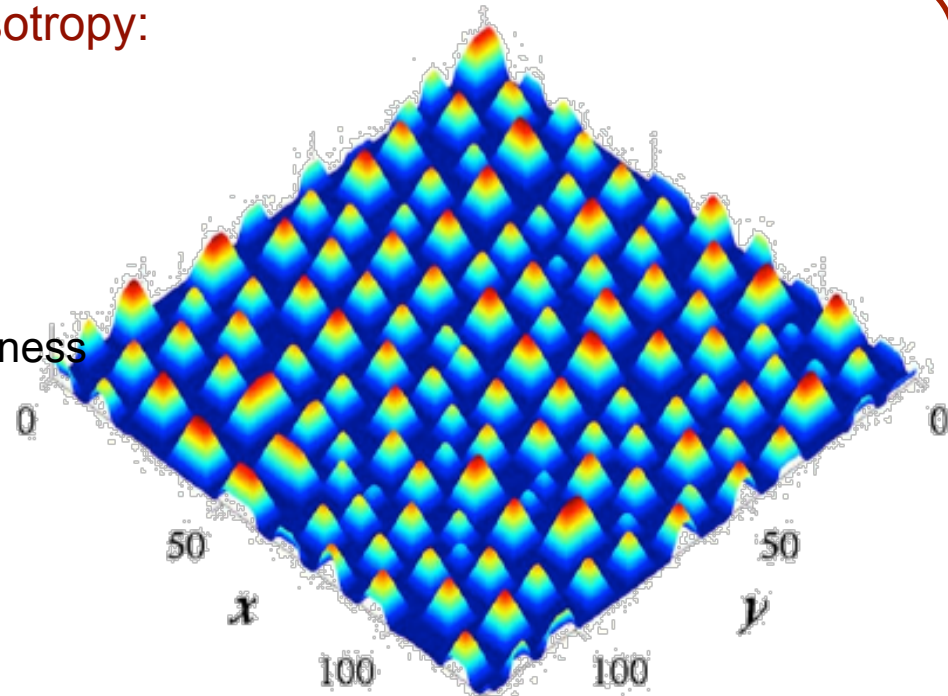
$$\text{In 2D: } \gamma = \gamma(\theta)$$

$$\mu \downarrow \gamma = \kappa (\gamma + d^2 \gamma / d\theta^2)$$

$$\gamma + d^2 \gamma / d\theta^2 = \text{surface stiffness}$$



M. Albani, *Master Thesis* (2015)

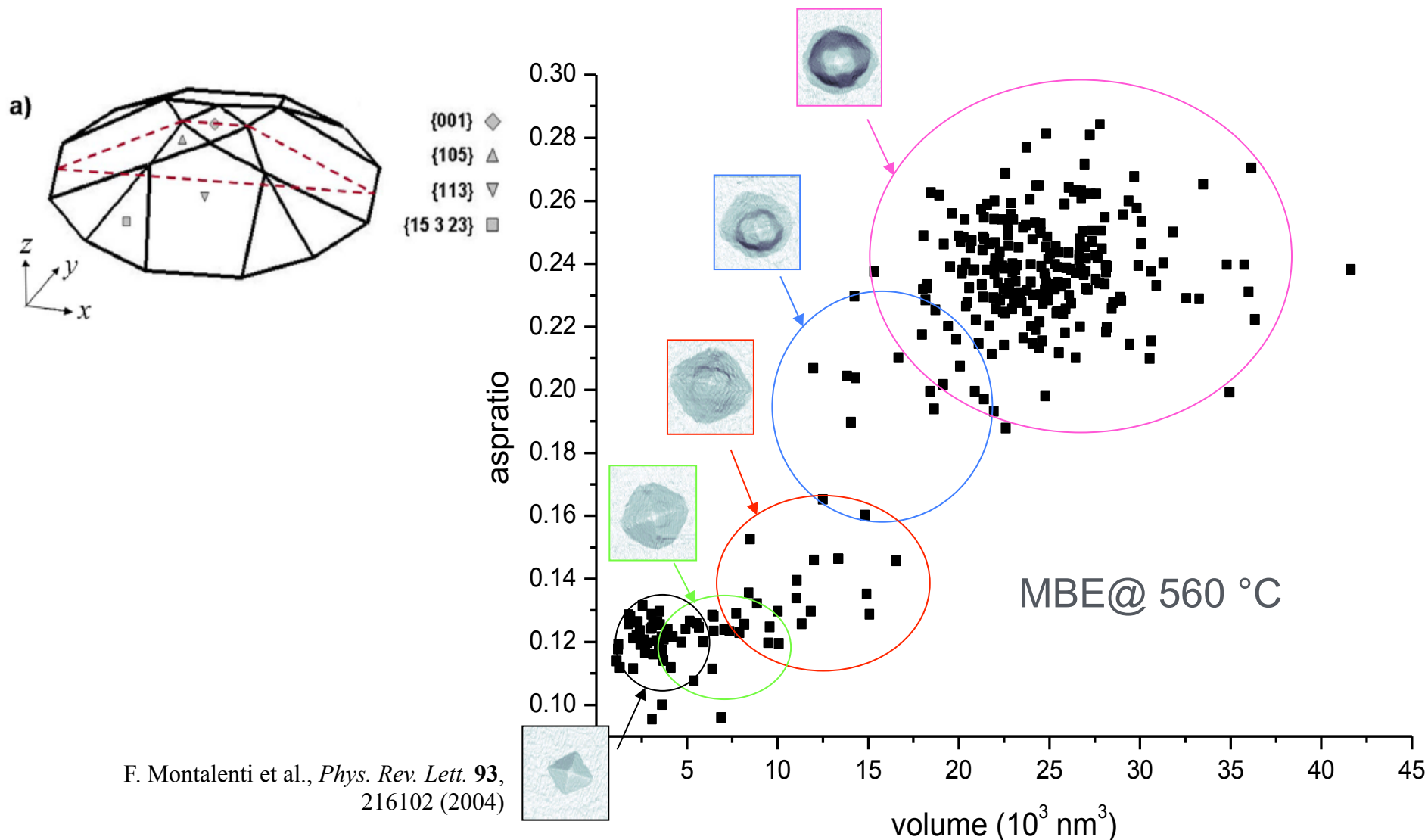


J.-N. Aqua & T. Frisch, *Phys. Rev. B*
82, 085322 (2010)

Morphology evolution to higher a.r. with V



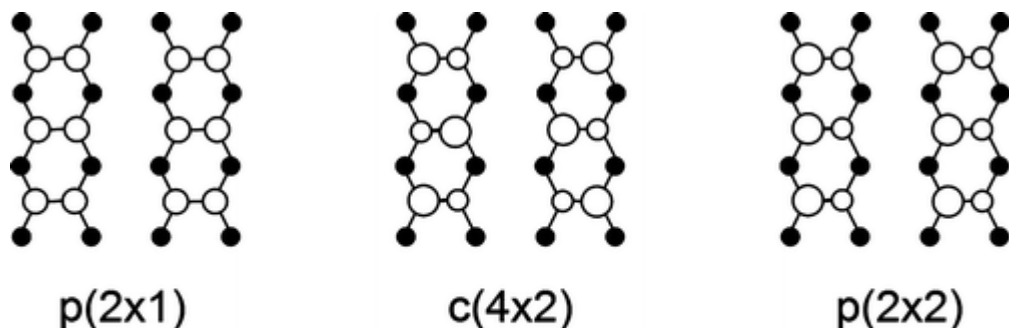
During deposition islands **grow in volume** and **aspect ratio increase** in order to maximize the elastic relaxation: **facetting** minimizes the surface energy




Ge(001) surface with strain: role of dimers



Dimer pairs provide different reconstructions. Surface energy change with strain because **the dimers are tensile strained**.



 Loscutoff PW, Bent SF. 2006.
Annu. Rev. Phys. Chem. 57:467–95

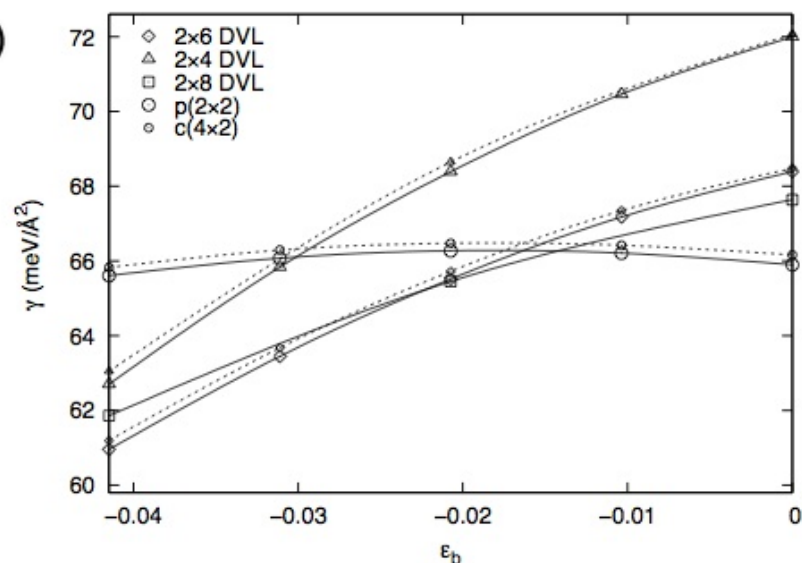
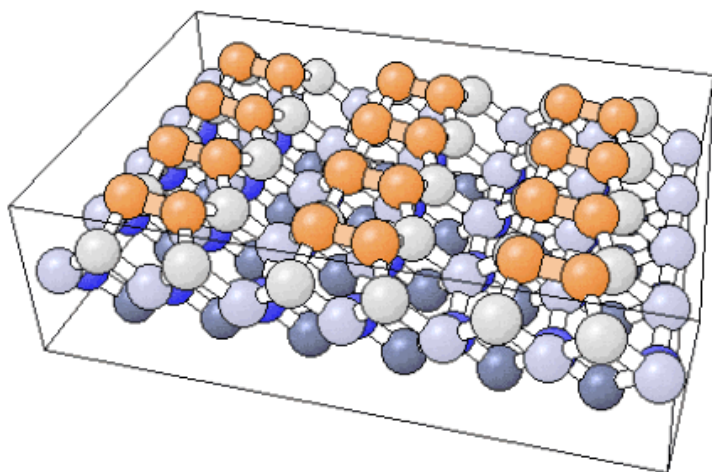


Figure 4.12. Ge (001) surface excess energy as a function of biaxial strain state, $\gamma_{\Theta}(\epsilon_b)$ for the $p(2 \times 2)$ -based (solid lines, larger symbols) 2×4 , 2×6 , and 2×8 and $c(4 \times 2)$ -based (dashed lines, smaller symbols) 4×4 and 4×6 DVL reconstructions, as well as the non-DVL $c(4 \times 2)$ and $p(2 \times 2)$ reconstructions.

The popular Ge(105) surface



Reconstruction provide a rebonded step configuration suppressing dangling bonds: low surface energy, especially for compressive strain

D.B. Migas et al., *Surf. Sci.* **556**, 121 (2004)

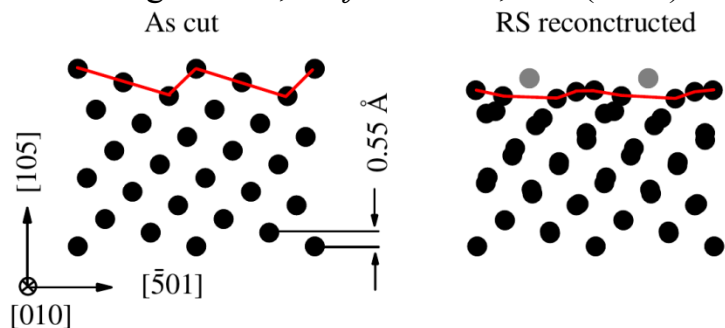


Fig. 2. Lateral view of the (1 0 5) surface in the case of “as cut” (left panel) and the RS reconstruction (right panel) as optimized by ab initio calculations for $a_{\parallel} = a_{\text{Ge}}$. Solid lines are used to sketch the average surface profiles. The distance between two adjacent (1 0 5) layers is also indicated. The topmost atoms for the (1 0 5)RS are in gray.

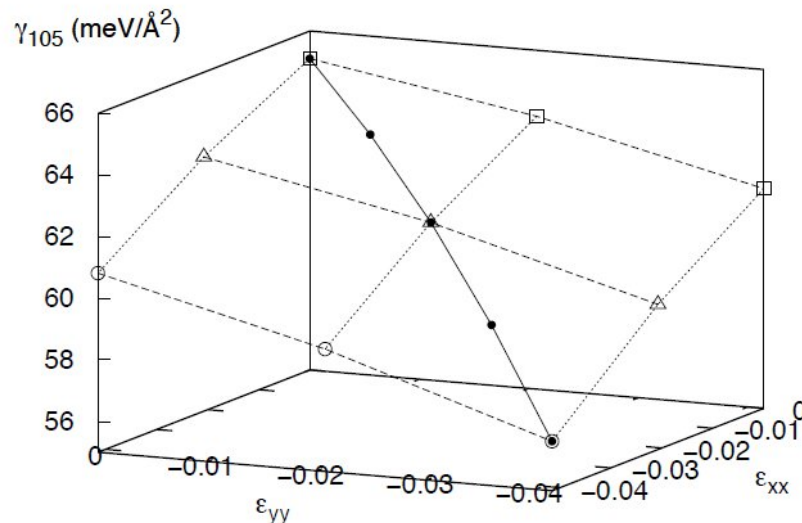
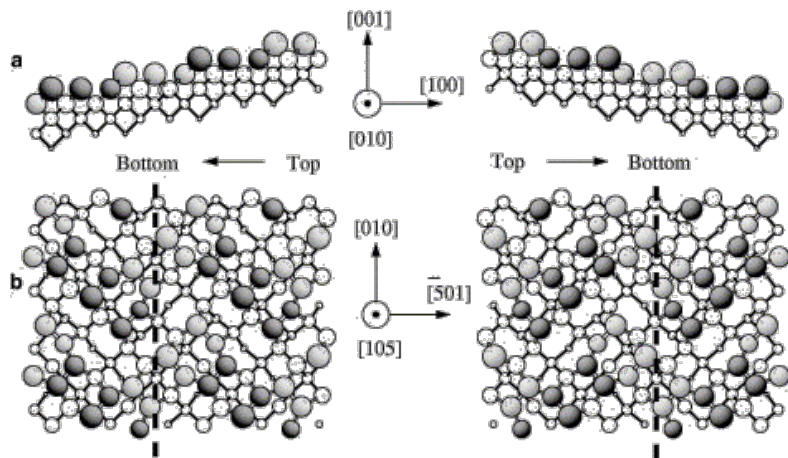


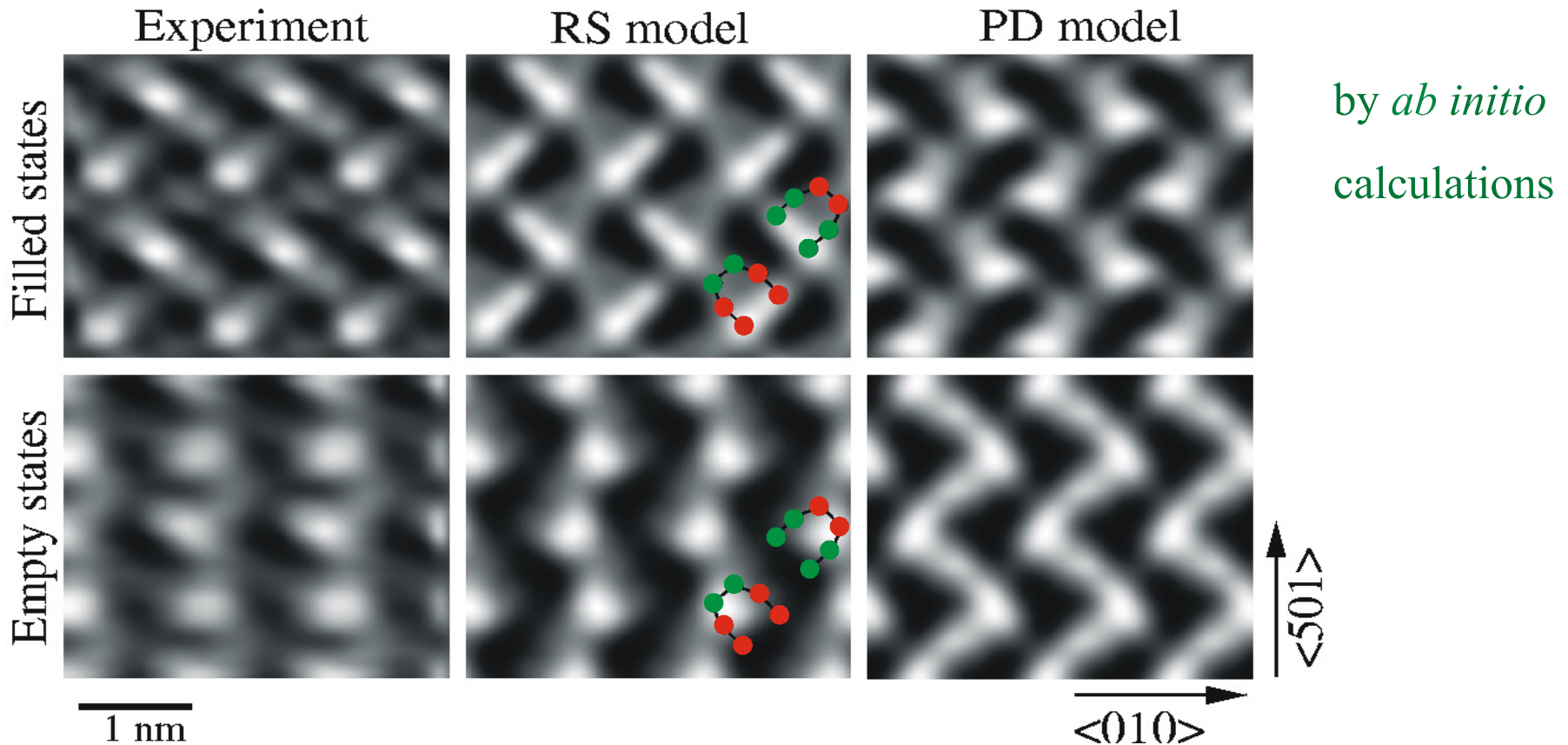
Figure 4.22. Ge (105) RS surface energy, γ_{105} , as a function of strain state, ϵ_{xx} and ϵ_{yy} , for \hat{y} along the [015] direction and \hat{x} along [100]. Dotted and dashed curves show surface energy for set of strains with constant ϵ_{xx} and ϵ_{yy} , respectively. Solid curve shows surface energy for ϵ_b .



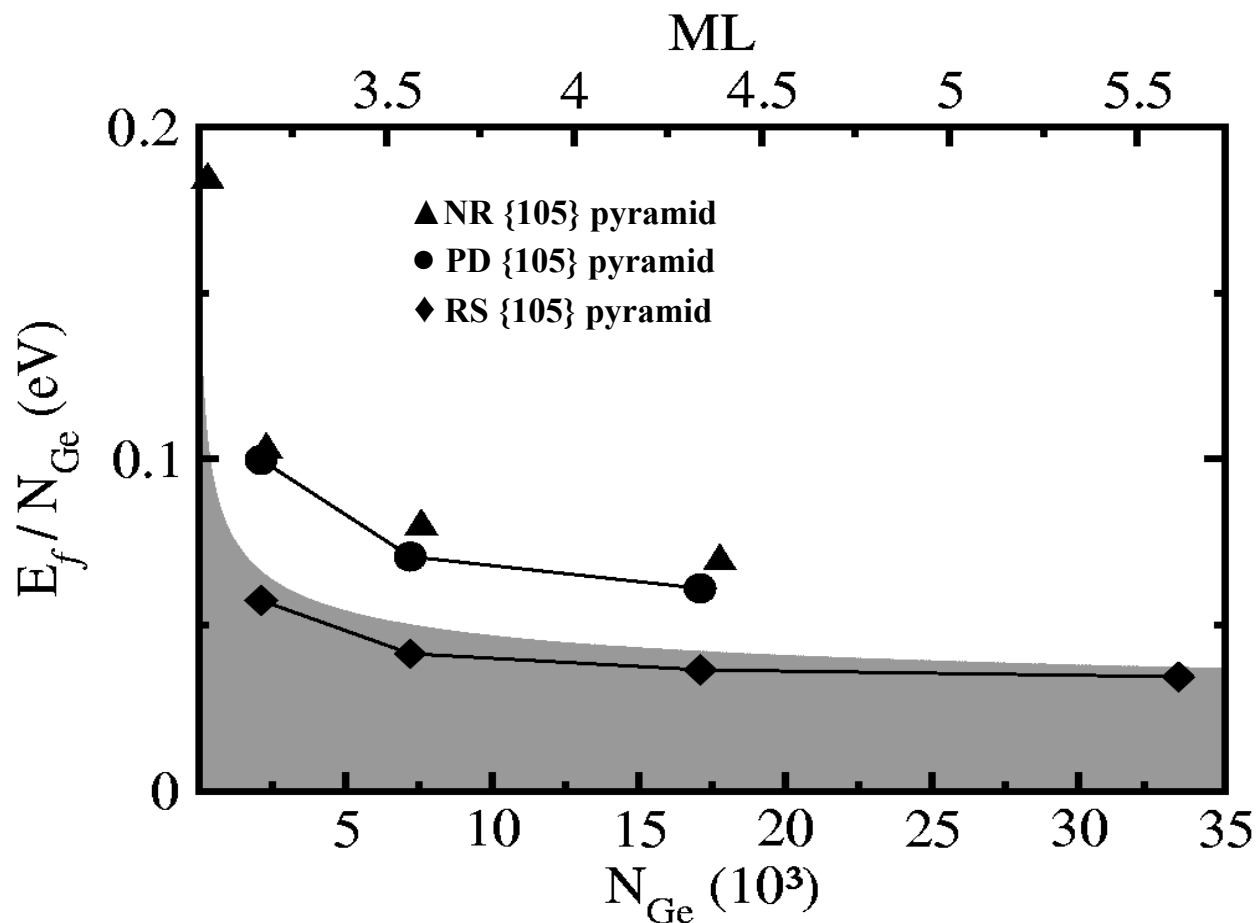
The Rebonded Step reconstruction



Measured and simulated STM images



P. Raiteri, D.B. Migas, L. Miglio, A. Rastelli, H. von Känel, *Phys. Rev. Lett.* **88**, 256103 (2002)



P. Raiteri, D.B. Migas, L. Miglio, A. Rastelli, H. von Känel, *Phys. Rev. Lett.* 88, 256103 (2002)



N Ge layers



+



1 layer of Ge
height: h_1

=

$N+1$ Ge layers



or

N Ge layers
+ island



?



and



have the same number of atoms

WL thickness vs Island formation



N Ge layers
+ island



Middle layers behave as
Ge-bulk, tetragonally strained due to
Si/Ge lattice mismatch

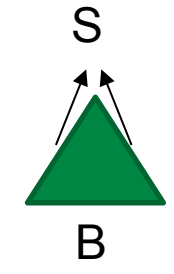
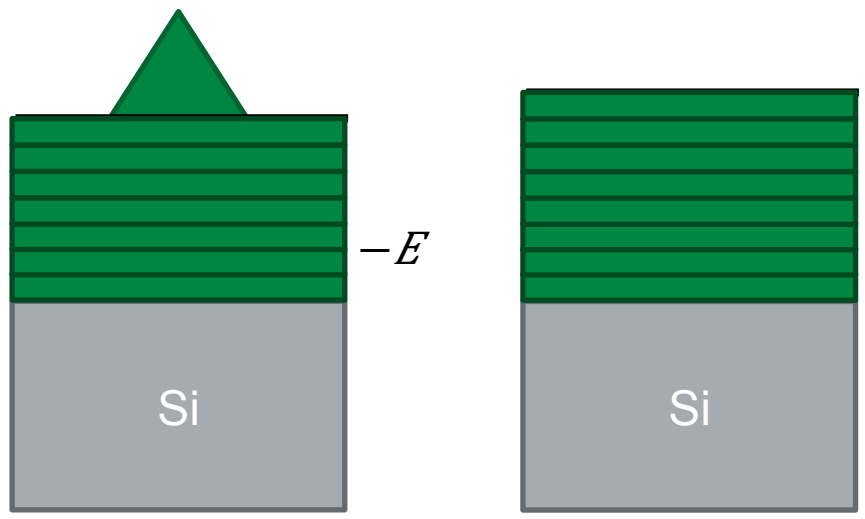
If I add 1 layer (keeping the same surface reconstruction), the elastic-energy difference between the $(N+1)$ -layer and the N layer structure is simply:

$$\Delta E = \rho \hat{t} \times V$$

where $\rho \hat{t}$ is the (well-known) volumetric density of elastic energy in tetragonally strained Ge



$$\Delta E = E$$



$$\rho_{\text{lis}} - \rho_{\text{lt}} < 0$$

for any (reasonable) shape

$$= V(\rho_{\text{lis}} - \rho_{\text{lt}}) + S\gamma_{\text{lis}} - B\gamma_{\text{lt}}$$

At sufficiently large V the island configuration is always favored. But at small volumes we have the flat wetting layer (3 monolayers in thickness).

The nucleation shape is determined by surface energies. Surface energy of the 105 pyramids always lower than the one of domes (multi-facetted).

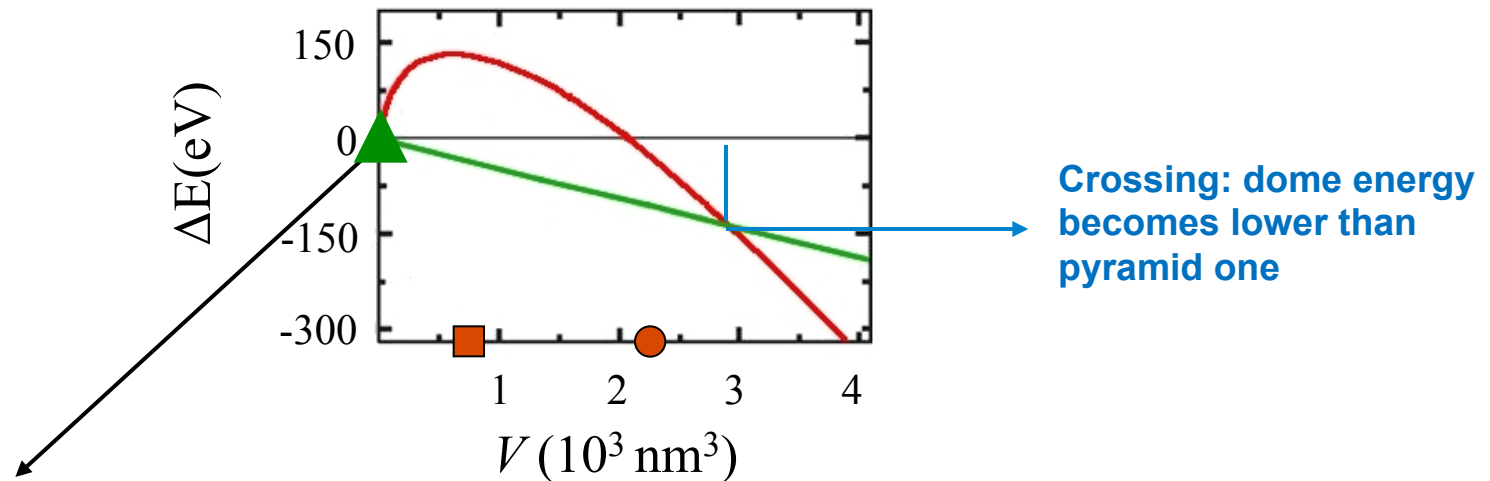
Energy density of domes always smaller than the one of 105 pyramids. First are expected pyramids, at larger V are expected domes.

Transition between pyramids and domes



Results for wetting layer thickness = 4 monolayers

We take the 105 surface energy for the pyramids ($0.52 \text{ eV}/\text{Å}^2$) and an average of $0.65 \text{ eV}/\text{Å}^2$ for the larger multi-faceted B of domes (113), (15 3 23), (105)



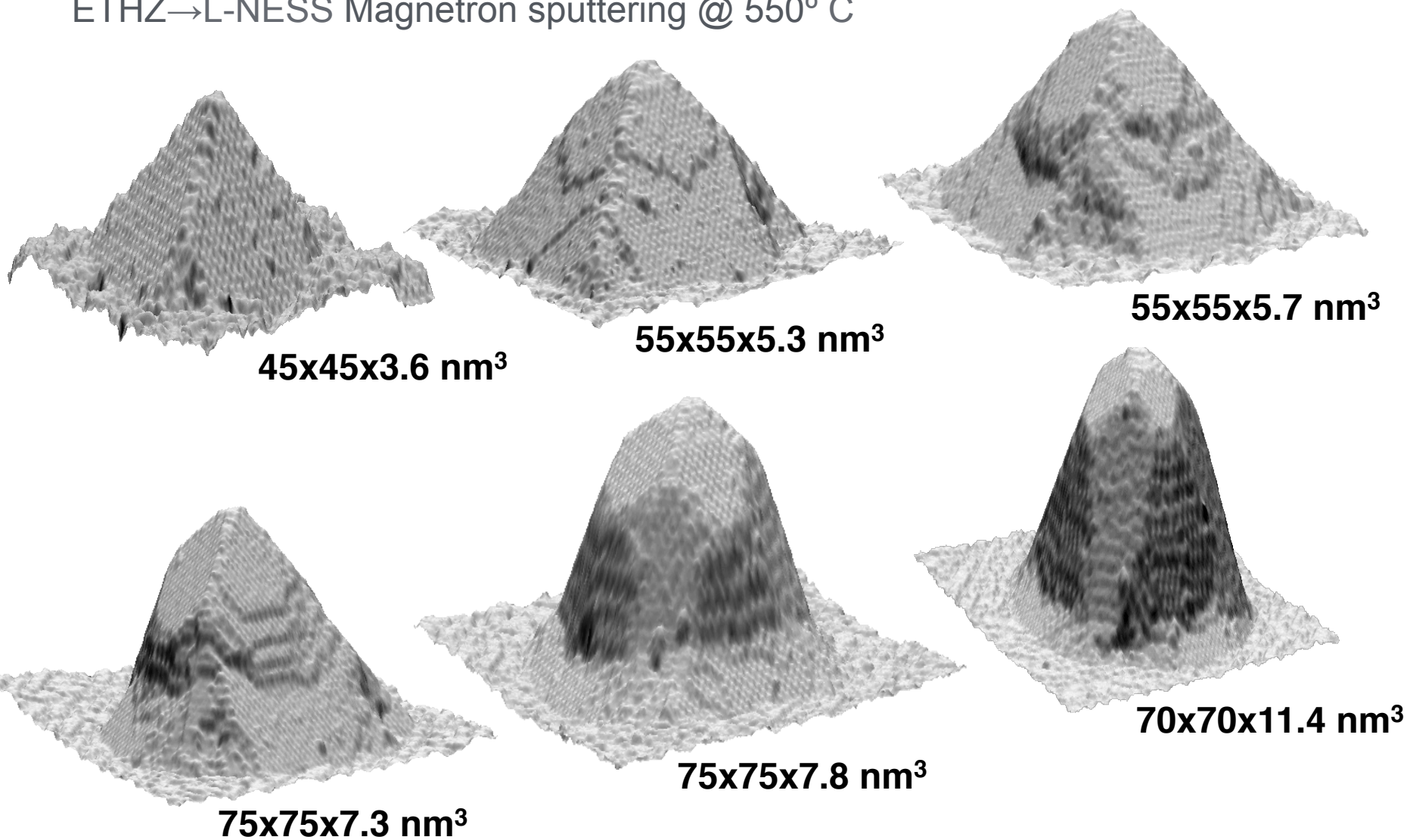
Volume above which pyramids become more stable than the WL.
At ML=4 this volume is vanishing small (barrier less formation).

By increasing deposition the volumes get larger and the dome configuration is more energetically convenient. Real transition via surface diffusion occurs when the volumetric chemical potential is lower (steeper slope of the dome curve).

How the transition takes place at atomic size



ETHZ → L-NESS Magnetron sputtering @ 550° C

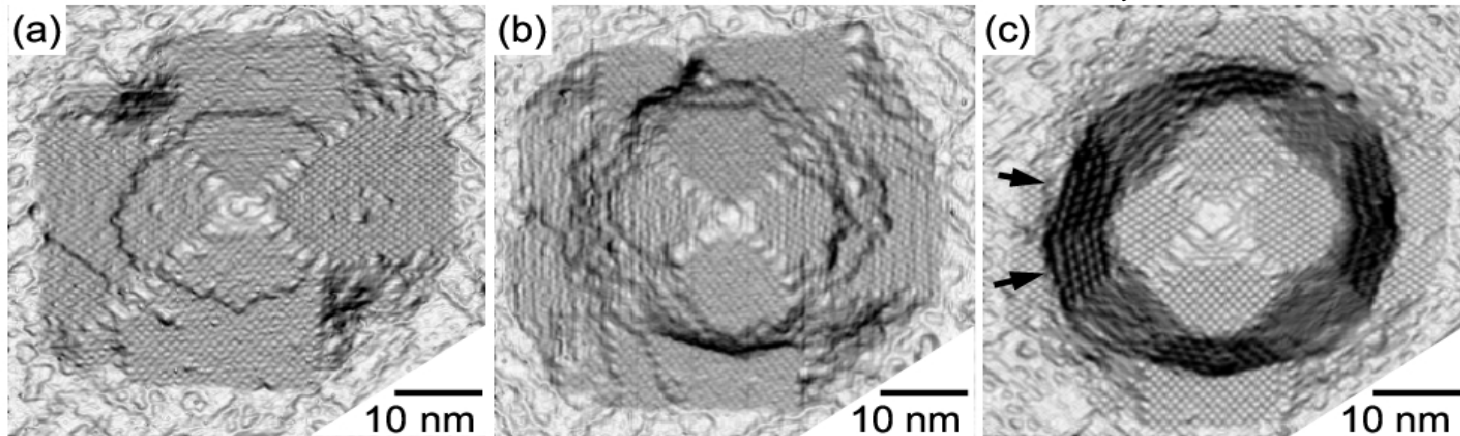


F. Montalenti et al. *Phys. Rev. Lett.* 93, 216102 (2004)

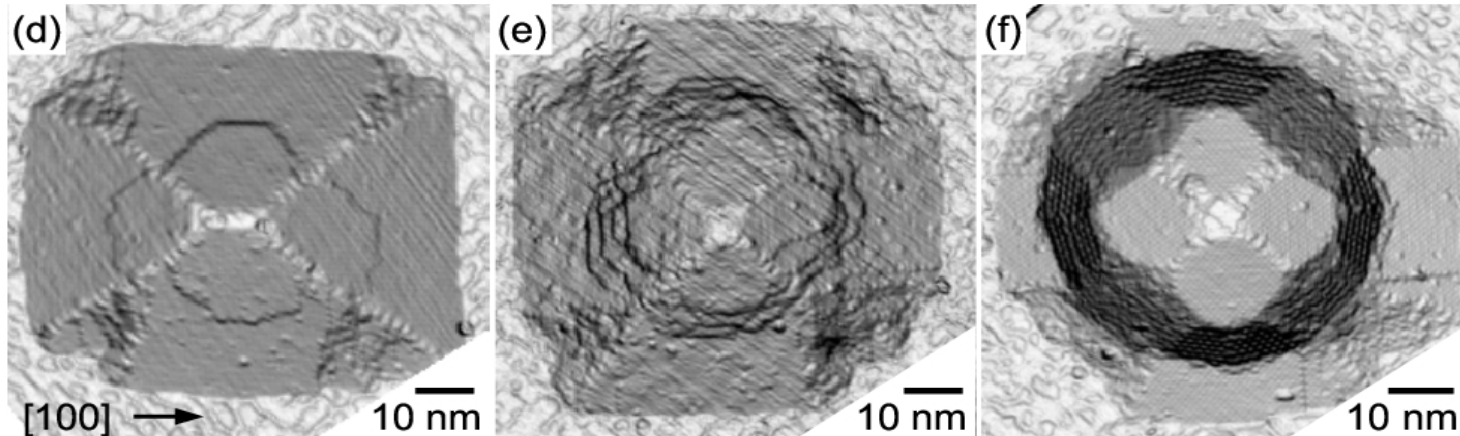


F. Montalenti et al. *Phys. Rev. Lett.* **93**, 216102 (2004)

Exp_A



Exp_B



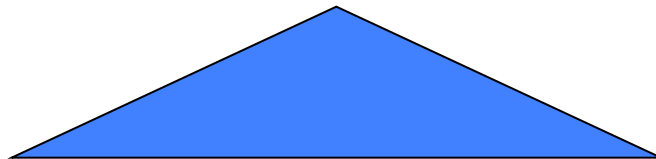
Exp_A: magnetron sputtering. 7ML Ge @ 550 °C; Flux: 0.3 ML/s

Exp_B: MBE. 6ML Ge @ 560 °C; Flux 0.04 ML/s + 10 min. anneal.

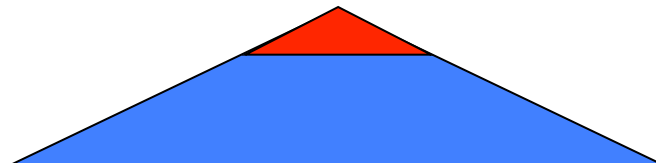
Small pyramids: proposed growth mode



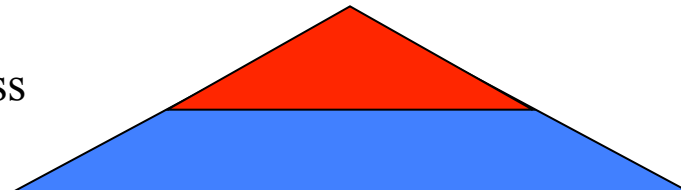
1) Flat layer with adatoms fast diffusing across the facet



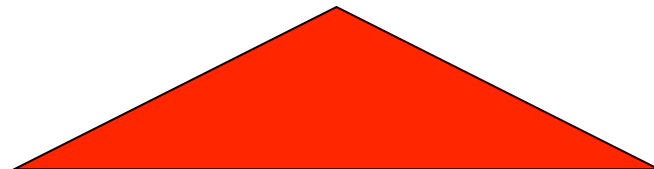
2) Next-layer nucleation starts on top



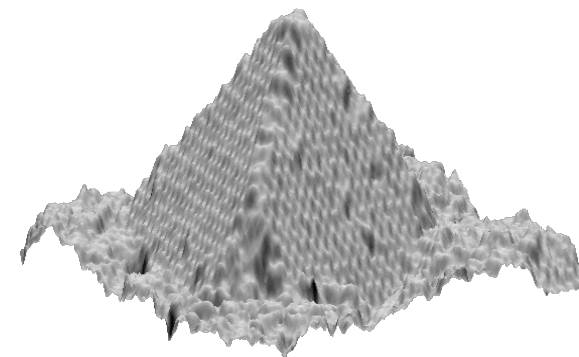
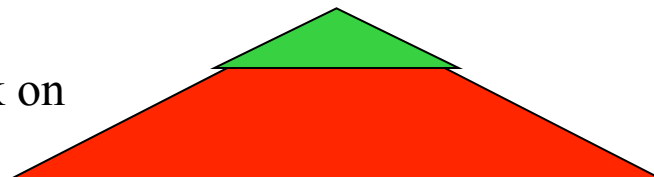
3) A fast step-flow process takes place



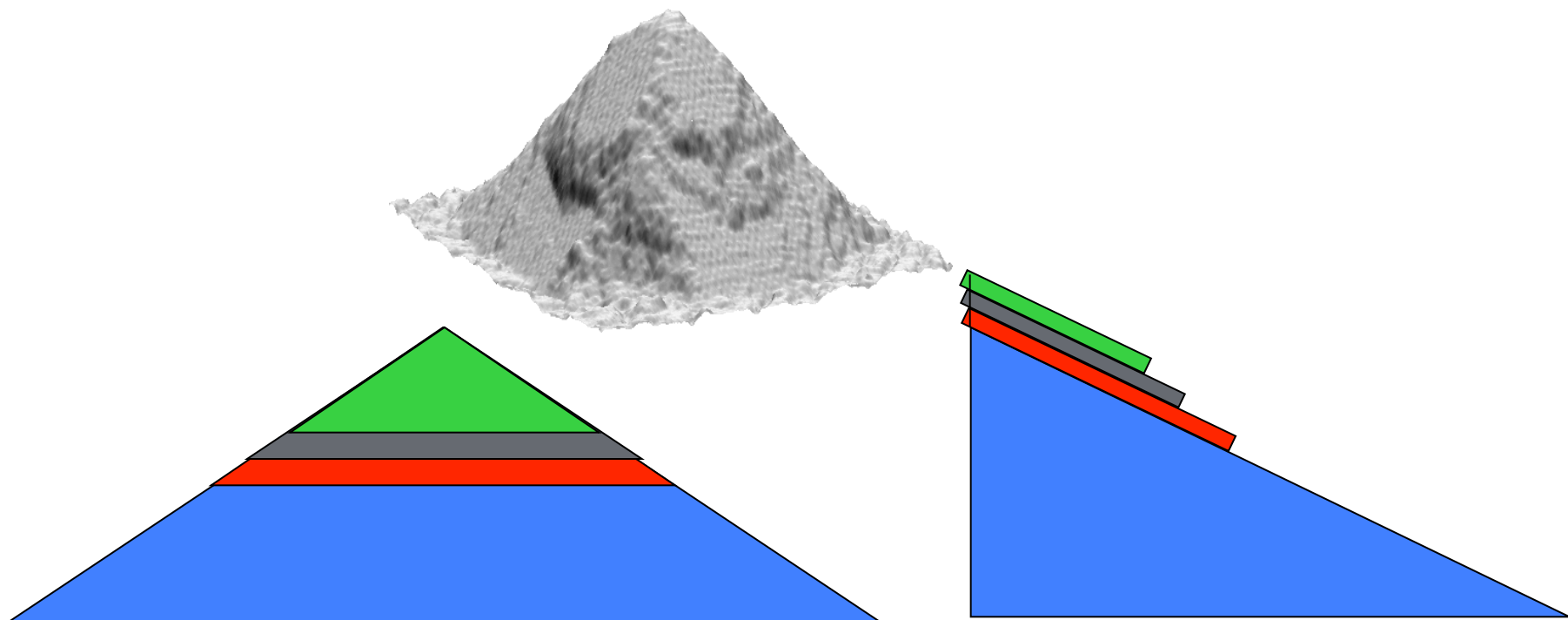
4) The layer is completed



5) The process starts back on the new layer



Step propagation is extremely fast, STM images report flat facets

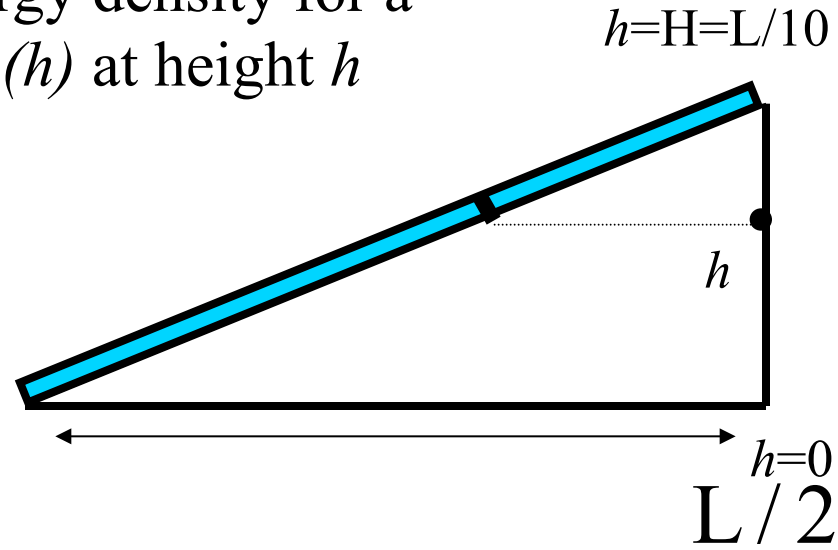
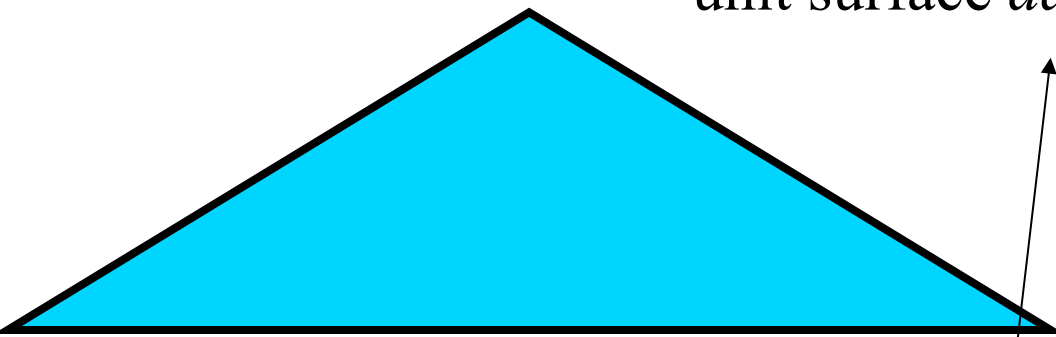


A trade off between the cost of generating steps and the gain in accumulating at the (relaxed) top? An estimation is needed



State S_0

Formation energy density for a unit surface $da(h)$ at height h

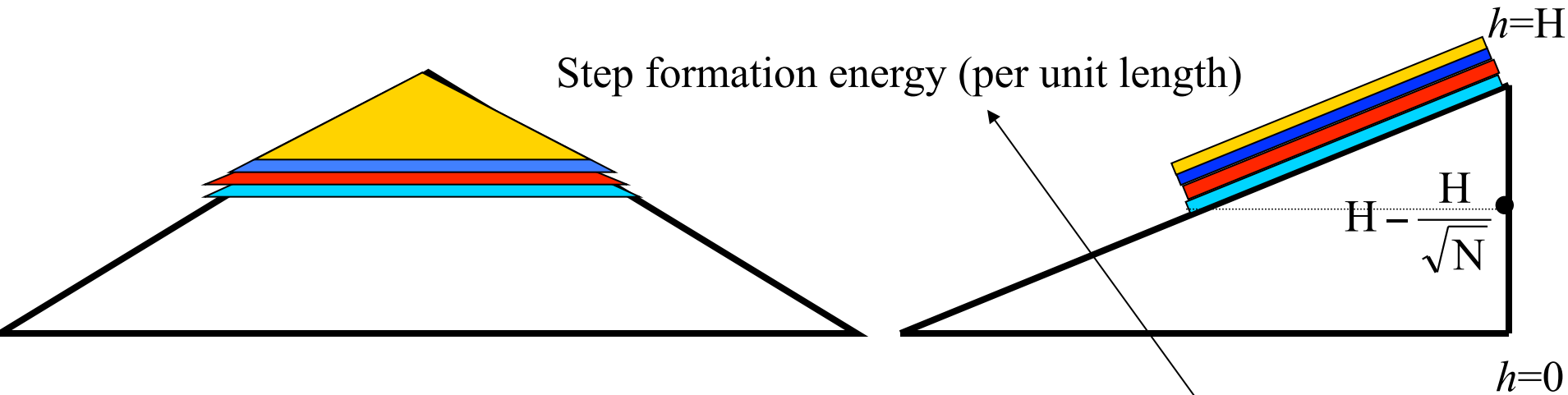


$$H \equiv L/10$$

$$E_{S_0} = \int_0^H E_{add.}(h) da(h)$$



State S_N the same atoms of state S_0
now form N steps bunched together

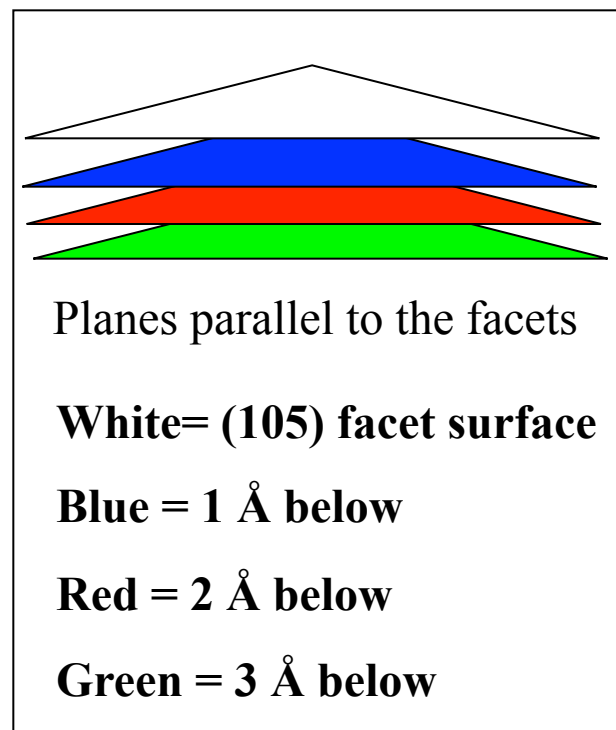
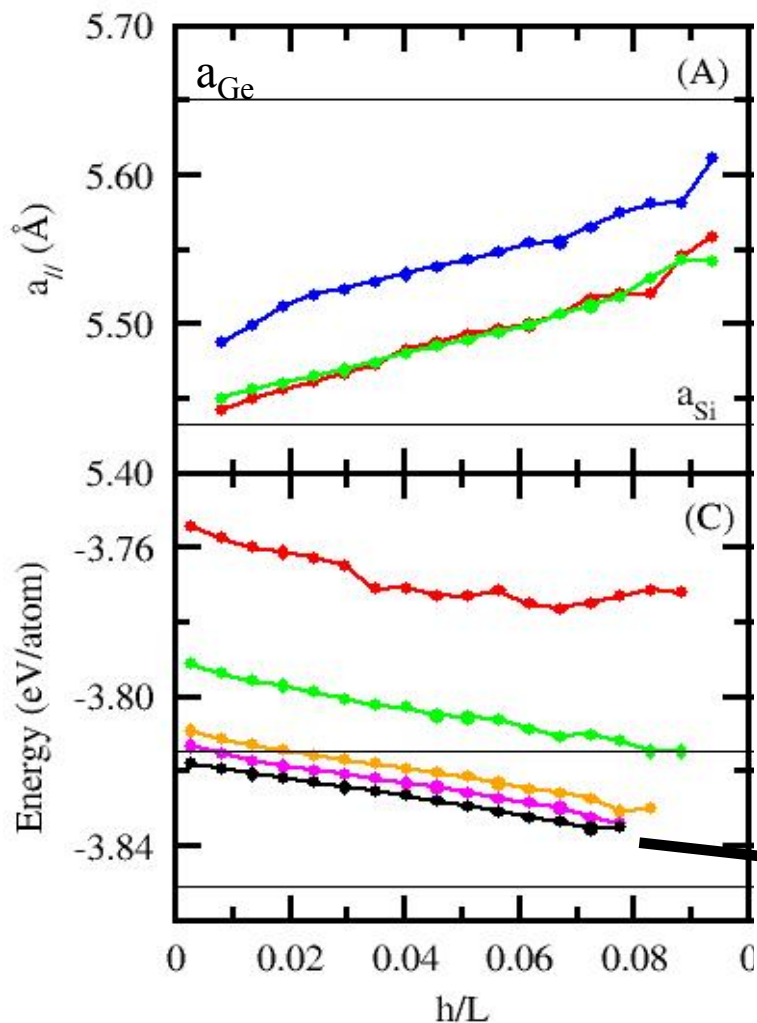


$$E_{S_N} = N \left\{ \left[\int_{H - H/\sqrt{N}}^{H \equiv L/10} E_{add.}(h) da(h) \right] + \frac{\Gamma L}{\sqrt{N}} \right\}$$

Energy for one additional layer vs h



Formation energy density for one additional layer is the one of the layer in depth.
Tersoff-MD results:



$$\times \sigma_{105} \Rightarrow E_{add.}(h) = B - A \frac{h}{L}$$

Atom per area in a $\{105\}$ plane

Competition between surface and edge terms



Tersoff-potential calculations for Ge pyramids on Si(001) show a linear trend with reduced height h/L : fitting the converged line

$$E_{add.}(h) = -A \frac{h}{L} + B \quad A \approx 6 \text{ meV}/\text{\AA}^2$$



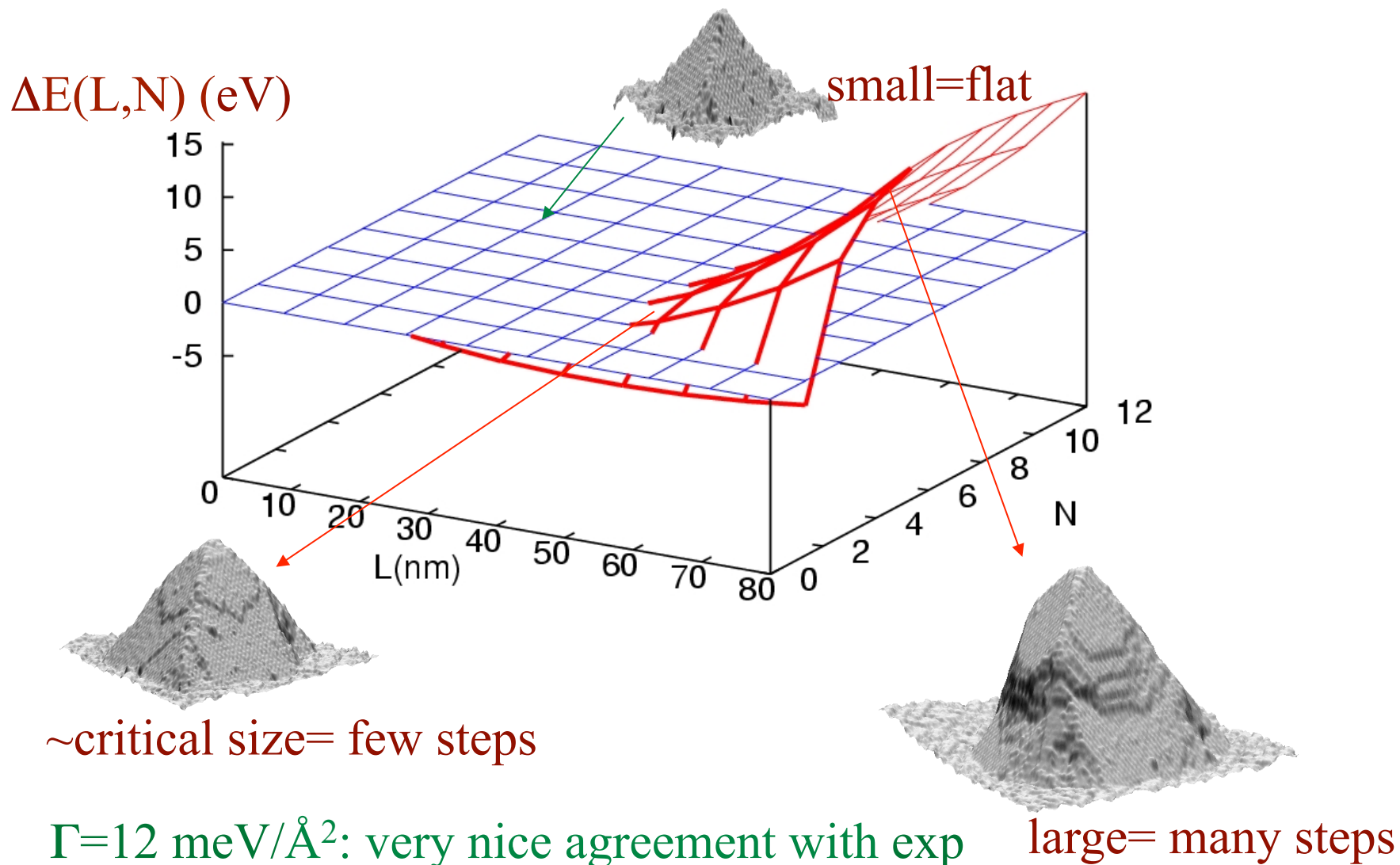
$$\begin{aligned} \Delta E(L, N) &\equiv E(S_0) - E(S_N) = \\ &= \frac{A}{300 \sin(11.31^\circ)} L^2 \left(1 - \frac{1}{\sqrt{N}} \right) - L\Gamma\sqrt{N} \end{aligned}$$

Surface term: Lowers the energy of the stepped state with $\sim L^2$

Linear term: Increases the energy of the stepped state with $\sim L$

Γ is the only unknown parameter

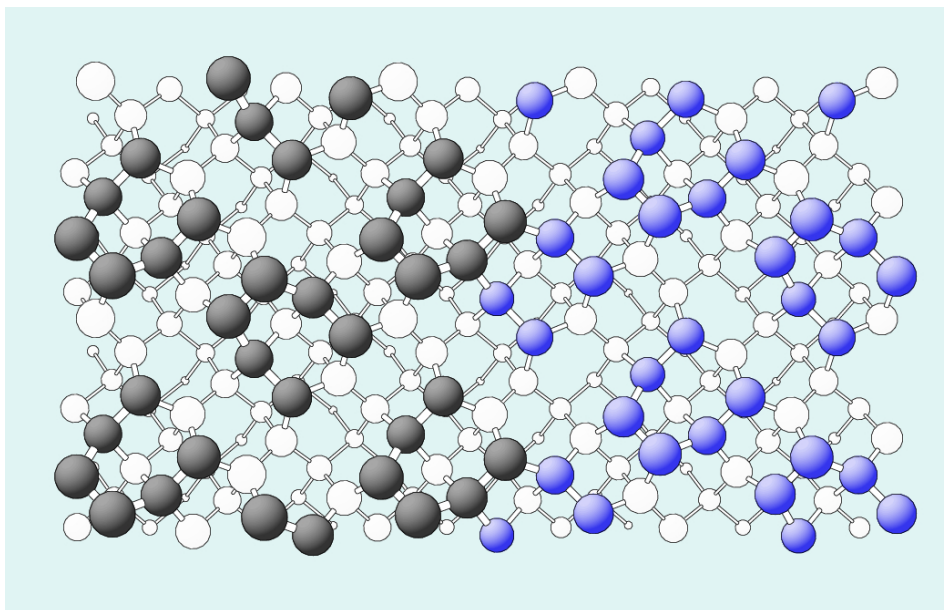
Best fit of step energy to STM results



Independent estimation of step energy



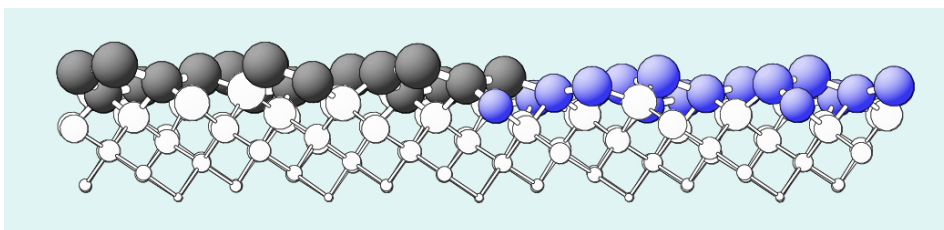
Independent and subsequent simulations of ours by Tersoff potential for (105) step energy



Step energy of

12 meV/Å

(surprisingly close to our fitting parameter..)



↕ single (105) layer

S. Cereda, F. Montalenti & L. Miglio, *Surf. Sci.* **591**, 23 (2005)



Porquerolles,
September 14th

Semiconductor epitaxy



Ordering, intermixing and plastic relaxation



P. Raiteri et al., *Appl. Phys. Lett.* **80**, 3736 (2002)

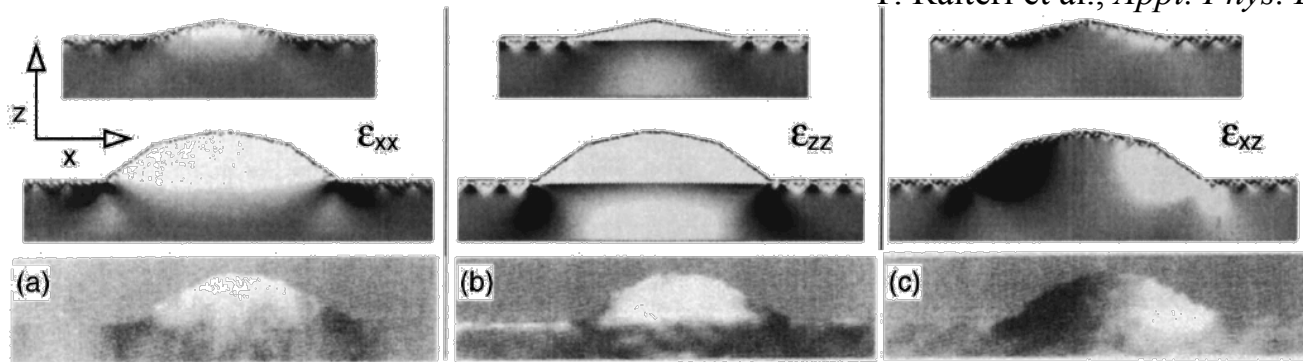


FIG. 1. Strain maps in a (010) cross view for one pyramid (22 nm wide, top panels) and for one dome (32 nm wide, middle panels) compared to Fourier transform maps of transmission electron micrographs for a real dome (approximately 75 nm wide, bottom panels) (see Ref. 10). The scale for simulated ϵ_{xx} and ϵ_{zz} ranges from -1% (black) to 0.5% (white) while for ϵ_{xy} from -0.5% (black) to 0.5% (white).

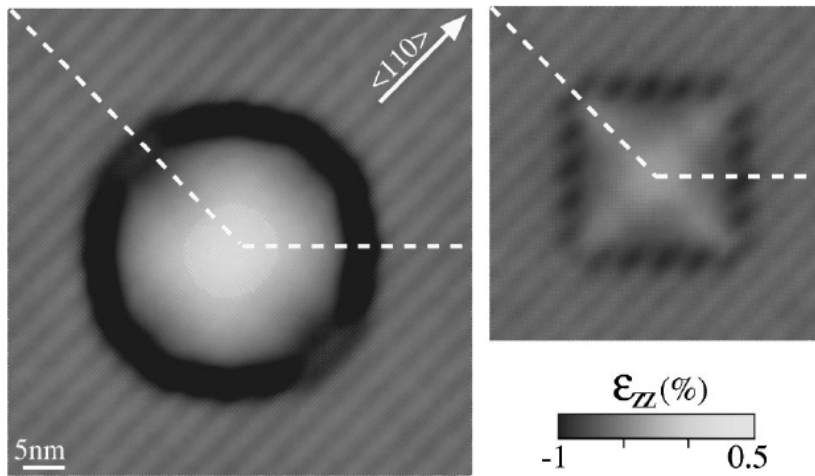
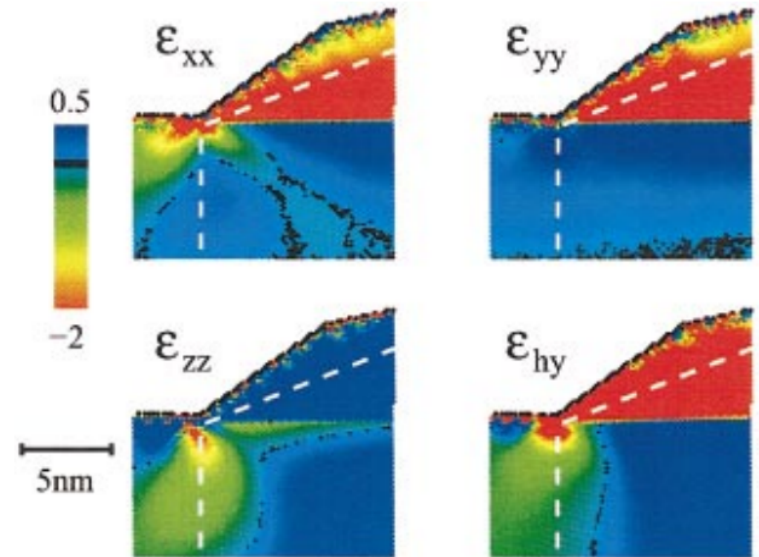


FIG. 2. Plan view of ϵ_{zz} for the dome (left-hand side) and for the pyramid (right-hand side) as computed across the Si substrate 2 nm below the Si/Ge interface.



Strain maps in a (010) cross view of the dome edge. The scale is in percentage with respect to the bulk lattice parameter of Si and Ge independently. The black color indicates atoms with zero strain.



Ideal alloy

$$G_{mix} = H_{mix} - TS_{mix} \approx kT \int V \left[c \ln c + (1-c) \ln(1-c) \right] dr$$

$$\mu_{\nu} = \delta G_{mix} / \delta N_{\nu} = \kappa_{\nu} + 1/2 \sum_{ijkl} S_{ijkl} \sigma_{ij} \sigma_{kl} + \eta_{\nu} \sum_{kk} \sigma_{kk} + kT \ln c_{\nu}$$

for component ν

B.J. Spencer, P.W. Voorhees & J. Tersoff, *Phys. Rev. Lett.* **84**, 2449 (2000)



... entropy opposes to component separation and keeps them mixed

Si-Ge intermixing: entropic contribution



Ideal alloy

$$G_{mix} = H_{mix} - TS_{mix} \approx kT \int V \left[c \ln c + (1-c) \ln(1-c) \right] dr$$

$$\mu_{\nu} = \delta G_{mix} / \delta N_{\nu} = \kappa_{\nu} + 1/2 S_{ijkl} \sigma_{ij} \sigma_{kl} + \eta_{\nu} \sigma_{kk} + kT \ln c_{\nu}$$

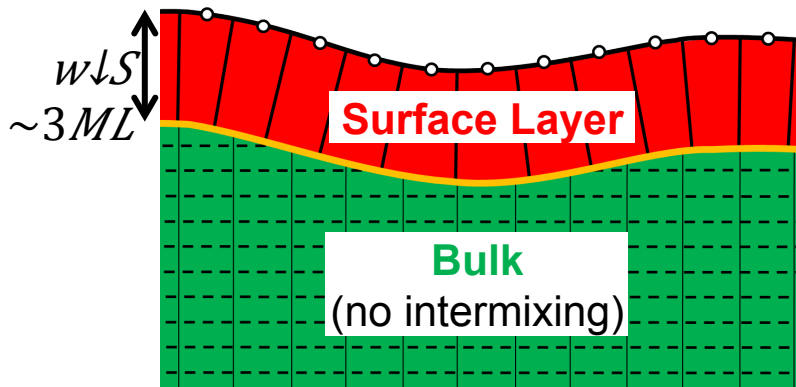
for component ν

B.J. Spencer, P.W. Voorhees & J. Tersoff, *Phys. Rev. Lett.* **84**, 2449 (2000)

Ge mixes only within a finite thickness layer below the surface

Uberuaga et al., *Phys. Rev. Lett.* **84**, 2441 (2000)

Zipoli et al., *Appl. Phys. Lett.* **92**, 191908 (2008)



J. Tersoff, *Appl. Phys. Lett.* **83**, 353 (2003)

$$\rightarrow v_{\nu n} = \sum_{\nu} v_{\nu} \nabla \cdot [M_{\nu} \nabla \mu_{\nu}] + \Phi_{\nu}$$

$$w_s \frac{d\xi_{\nu}}{dt} = \nabla \cdot [M_{\nu} \nabla \mu_{\nu}] + \Phi_{\nu} - c_{\nu} v_{\nu n}$$

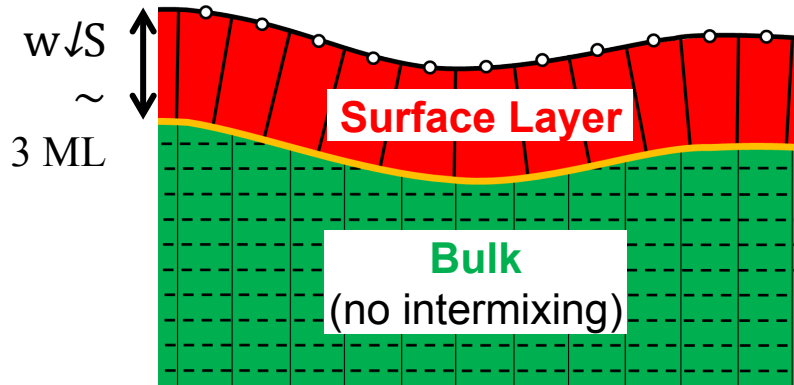
$$c_{\nu} = \begin{cases} \xi_{\nu} & v_{\nu n} \geq 0 \\ 0 & v_{\nu n} < 0 \end{cases}$$

Critical thickness to islands with flux composition



Ge mixes only within a finite thickness layer below the surface

Uberuaga et al., Phys. Rev. Lett. **84**, 2441 (2000)
Zipoli et al., Appl. Phys. Lett. **92**, 191908 (2008)

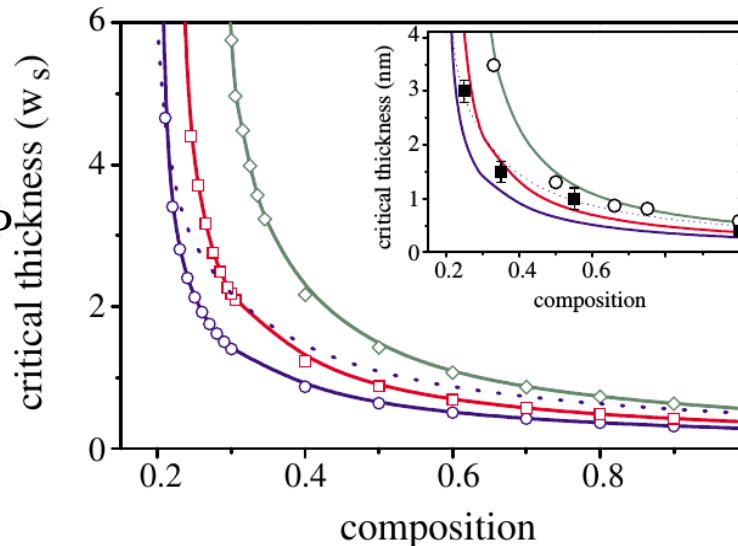
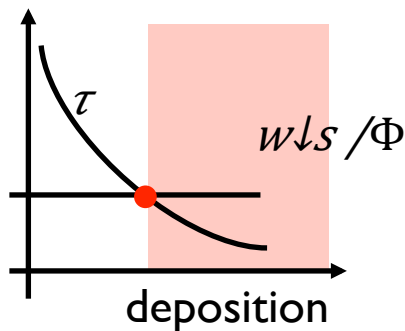


$$\rightarrow v \downarrow n = \sum v \uparrow \nabla \cdot [M \downarrow \nabla \mu \downarrow] + \Phi \downarrow v$$

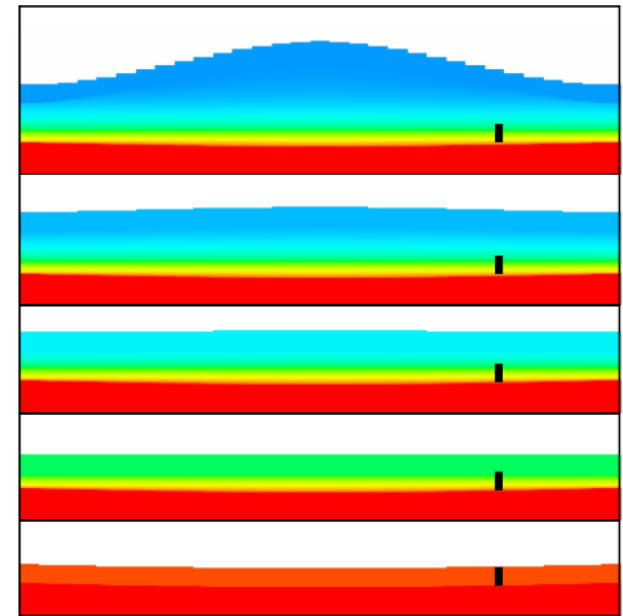
$$w_s \frac{d\xi \downarrow v}{dt} = \nabla \cdot [M \downarrow \nabla \mu \downarrow] + \Phi \downarrow v - c \downarrow v v$$

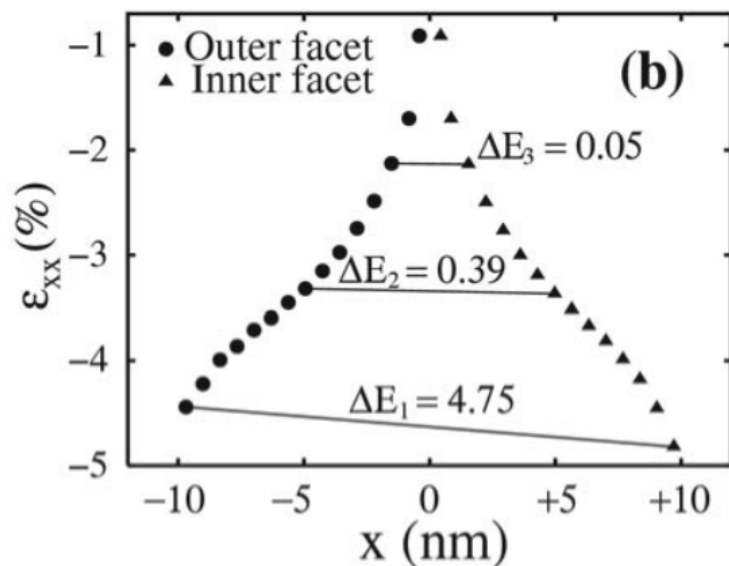
$$c \downarrow v = \{ \dots \xi \downarrow v \ \& \ v \downarrow n \geq \dots \}$$

J. Tersoff, Appl. Phys. Lett. **83**, 353 (2003)

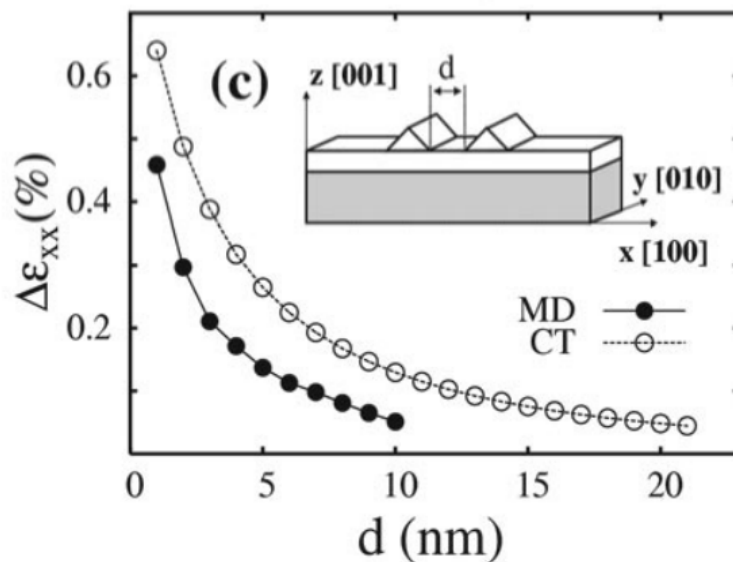


Y. Tu & J. Tersoff, Phys. Rev. Lett. **93**, 216101 (2004)





Asymmetric strain component ϵ_{xx} estimated by MD along the surface profile of the inner (triangles) and outer (circles) facets of one Ge ridge at a distance $d=1$ nm from another one. The differences in the elastic energy between opposite facets, as produced by the full strain tensor, are also reported at selected island heights ($\Delta E_{\downarrow 1}$, $\Delta E_{\downarrow 2}$, and $\Delta E_{\downarrow 3}$ in meV/atom).

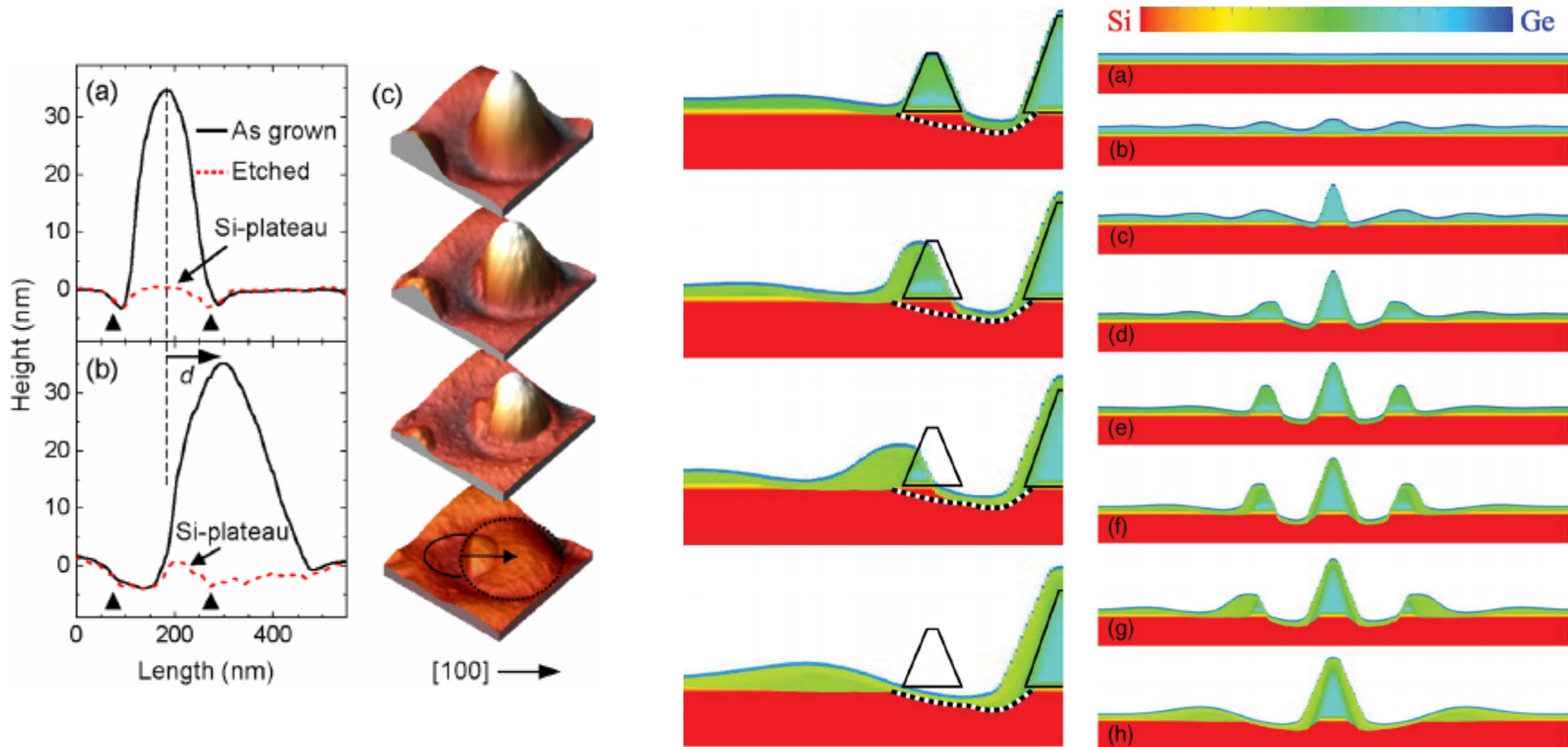


Difference between the xx strain component at the opposite edges of the ridge base $\Delta \epsilon_{xx}$ vs d : MD simulations (solid circles) and continuum approach (open circles). Inset: Geometry of the simulation cell.

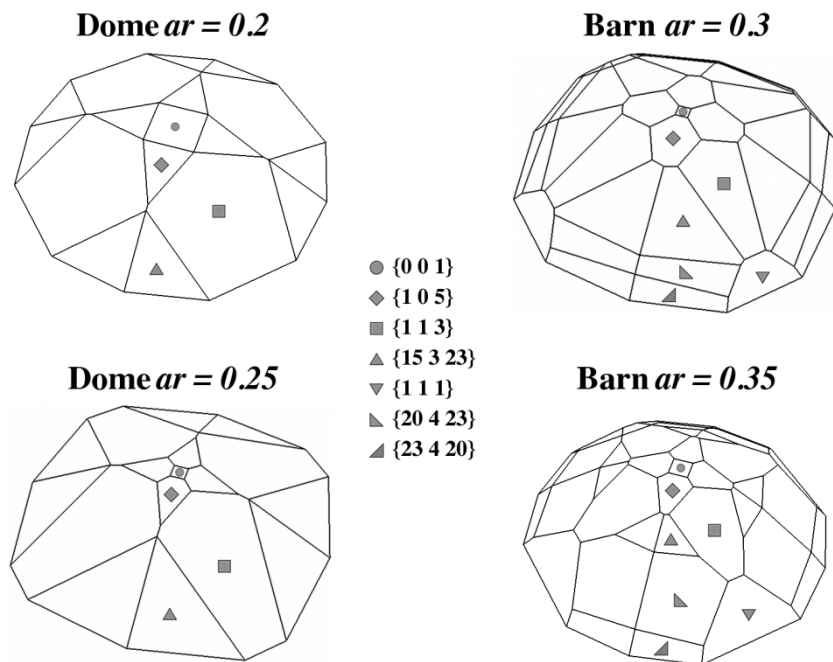


Island displacement via surface diffusion with intermixing

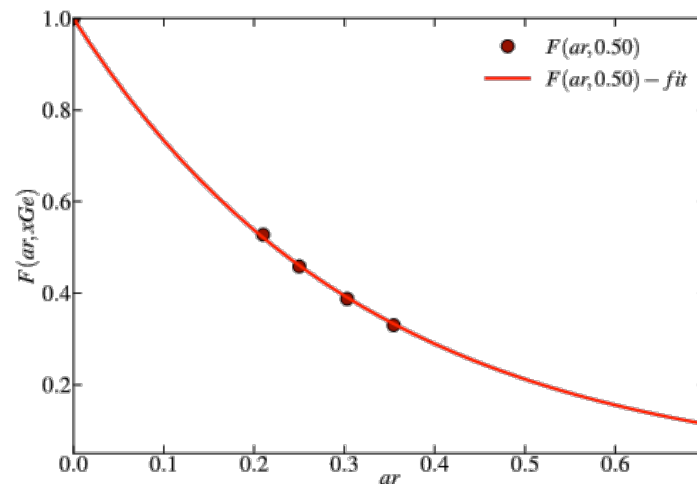
Y. Tu & J. Tersoff, *Phys. Rev. Lett.* **98**, 096103 (2007)



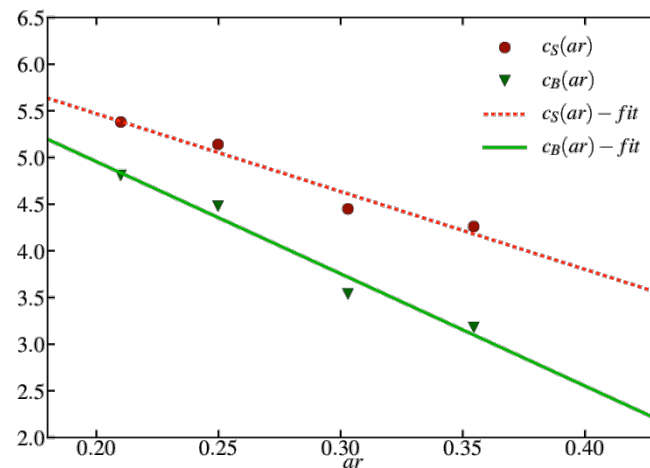
A simplified model for dome to barn transition with V



F is a geometric parameter for the volumetric strain relaxation with shape



C are geometric parameters for surface energy with shape



$$\Delta E_{is}(V, x_{Ge}) = V \rho_{WL}(x_{Ge}) [F_{is}(x_{Ge}) - 1] + V^{\frac{2}{3}} (c_S^{is} \gamma_{is} - c_B^{is} \gamma_{WL})$$

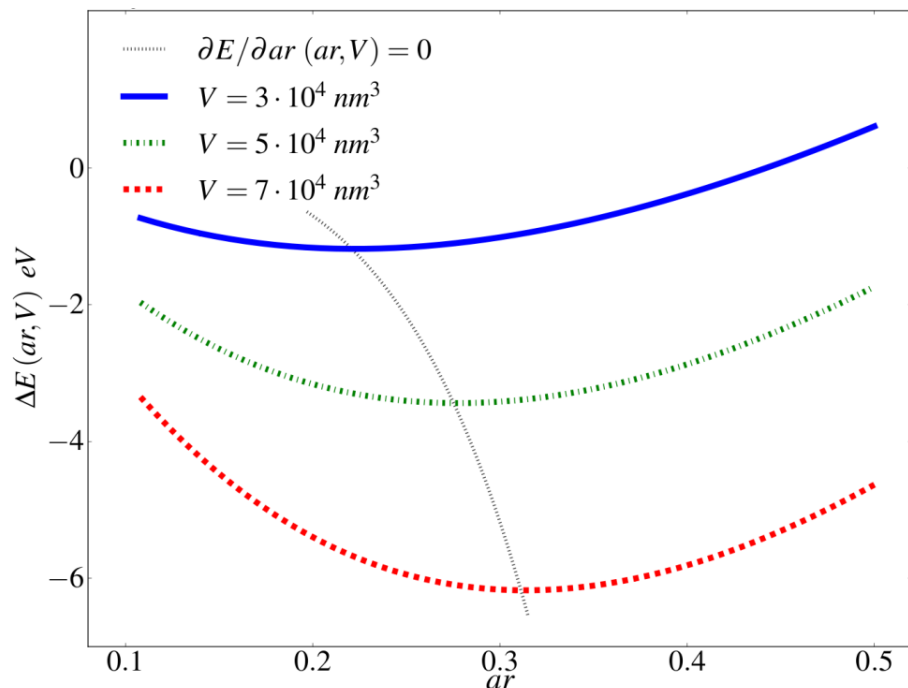
elastic energy referred to Wetting Layer

island surface energy referred to the one of the Wetting Layer

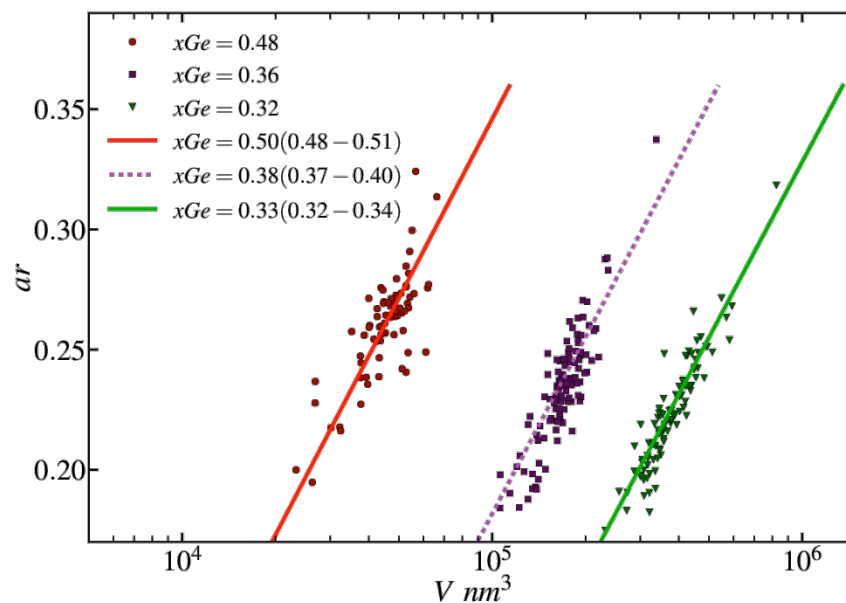
Predicting the mean composition by size



By increasing the volume, the aspect ratio minimizing the total energy increases, because of a smaller surface to volume ratio: stable shape; ar vs misfit, i.e. vs composition, can be obtained.



Very good comparison to experimental data



$$ar_{\min}(V, x_{Ge}) = \frac{1}{k(x_{Ge})} \left\{ \frac{\ln V}{3} - \ln(-\gamma_{is} k_s + \gamma_{WL} k_B) + \ln[k(x_{Ge}) \rho_{WL}(x_{Ge})] \right\}$$

R. Gatti et al., *J. Phys. Condens. Matter* **24**, 104018 (2012)

Little lateral ordering via elastic repulsion



G. Capellini et al., *Phys. Rev. Lett.* **96**, 106102 (2006)

Increasing the island size by Si deposition provides some angular ordering

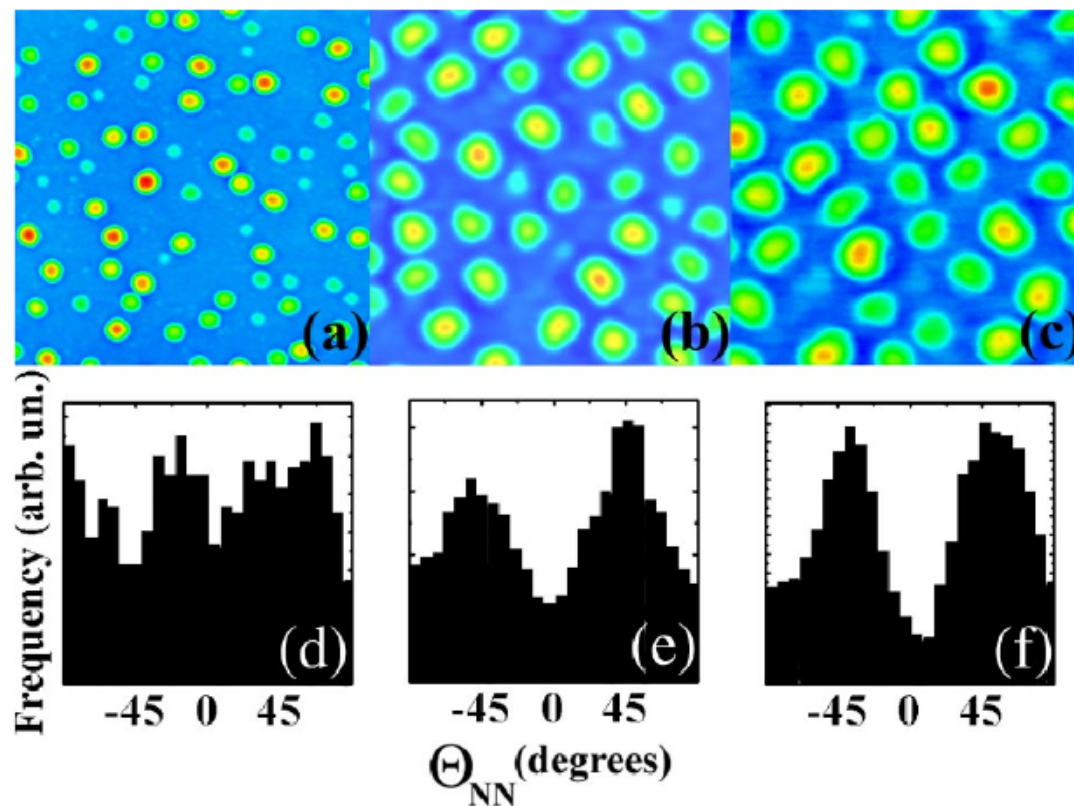


FIG. 1 (color online). $2 \times 2 \mu\text{m}^2$ AFM images of samples belonging to experimental series A: (a) As-grown, (b) with a 4.5-nm and (c) with 6 nm-thick Si deposition. Image sides are oriented along [011] directions. In (d)–(f), we display the corresponding angular distribution of the four nearest neighbors.



F. Montalenti et al., *J. Phys: Condens. Matter*
19, 225001 (2007)

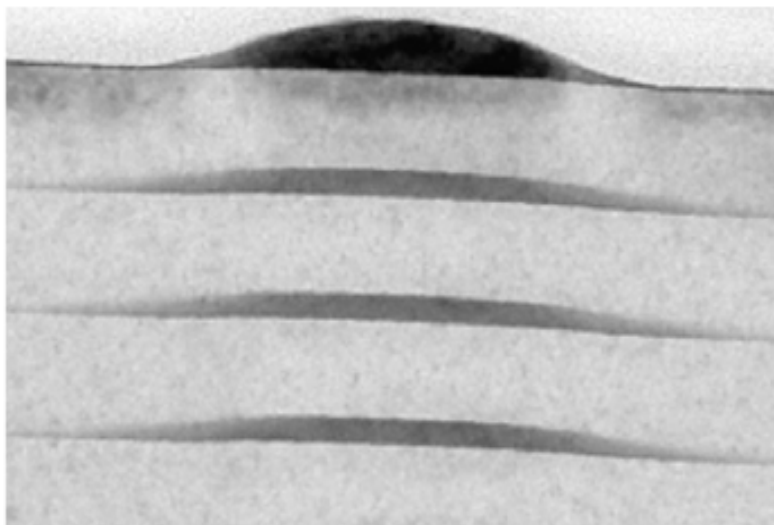


Figure 7. Cross-sectional TEM image of a multilayer grown at 750°C. The buried islands are the evolution of the multifaceted dome visible in the topmost layer after capping with a 65 nm thick silicon layer. The flattened buried islands have typical base width $b = 220$ nm and height $h = 10$ nm while the uncapped dome is characterized by $b = 180$ nm and $h = 35$ nm.

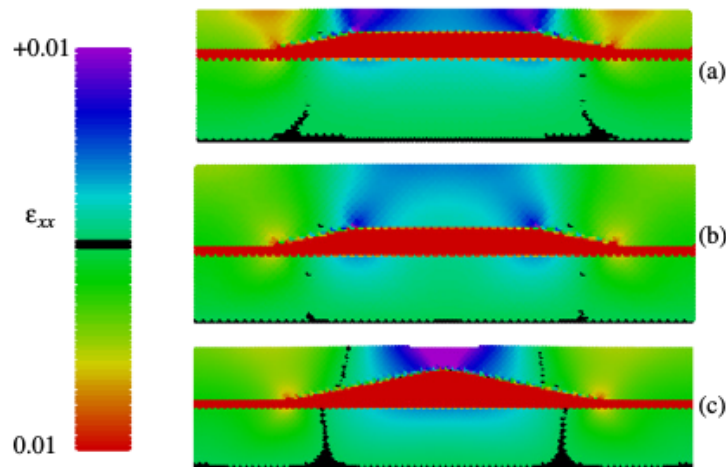


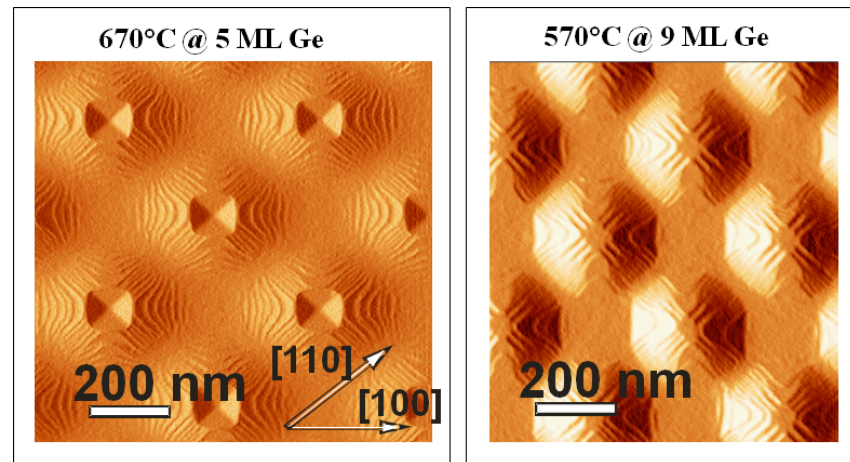
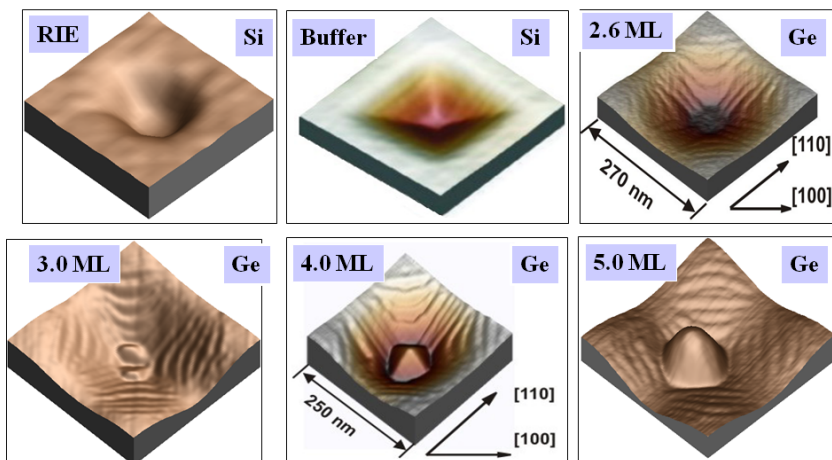
Figure 4. Plots of the ϵ_{xx} component of the strain tensor. (a) Truncated {105} pyramid; thin ($H = 2.5$ nm) CL. (b) Truncated {105} pyramid; thicker ($H = 5.4$ nm) CL. (c) Complete {105} pyramid. While the data reported in panels (a) and (b) exactly correspond to those displayed in figure 1 of [36], with the cell size specified in section 4, the complete pyramid data were taken from a different set of simulations [37], where the base length was set to 27 nm, $H = 4.6$ nm, while the extension of the cell in x and y was 44 nm (the same number of Si substrate layers was used). Black dots are just an artifact of our plotting code: they correspond to *exactly* zero-strain regions.

R. Marchetti et al., *Appl. Phys. Lett.* **87**, 261919 (2005)

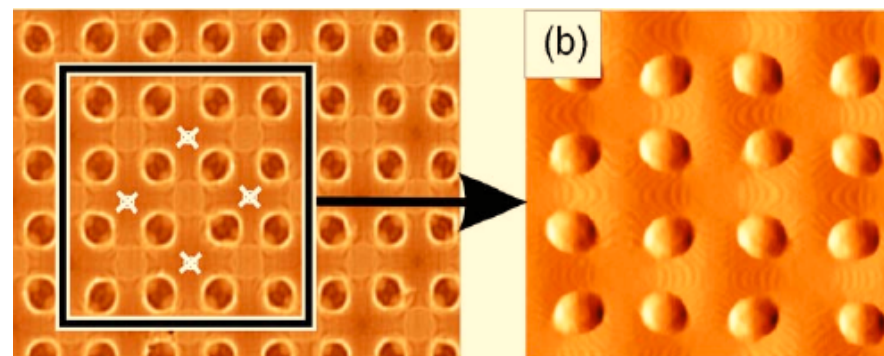
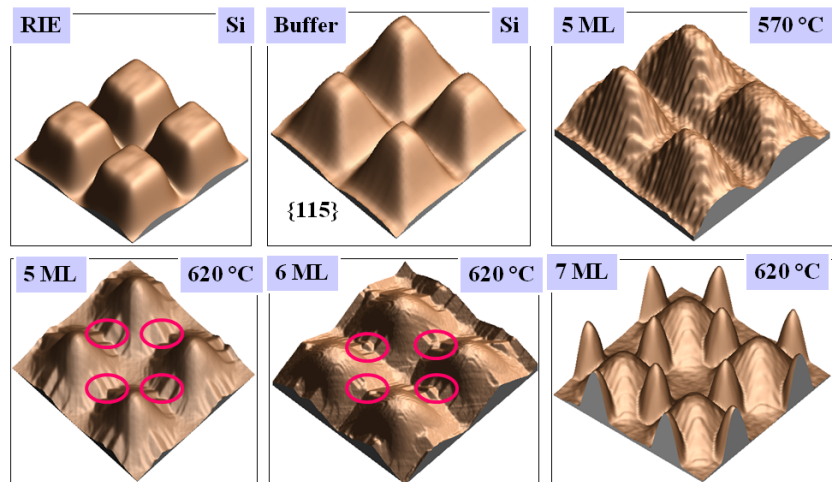
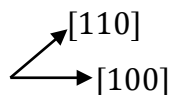
Ordering depends on pattern geometry



Morphology evolution in PIT-patterned template



Morphology evolution in HILL-patterned template

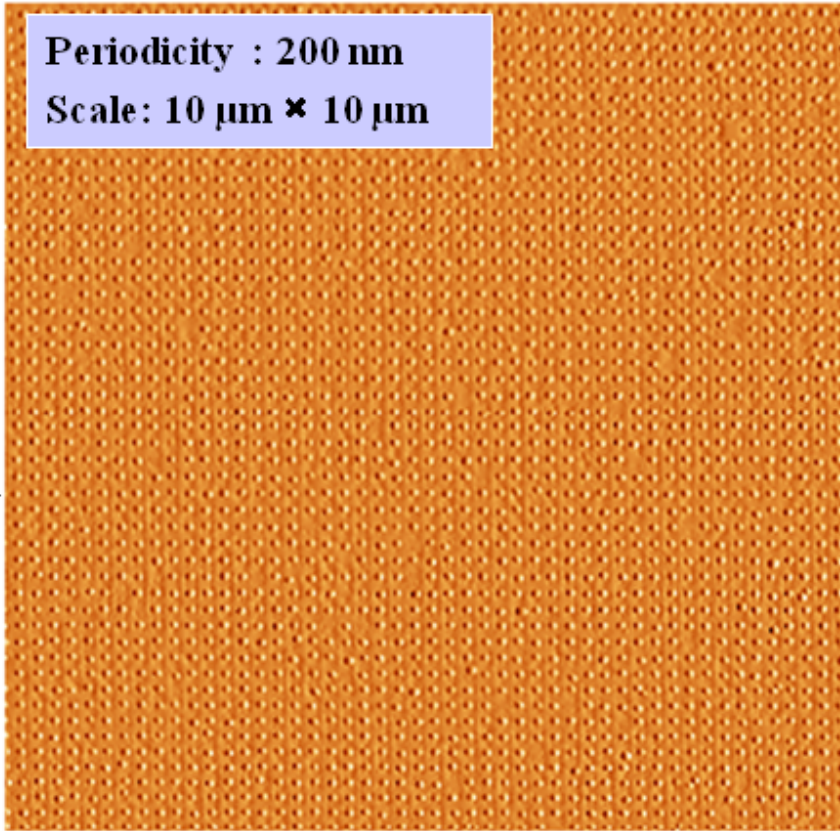


G. Chen et al., *Appl. Phys. Lett.* **92**, 113106 (2008)

Very effective, still depends on T and spacing

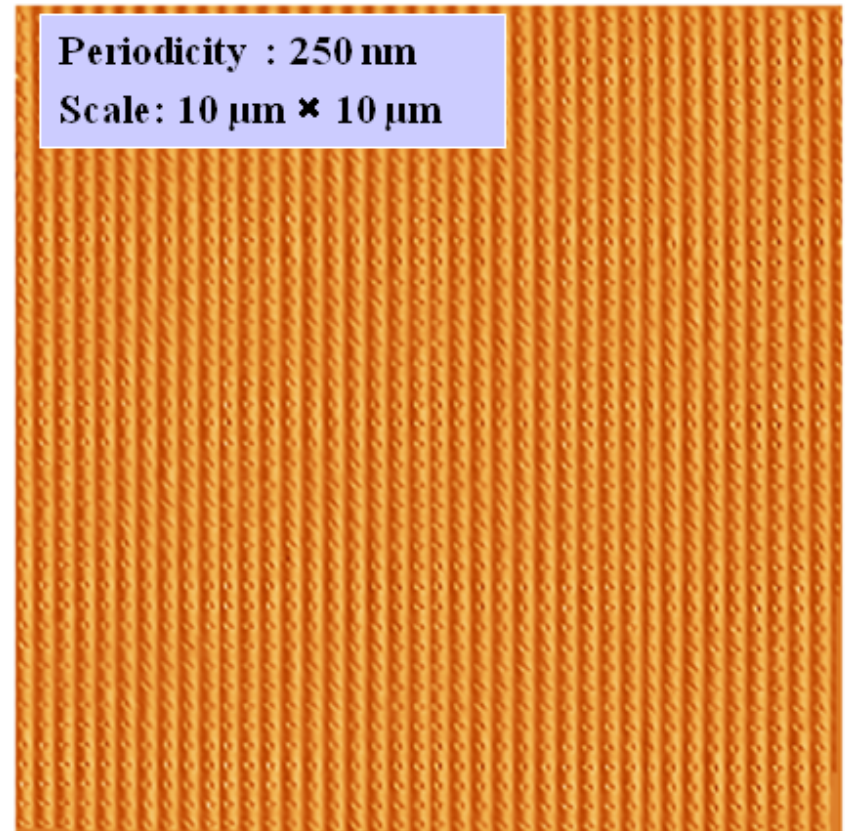


Periodicity : 200 nm
Scale: 10 μm \times 10 μm



620°C @ 5 ML Ge
Total Pits: 2500
Missing Pits: 49, **1.96%**
Substitutional Pits: 11, **0.43%**

Periodicity : 250 nm
Scale: 10 μm \times 10 μm



620°C @ 5 ML Ge
Total Pits: 1600
Missing Pits: 0, **0%**
Substitutional Pits: 0, **0%**

Courtesy of G. Chen, JKU

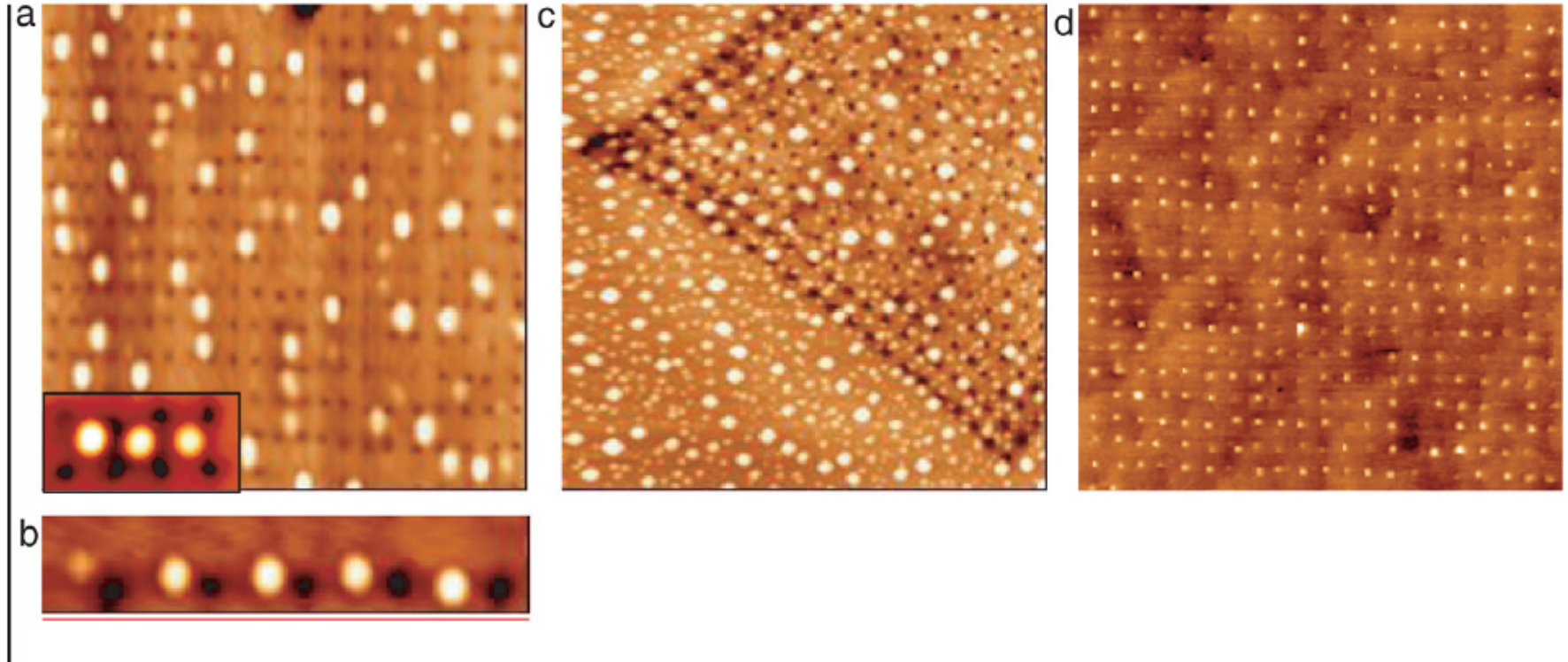
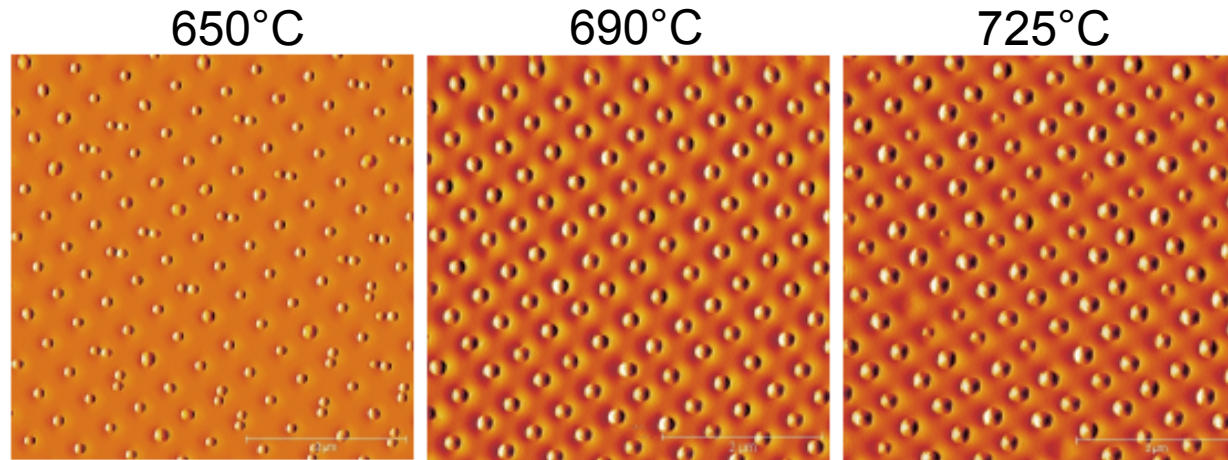


Fig. 67. AFM images (scan size $1.5 \mu\text{m}$) of FIB patterned areas after 8 ML Ge deposition at different temperatures (T_s): (a) $T_s = 750 \text{ }^\circ\text{C}$. In this situation the size of QD (100 nm) is in the range of the hole-hole distance (180 nm). The inset shows a higher magnification image of three Ge QD situated on terraces between the FIB pits; (b) $T_s = 750 \text{ }^\circ\text{C}$. In this situation the size of the QDs is three times smaller than the hole-hole distance (350 nm). Ge QDs are located close to FIB pits; (c) $T_s = 650 \text{ }^\circ\text{C}$, hole-hole distance is 180 nm. At this temperature the Ge QDs are located randomly both in the holes and out of the holes; (d) $T_s = 550 \text{ }^\circ\text{C}$, In this situation, Ge QDs are located only in the holes.

A. Pascale, I. Berbezier, A. Ronda & P. C. Kelires, *Phys. Rev. B* **77**, 075311 (2008)

Optimal conditions for ordering



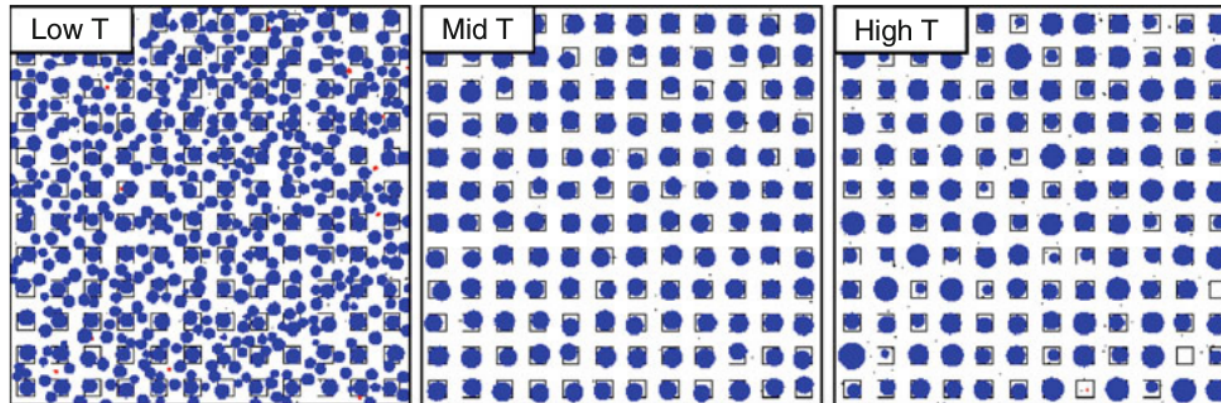
Courtesy of
M. Grydlik,
JKU

$\Delta = 400\text{nm}$

Disorder

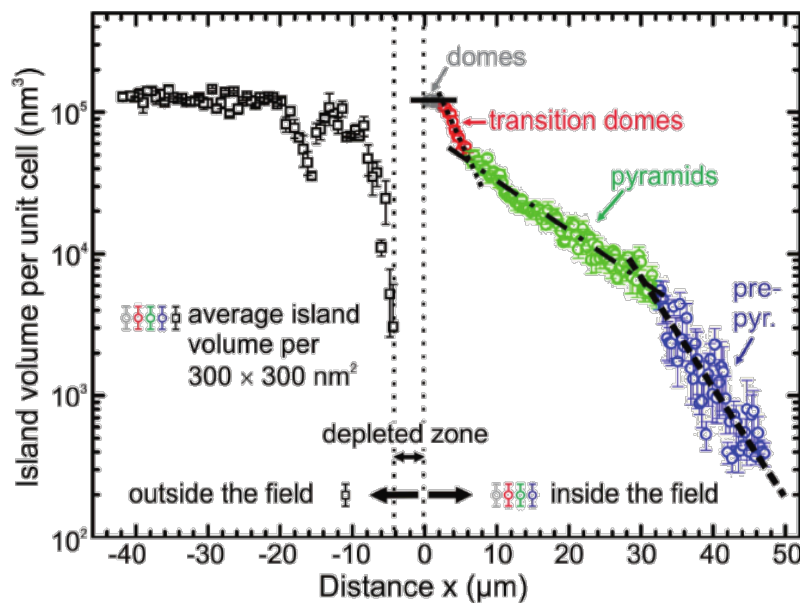
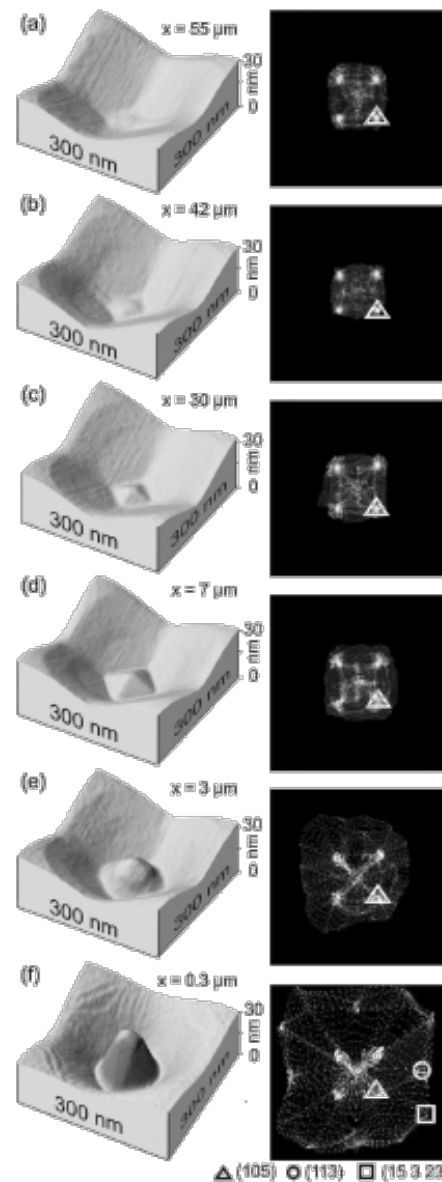
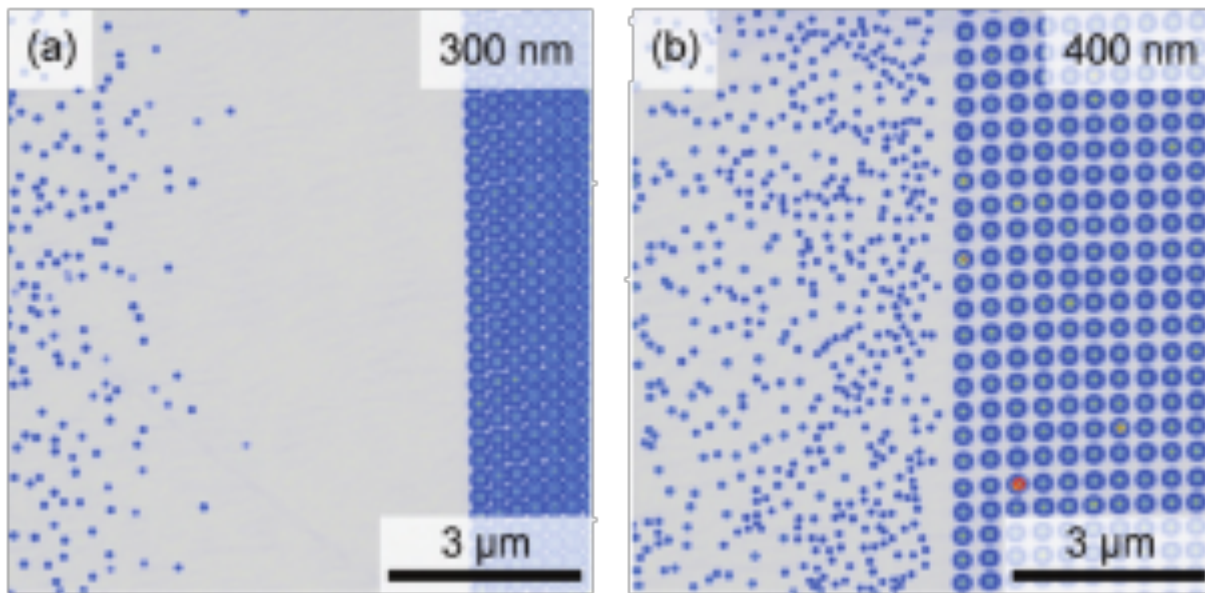
Optimal ordering

Positional order
but size disorder



R. Bergamaschini et al., *Nanoscale Res. Lett.* **5**, 1873 (2010)

Surface diffusion length drives the ordering

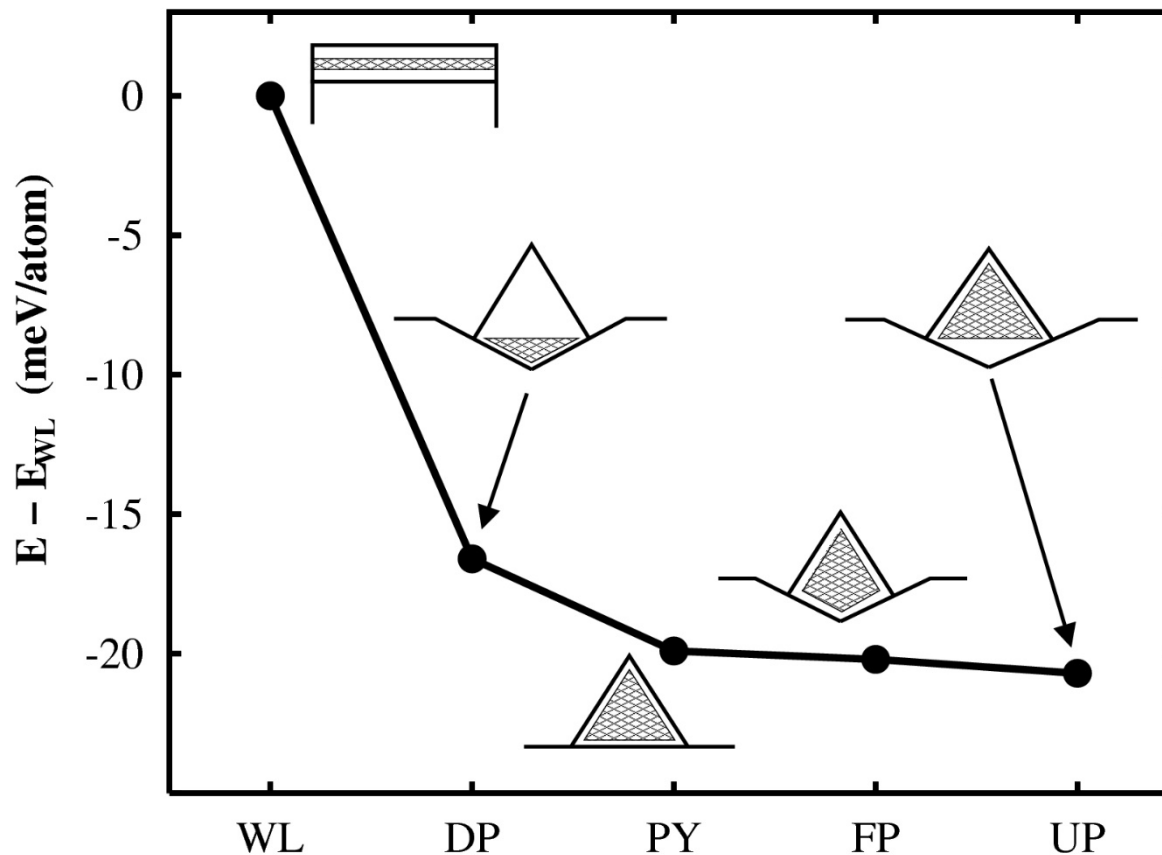


M. Grydlik et al., *Phys. Rev. B* **88**, 115311 (2013)



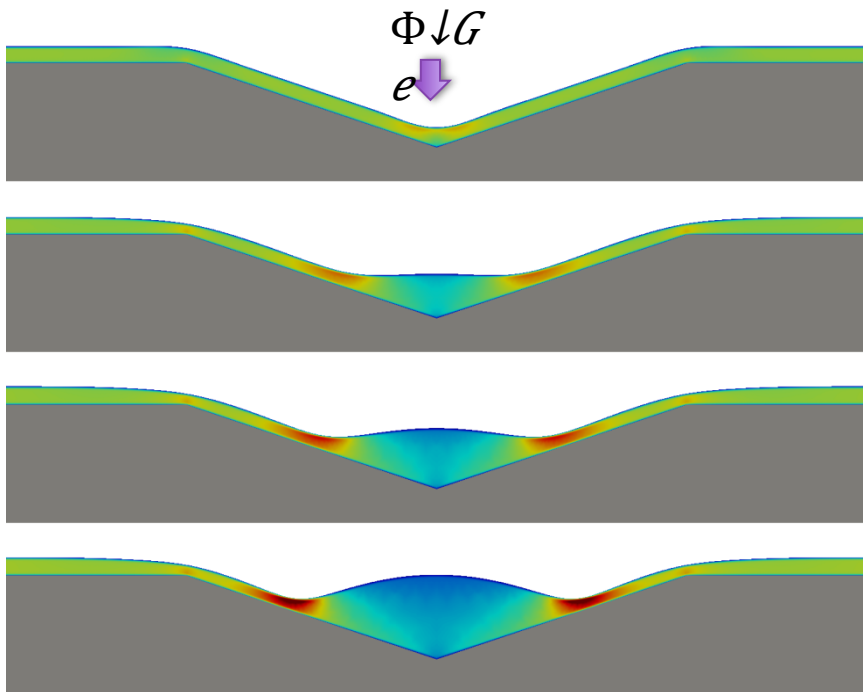
Delayed Plastic Relaxation on Patterned Si Substrates: Coherent SiGe Pyramids with Dominant {111} Facets

Zhenyang Zhong,^{1,3} W. Schwinger,¹ F. Schäffler,¹ G. Bauer,¹ G. Vastola,² F. Montalenti,² and L. Miglio²





Simulation with exact elastic field from FEM
M. Albani, *Master Thesis* (2015)



J.-N. Aqua & X. Xu, *Phys. Rev. E* **90**, 030402(R) (2014)

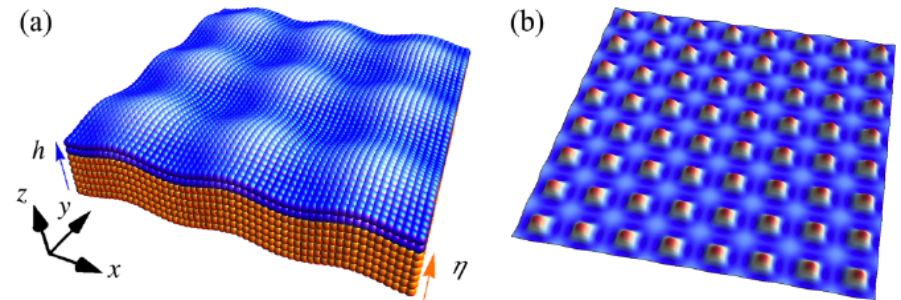


FIG. 1. (Color online) (a) Film with a free surface at $z = h(x, y, t)$ deposited on a pattern at $z = \eta(x, y)$. (b) Best-ordered stationary islands sitting in the pattern valleys, resulting from the numerical integration of Eq. (1) for $\lambda_\eta/\lambda_{\text{ATG}} = 1$ and $\bar{H}/H_c = 1.8$.

ATG & substrate patterning with intermixing

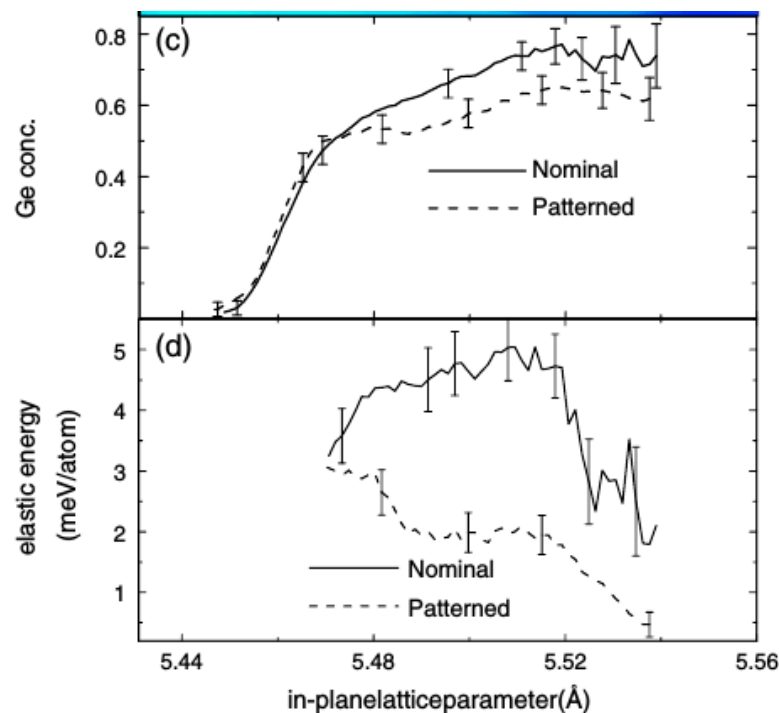
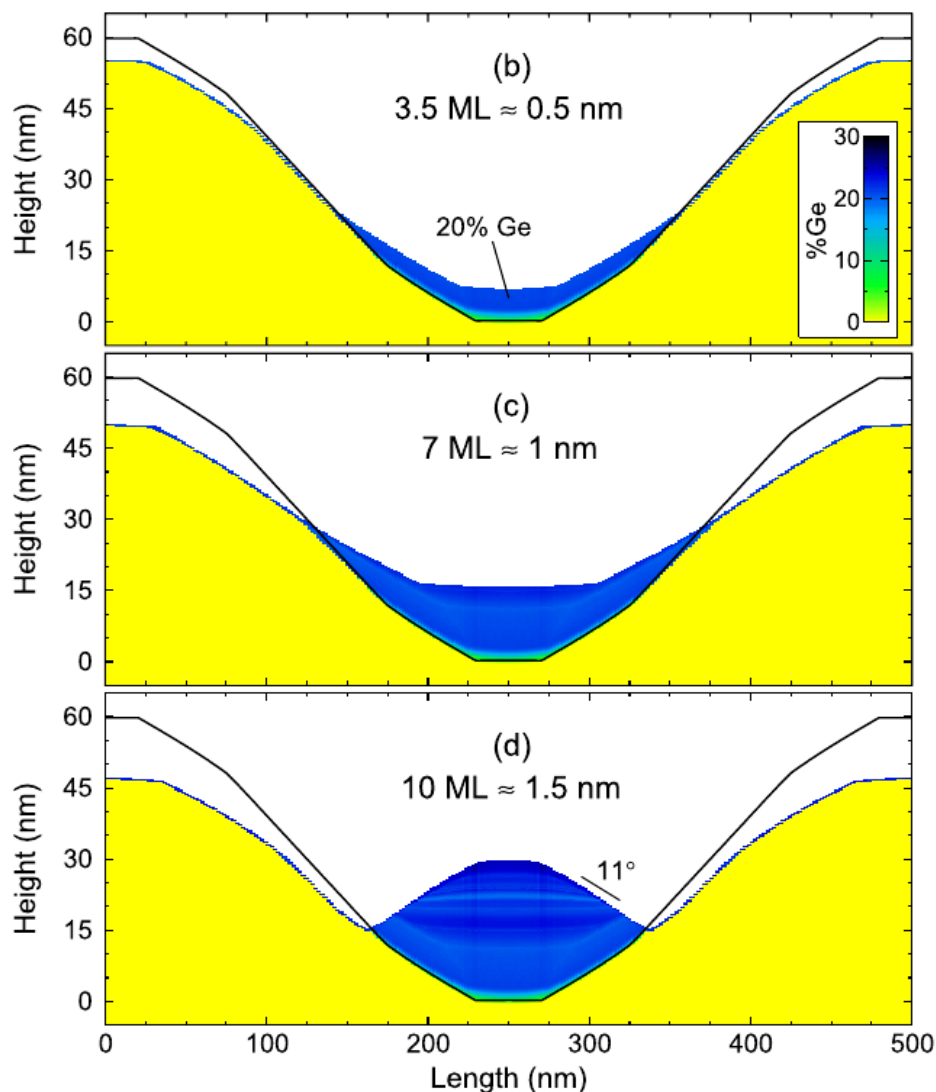


FIG. 1 (color online). Logarithmic intensity distribution in the vicinity of the (400) Bragg reflection for Ge islands grown on the flat (a) and patterned (b) sample part. Corresponding AFM images ($1 \mu\text{m}^2$ in size) are shown as insets. (c) Ge content inside the islands as a function of lattice parameter for growth on the flat (full line) and on the patterned part (dashed line). (d) elastic energy as a function of lattice parameter as extracted from the x-ray data. All figures correspond to the same lattice-parameter scale.

R. Bergamaschini et al., *Phys. Rev. Lett.* **109**, 156101 (2012)

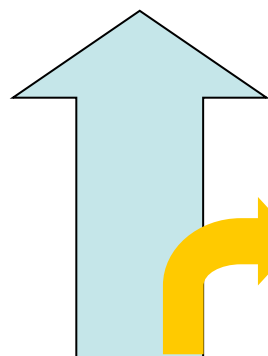
Plastic relaxation onset



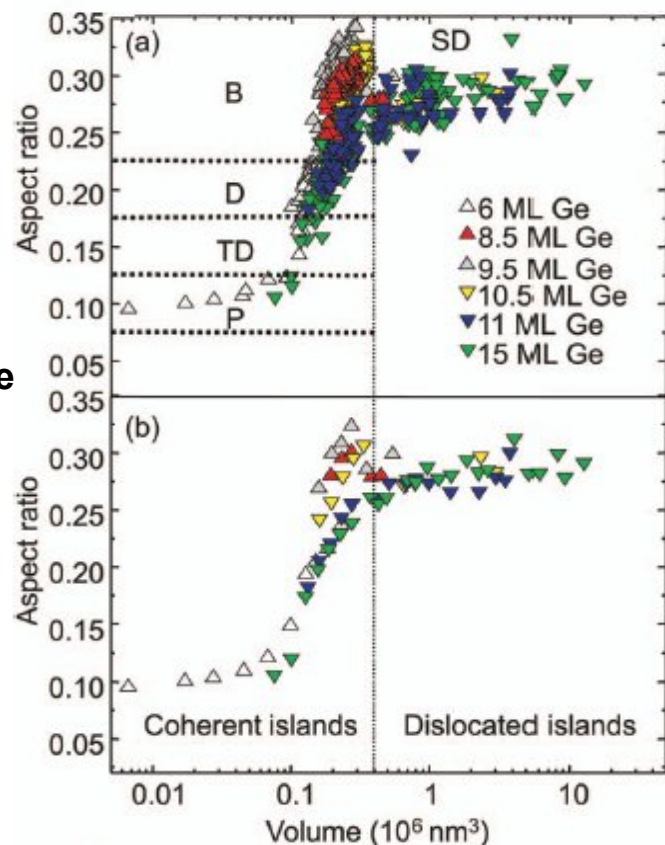
Plastic relaxation is a different path for the strain relaxation

Higher aspect ratio

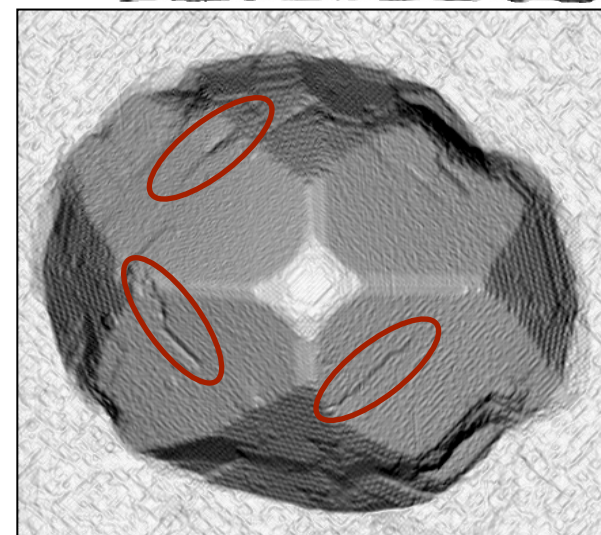
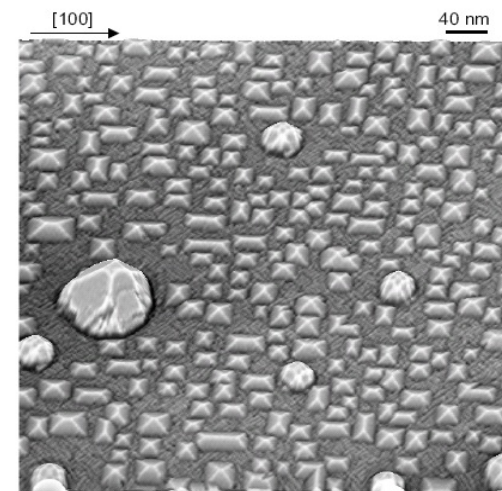
Further elastic relaxation



Plastic relaxation takes place



M. Stoffel et al., *Phys. Rev. B* 74, 155326 (2006)



0 48° STM 120x120x27 nm³

A. Rastelli, MPI-FKF, Stuttgart, IFW, Dresden private communication and Phd. thesis

When islands reach a **critical size** a different path for relaxation becomes favorable: **plastic relaxation** occurs



PHYSICAL REVIEW B, VOLUME 63, 205424

Stresses and first-order dislocation energetics in equilibrium Stranski-Krastanow islands

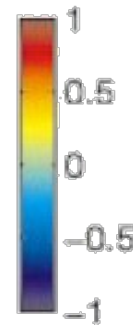
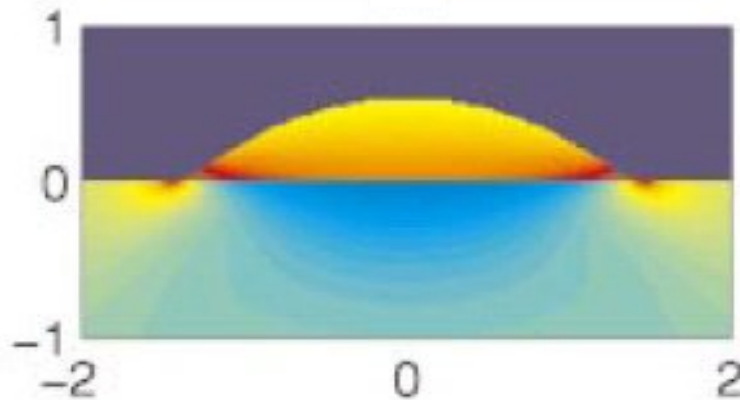
B. J. Spencer

Department of Mathematics, State University of New York at Buffalo, Buffalo, New York 14260-2900

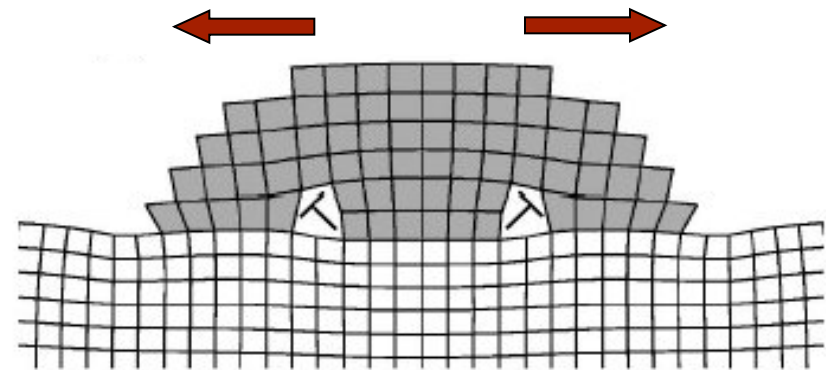
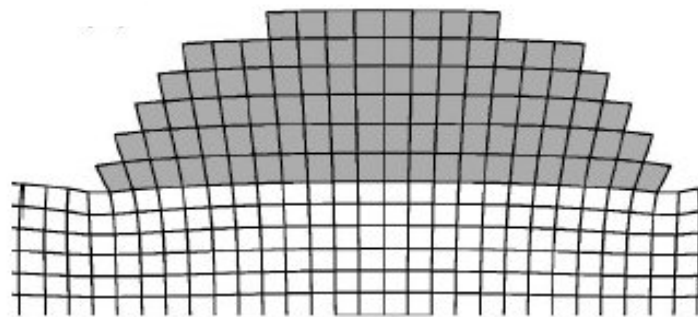
J. Tersoff

IBM Research Division, Thomas J. Watson Research Center, P.O. Box 218, Yorktown Heights, New York 10598

(Received 15 September 2000; published 7 May 2001)

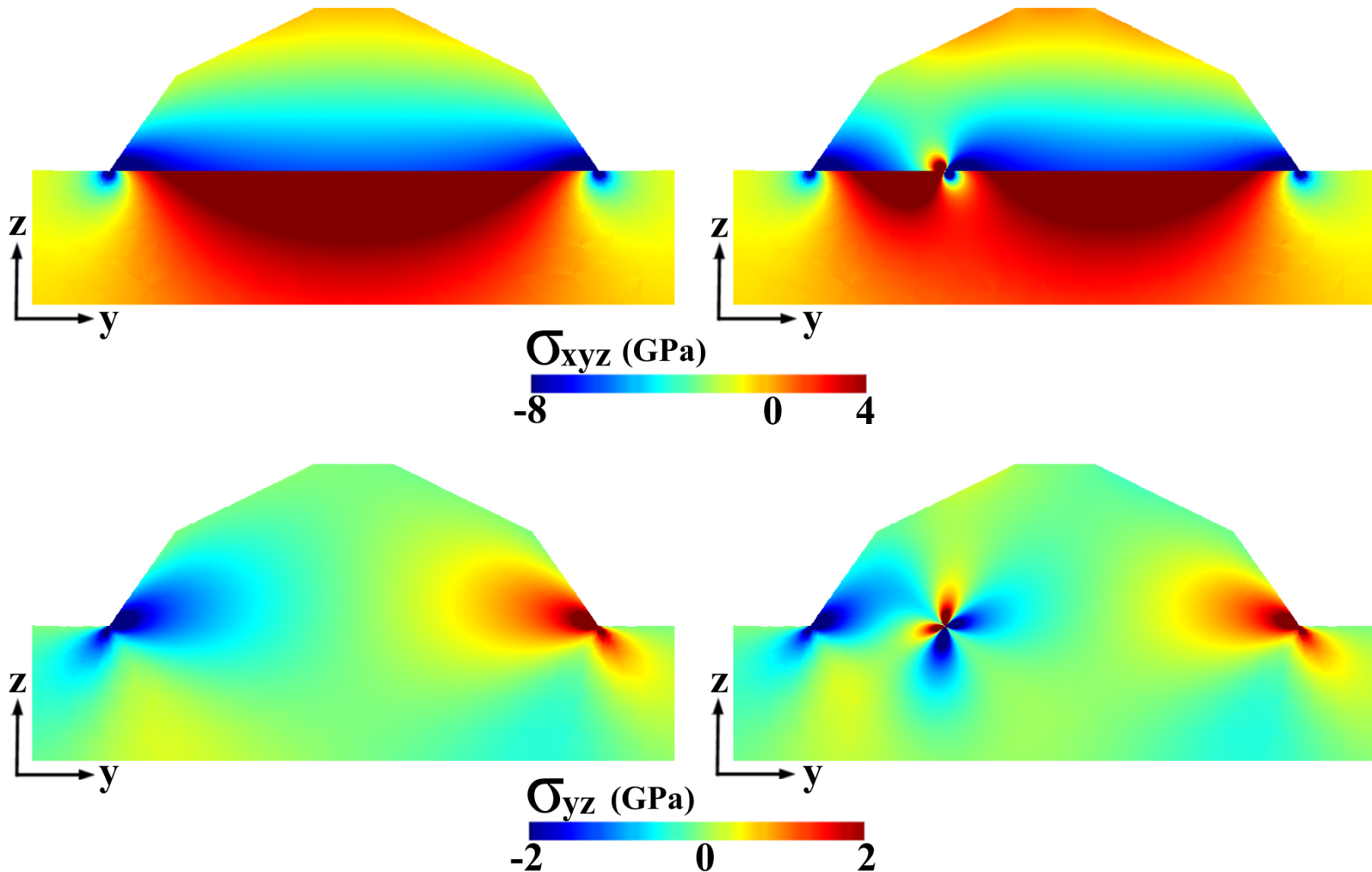


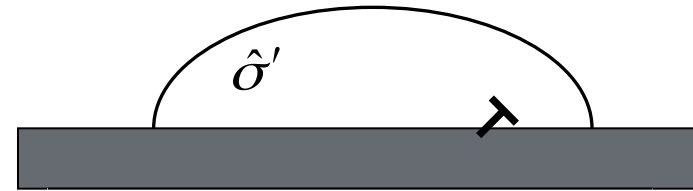
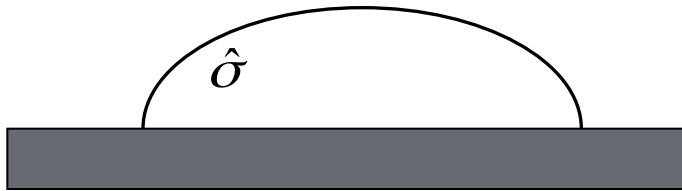
σ_{xx} scaled relative to the misfit stress for a planar film





60° dislocation straight segment,





Plastic relaxation occurs when:

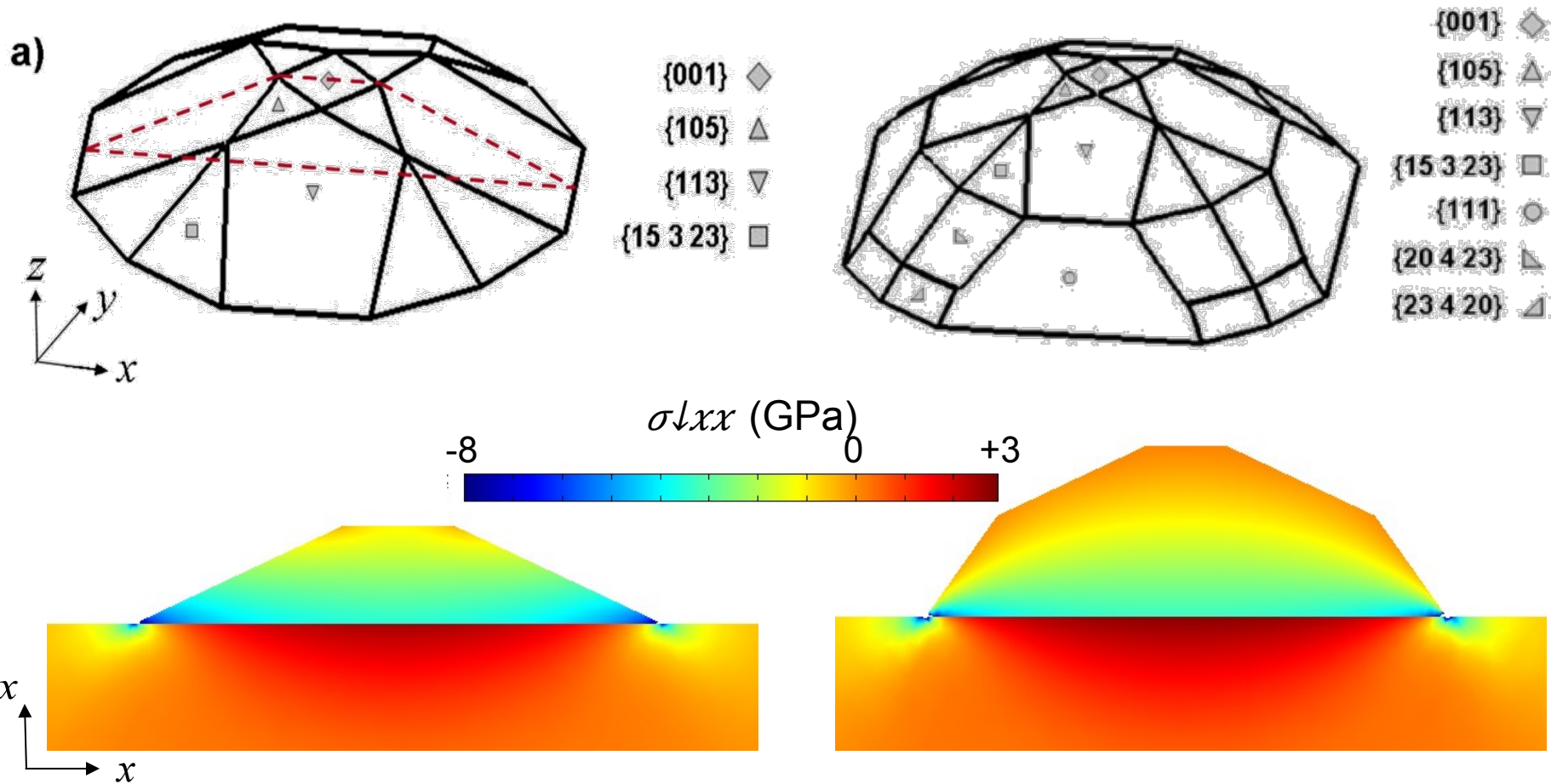
$$\Delta E_{el}(\hat{\sigma} \rightarrow \hat{\sigma}') \leq 0$$

The **direct calculation** of the **exact** total elastic energy in a **dislocated** island *seems* to be impossible, analytical modeling is needed.

$$\Delta E_{el} = E_{gain} + E_{cost}$$

Energy reduction due to the interaction between the dislocation field and the coherent island elastic field

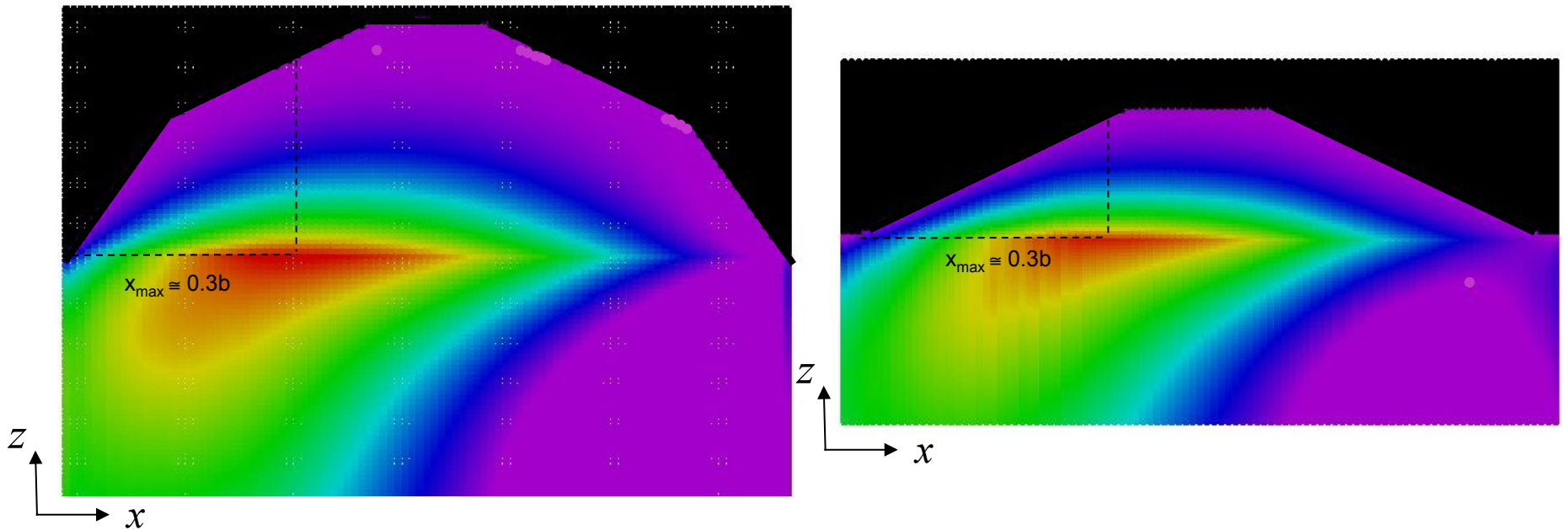
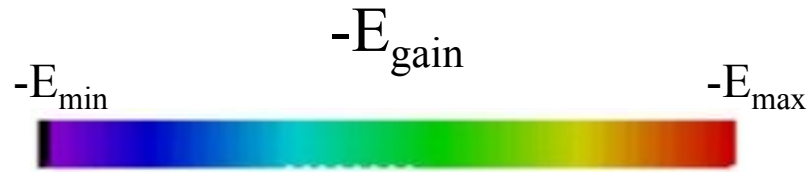
Energy enhancement due to the introduction of the dislocation field itself, as in a bulk system



Elastic field has been calculated for **typical experimental SiGe island composition** imposing a different initial compression

A. Marzegalli et al., *Phys. Rev. Lett.* **99**, 235505 (2007)

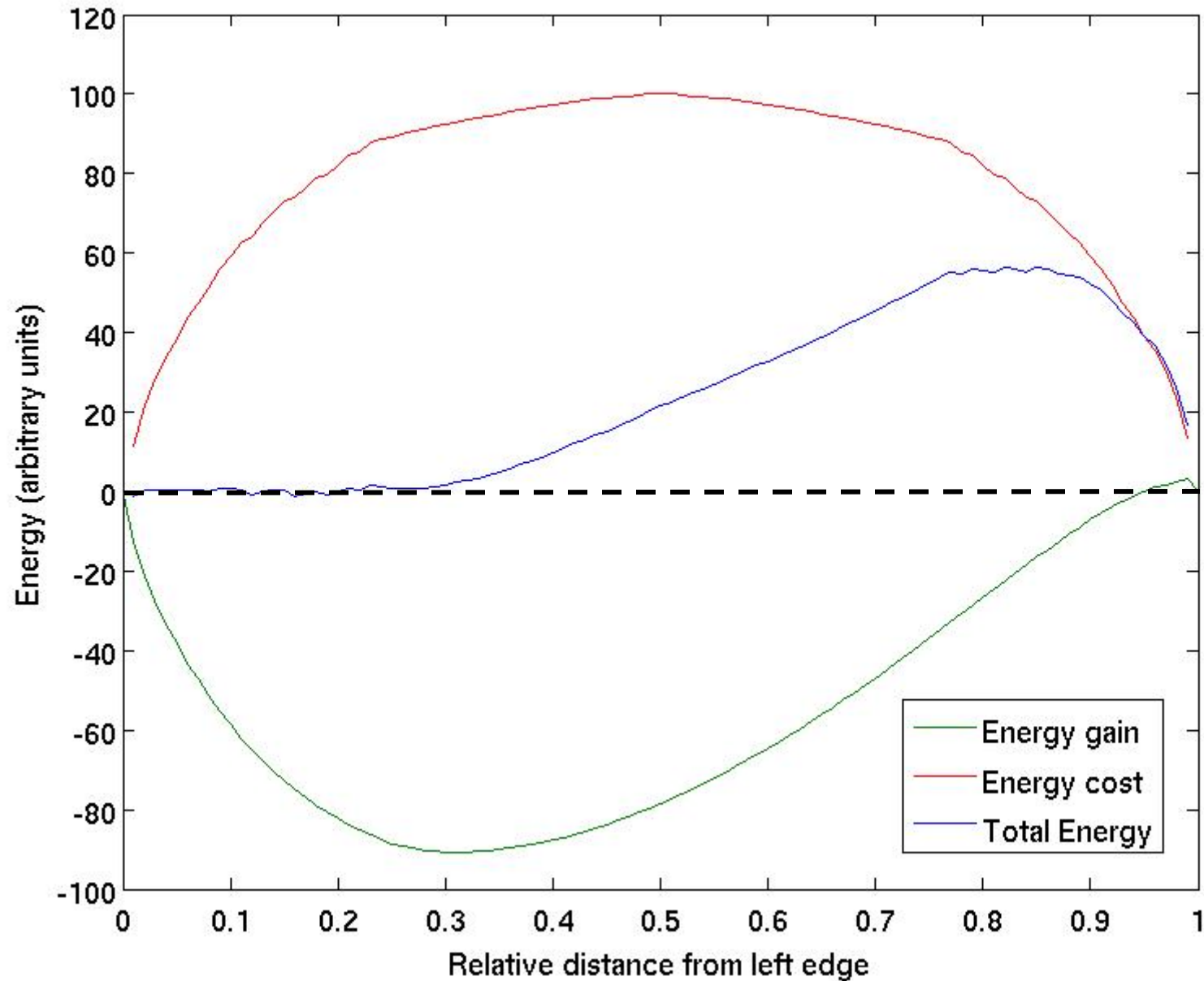
Energy gain: results for barns and domes



In the island it exists a **position that maximize the energy gain:** there, in first approximation, the dislocation will be placed

A. Marzegalli et al., *Phys. Rev. Lett.* **99**, 235505 (2007)

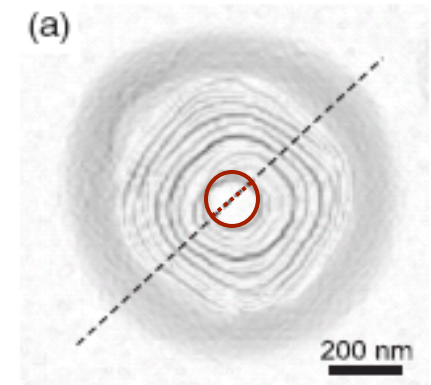
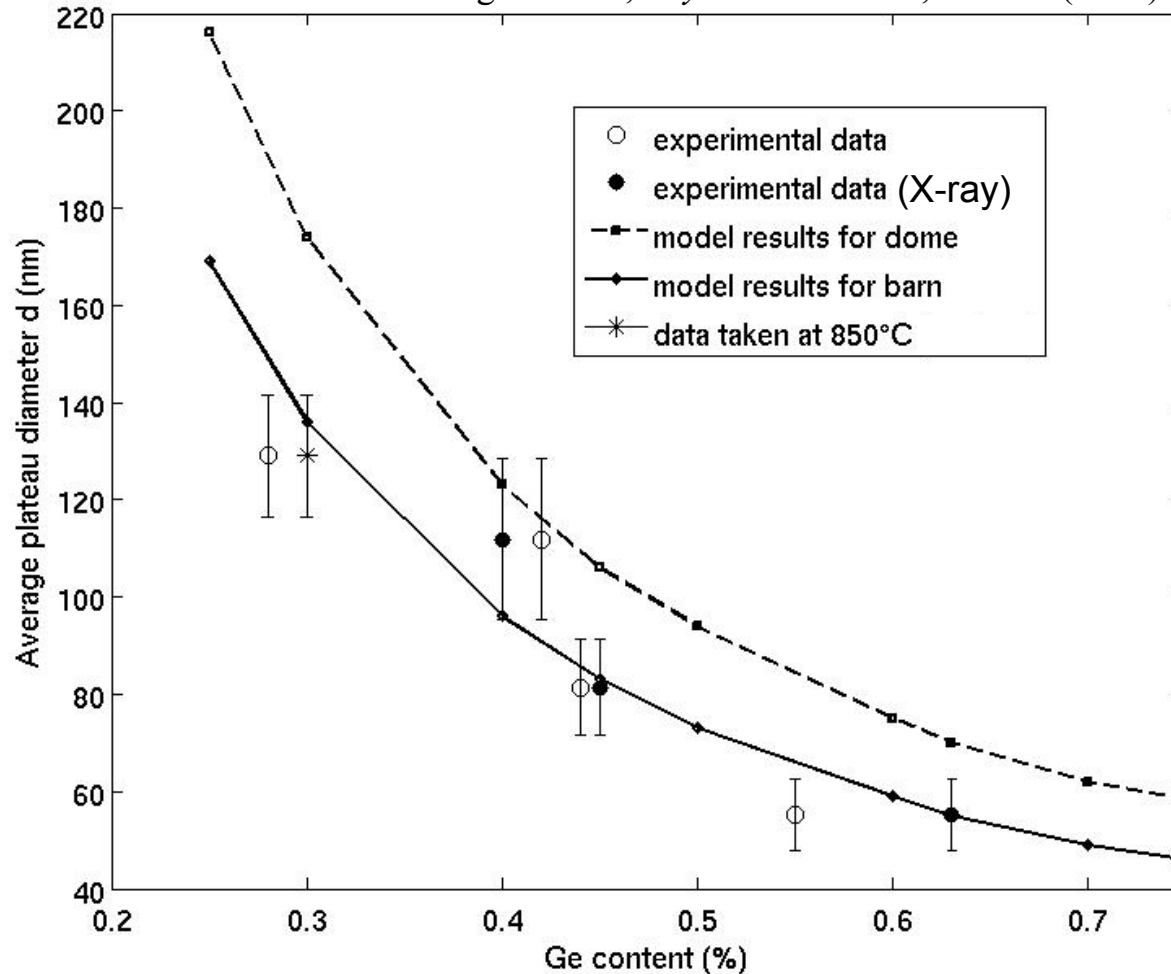
Gain and cost at the critical size



Plastic relaxation onset in barn shape, first



A. Marzegalli et al., *Phys. Rev. Lett.* **99**, 235505 (2007)



Good correspondence with the mean Si plateau size of largest coherent islands before plastic relaxation onset

First theoretical evidence that **BARNs** are the actual island shaped in which plastic relaxation occurs

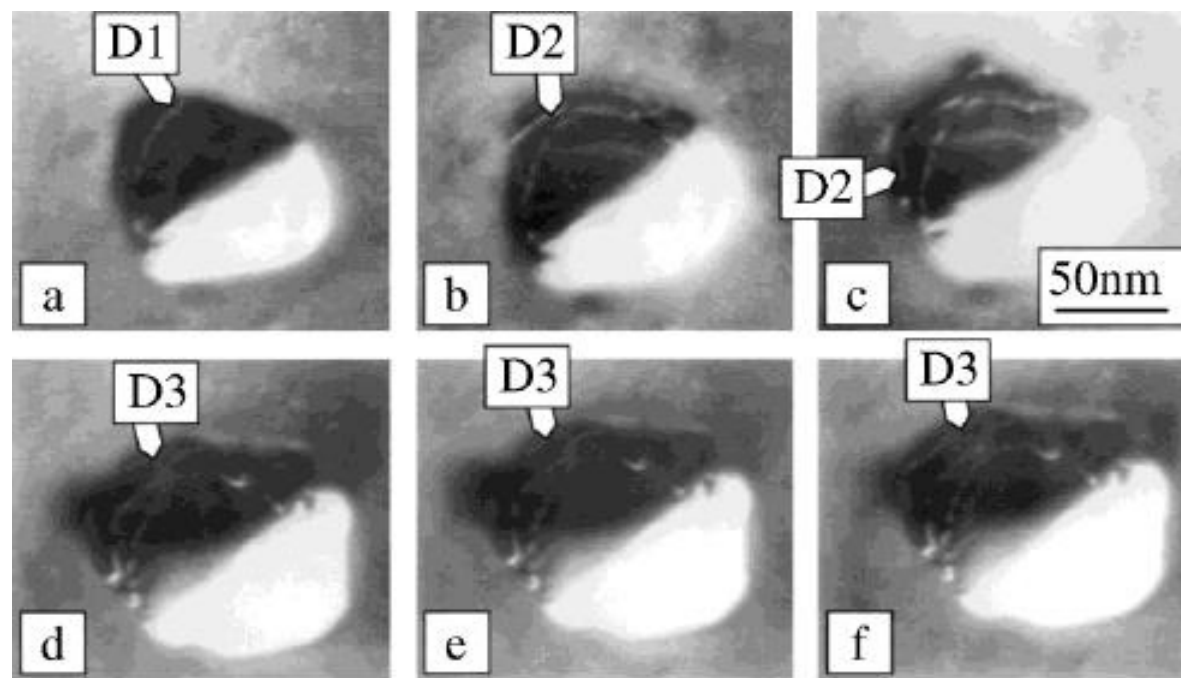


Cyclic Growth of Strain-Relaxed Islands

F. K. LeGoues, M. C. Reuter, J. Tersoff, M. Hammar, and R. M. Tromp

IBM Research Division, T.J. Watson Research Center, Yorktown Heights, New York 10598

(Received 8 March 1994)

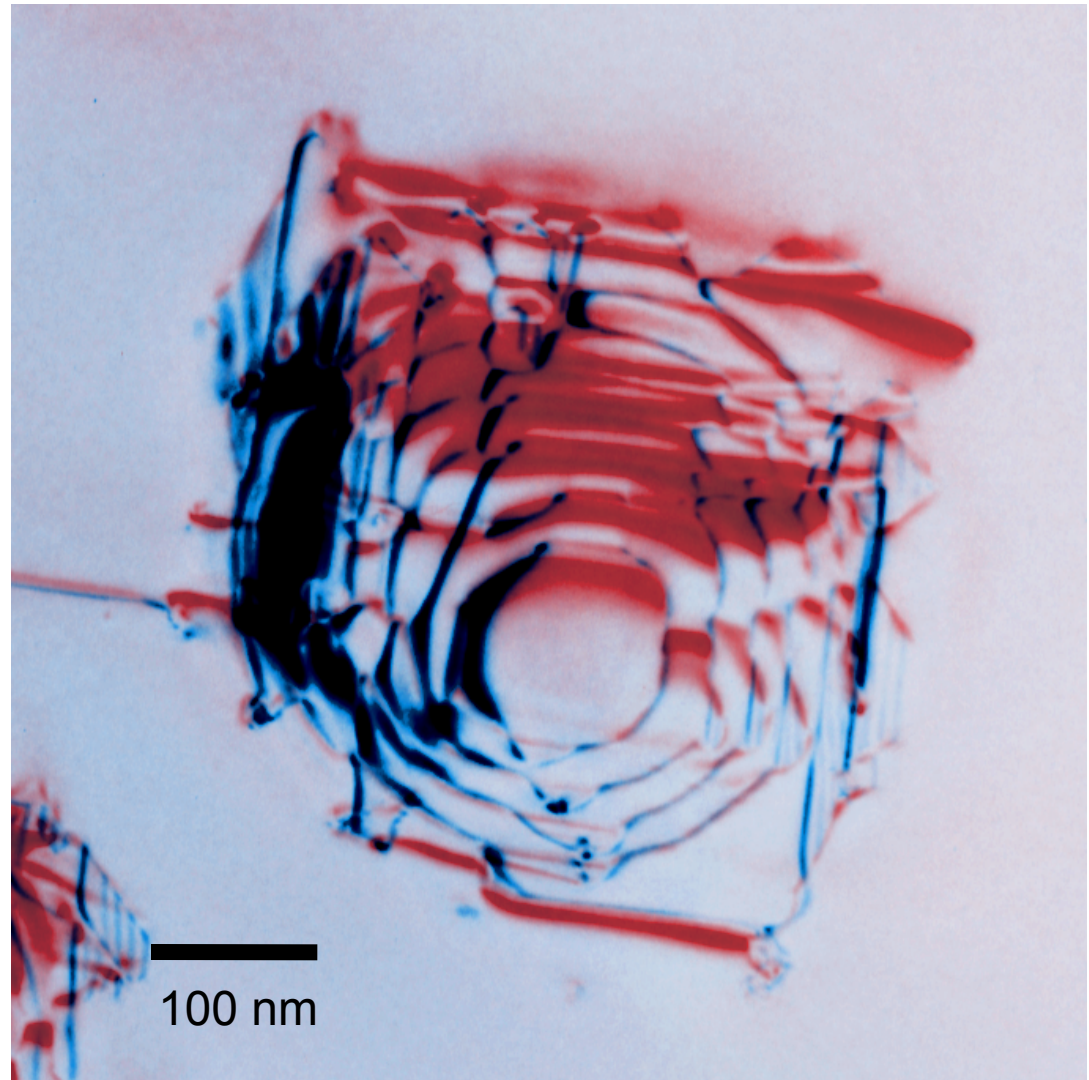


TEM images of Ge islands



TEM image of Ge island grown by UHV-CVD on Si (001) in situ by Francis Ross (IBM)

T = 700 °C

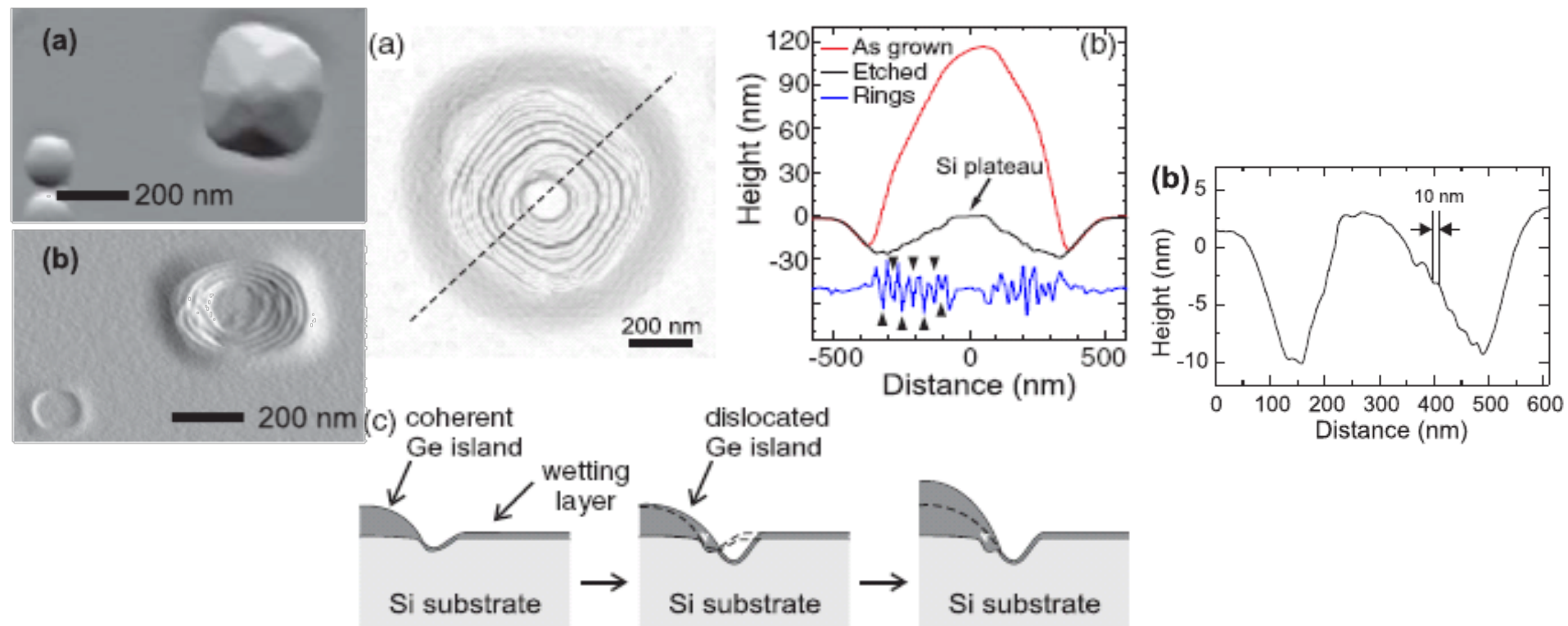


A. Portavoce et al., *Phys. Rev. B* **76**, 235301 (2007)

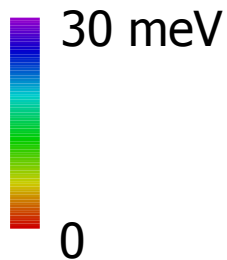


Dendrochronology of Strain-Relaxed Islands

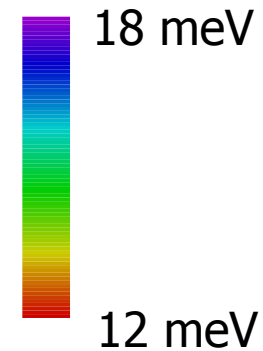
T. Merdzhanova,* S. Kiravittaya, A. Rastelli, M. Stoffel, U. Denker, and O. G. Schmidt
Max-Planck-Institut für Festkörperforschung, Heisenbergstrasse 1, D-70569 Stuttgart, Germany
(Received 19 December 2005; published 6 June 2006)



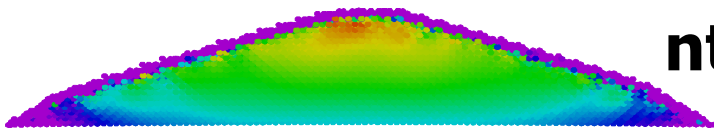
Dislocation creates a preferential side ..



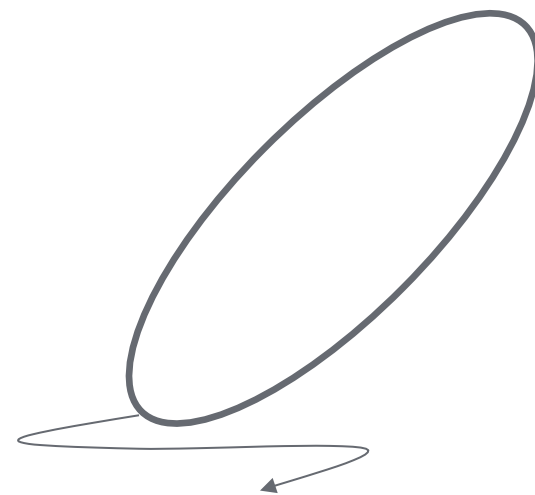
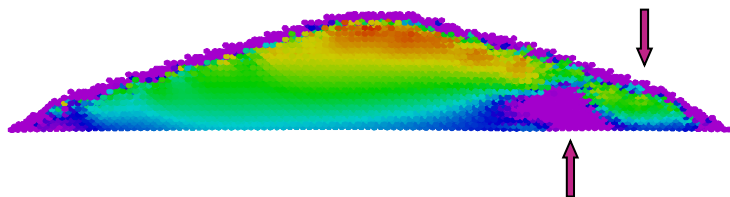
$$\Delta E_{\text{atom}} = E_{\text{bulkGe}} - E_{\text{dome}}$$



coherent

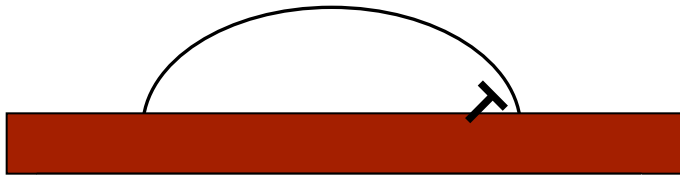


dislocated

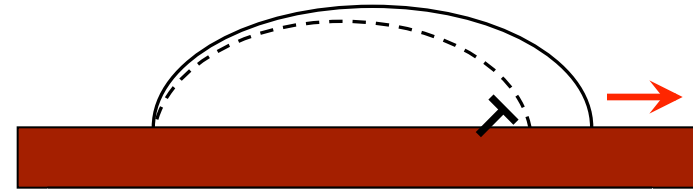


preferential side for dome expansion

Cyclic growth mechanism



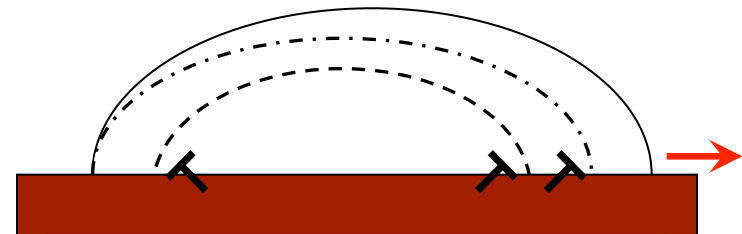
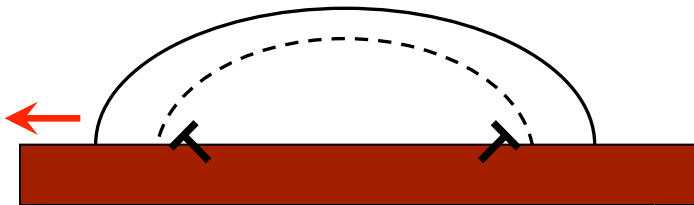
Metastable state



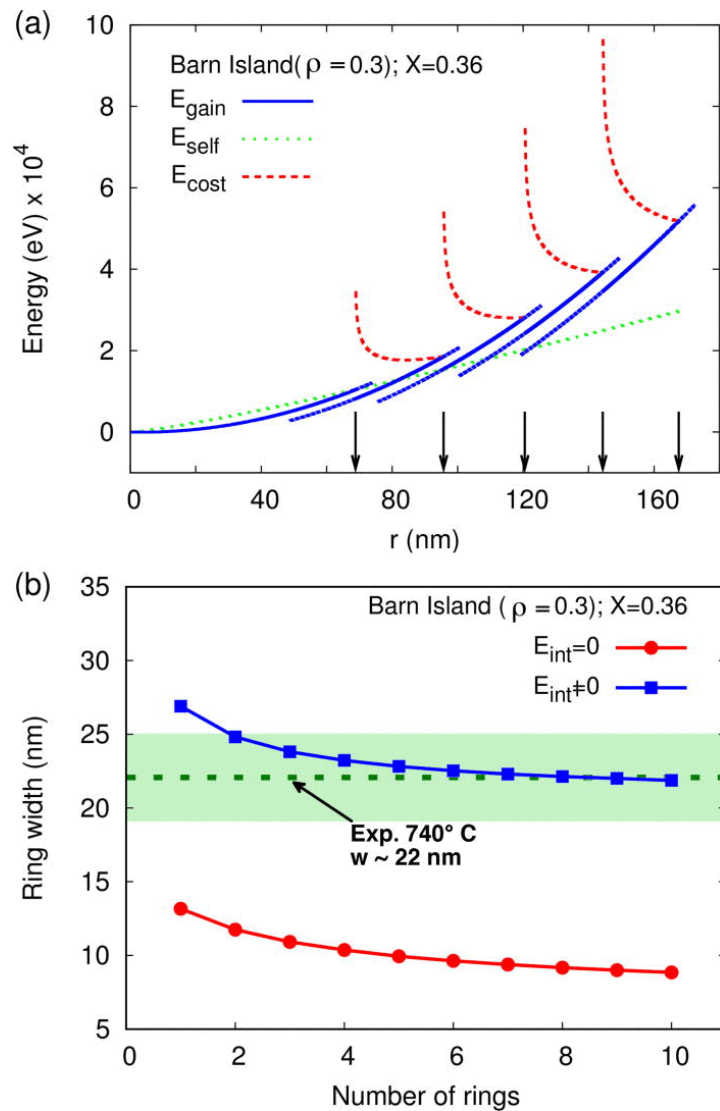
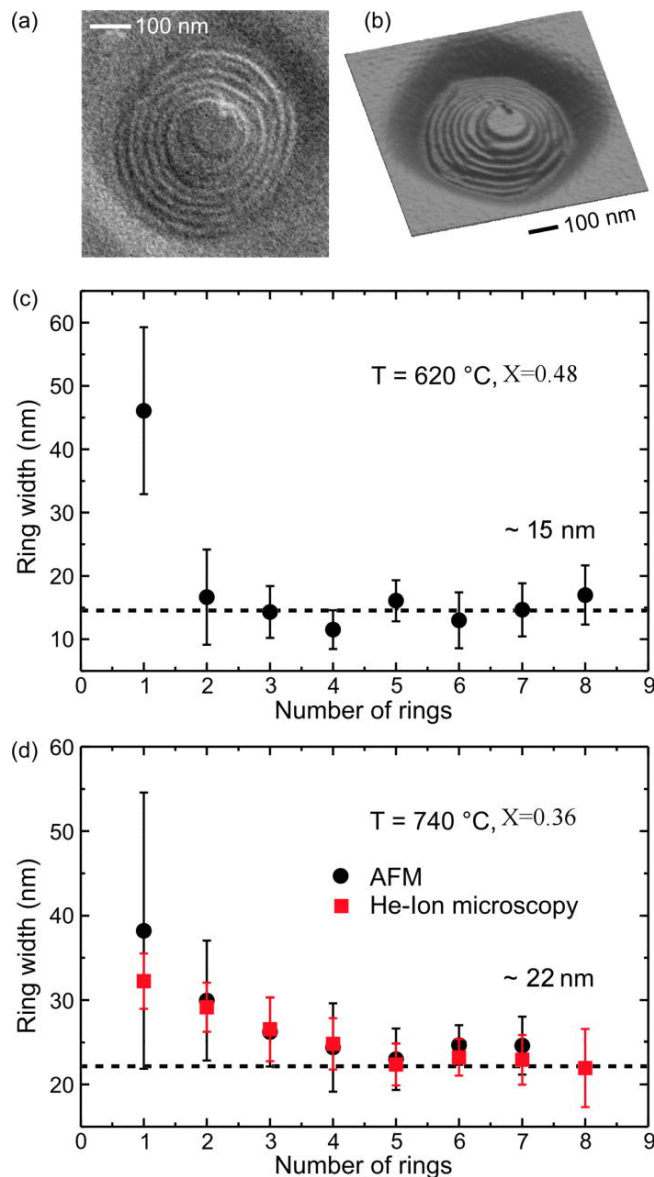
Stable state

New material will be incorporated at the same edge where plastic relaxation has already occurred and the dislocation is moved in the equilibrium position

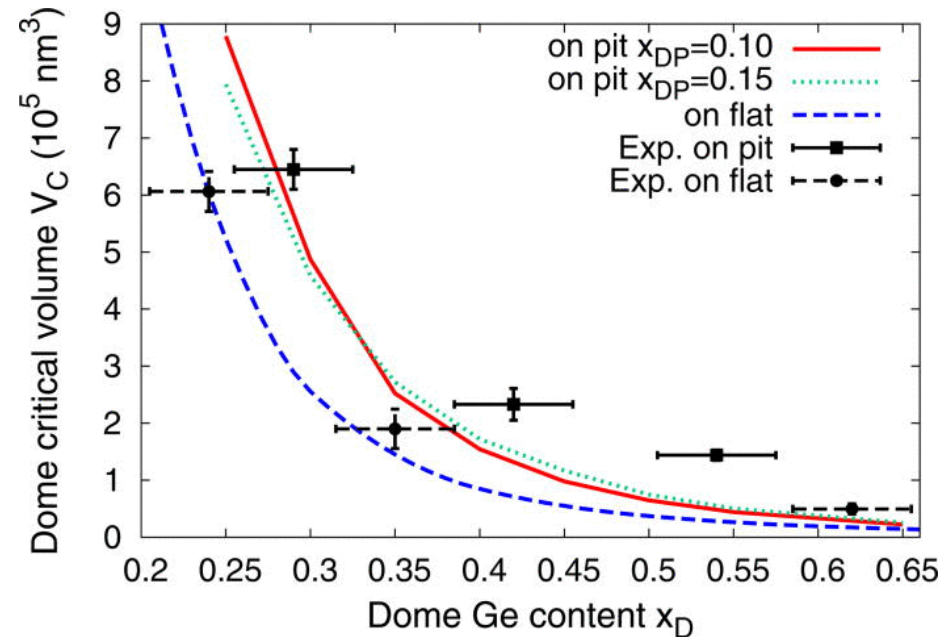
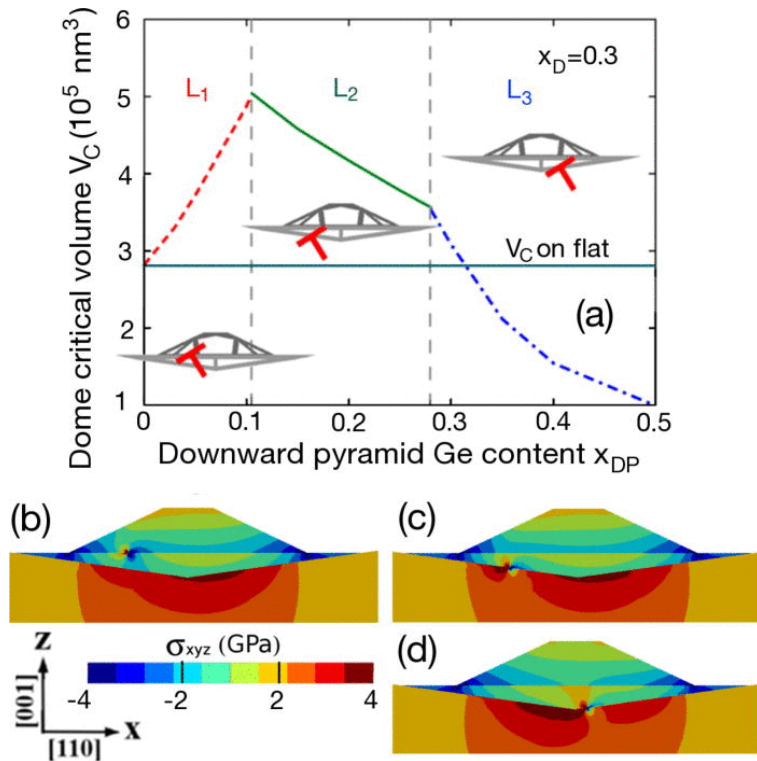
The process goes on during the growth



Ring size estimation by ring-shaped dislocat.



Last issue: plastic relax. in pits and intermix.



Critical volumes V_C for plasticity onset in $\text{Si}_{0.7}\text{Ge}_{0.3}$ domes on pit-patterned $\text{Si}(001)$ substrates as a function of the DP Ge content x_{DP} . For $x_{DP} = 0.2$, we show the hydrostatic stress map in the xz -plane, perpendicular to the $[110]$ direction, with the dislocation at the (001) dome/DP interface (b), where only the island is relaxed, and at the DP/Si interface, in its minimum energy position (c) and on the right handed pit side (d), where the dislocation relaxes mainly the DP.

Critical volumes V_C for plasticity onset in $\text{Si}_{1-xD}\text{Ge}_{xD}$ islands on flat and on pit-patterned $\text{Si}(001)$ substrates as a function of the dome Ge content x_D .



Selfassembly in apparently simple system, such as Ge(Si)/Si reveals to be unexpectedly complex

- Elastic relaxation by aspect ratio
- Morphology by surface energies
- Oswald ripening and pit patterning order
- Intermixing and island displacements
- Plastic relaxation on flat and in pits...

Thermodynamics drives the system and you have limited chance to modify the route

Latest ICT applications needs better control to nano+micro 3D vertical structures (Fin FET)

Move epitaxy to kinetic growth modalities, with very short surface diffusion length: non equilibrium 3D structures.
(see poster by M. Salvalaglio starting from non-equilibrium 3D structures)